ELECTRONIC EMISSION SPECTRA OF DIATOMIC FREE RADICALS SeO AND SbO

KUMAR KRISHNA VERMA

NOTICE

The quality of this microfiche is heavily dependent upon the quality of the original thesis submitted for microfilming. Every effort has been made to ensure the highest quality of reproduction possible.

If pages are missing, contact the university which granted the degree.

Some pages may have indistinct print especially if the original pages were typed with a poor typewriter ribbon or if the university sent us a poor photocopy.

Previously copyrighted materials (journal articles, published tests, etc.) are not filmed.

Reproduction in full or in part of this film is governed by the Canadian Copyright Act, R.S.C. 1970, c. C-30. Please read the authorization forms which accompany this thesis.

THIS DISSERTATION HAS BEEN MICROFILMED EXACTLY AS RECEIVED

AVIS

La qualité de cette microfiche dépend grandement de la qualité de la thèse soumise au microfilmage. Nous avons tout fait pour assurer une qualité supérieure de reproduction.

S'il manque des pages, veuillez communiquer avec l'université qui a conféré le grade.

La qualité d'impression de certaines pages peut laisser à désirer, surtout si les pages originales ont été dactylographiées à l'aide d'un ruban usé ou si l'université nous a fait parvenir une photocopie de mauvaise qualité.

Les documents qui font déjà l'objet d'un droit d'auteur (articles de revue, examens publiés, etc.) ne sont pas microfilmés.

La reproduction, même partielle, de ce microfilm est soumise à la Loi canadienne sur le droit d'auteur, SRC 1970, c. C-30. Veuillez prendre connaissance des formules d'autorisation qui accompagnent cette thèse.

LA THÈSE A ÉTÉ MICROFILMÉE TELLE QUE NOUS L'AVONS REÇUE

ELECTRONIC EMISSION SPECTRA OF DIATOMIC FREE RADICALS SeO AND SbO

by

Kumar Krishna Verma, M.Sc.

A Thesis submitted in partial fulfillment of
the requirements for the degree of
Doctor of Philosophy

Department of Physics
Memorial University of Newfoundland

September, 1977

St. John's Newfoundland

TO MY PARENTS

ACKNOWLEDGEMENTS

It is my pleasure to express my gratitude to my supervisor, Professor S.P. Reddy, for his constant encouragement and guidance through all stages of the work presented in this thesis.

I am grateful to the chairman and other faculty members of the Physics Department for their understanding and goodwill throughout my graduate work at Memorial University.

My special thanks are due to Dr. N.H. Rich for helpful discussions, to Mr. P. Gillard for his assistance in some aspects of computer programming and to Mr. M. Azam for his help in the initial stages of the experimental work.

The financial support received from the Memorial University of Newfoundland is gratefully acknowledged. I would like to express my gratitude to Dr. F.A. Aldrich, Dean of the School of Graduate Studies, whose personal interest and encouragement were extremely helpful throughout my graduate programme.

I am thankful to Professor W.R. Jarmain, University of Western Ontario, for providing us a copy of his computer programme, "TRAPRB".

I wish to thank the following technical personnel for their invaluable assistance: Messrs. T.G. White, M. Ryan,

B. Moriarity, T. Vallis and A.J. Walsh for machine work; Messrs. D. Seymour, T. Perks and Martin Hatswell for glassblowing; Messrs. R.J. Penney and A.W. McCloy for assistance in electronics; Mr. R. Guest for drafting some diagrams and Educational Television (Photography) for photographic work.

I extend my sincere thanks to Mrs. D. Strange for a careful typing of the manuscript.

I owe my most cordial and special thanks to my wife, Gita and my son, Rajeev, for their patience and deep understanding; and to my brother-in-law, Dr. Avinash Singh, for his inestimable help especially during the preparation of this thesis. Last but by no means least, I must express my high regards and deep indebtedness to my Respected Parents whose blessings and inspirations have brought me to a stage where this work is possible.

CONTENTS

ABSTRACT

Experimental studies of several electronic transitions of the SeO free radical in the spectral region 2000 - 18 000 Å and of one electronic transition of the SbO free radical in the region 3240 - 4720 Å have been made.

The 0 - 0 bands at 10 296 and 10 491 Å of the near-infrared band system b - X of SeO have been photographed at high resolution and their rotational structures have been analyzed. The analysis shows that the bands represent the transition $b0^+ - X0^+,1$ (X being the case (c) $^3\Sigma^-$ ground state of SeO). Rotational constants of substates $X_1 0^+$, $X_2 1^-$ and $X_2 1^+$ of the ground state and that of state $b0^+$ have been derived. The observed isotope shifts of the rotational lines of ^{78}SeO from those of ^{80}SeO are in good agreement with the calculated values. Franck-Condon factors and r-centroids are reported for the b - X system.

Three electronic band systems of SeO in the spectral regions, around 18 000 Å, 6730 - 8570 Å and 2690 - 3190 Å have been observed for the first time at medium resolution. Vibrational constants for the upper and lower states of these transitions, whenever possible, have been derived. Vibrational analyses of these systems suggest that these arise from the transitions $a2 - X_2 1$; $A0,1,2 - X0^+,1$ and

C2,1,0 - $X0^+$,1, respectively. Approximate rotational constant B_o for state a or A is estimated from the separations of the observed R and Q heads or P and Q heads. The vibrational structure of two known brief band systems of SeO in the region 2070 - 2270 Å have been reanalyzed and the molecular constants derived. From the analysis, the transitions are labelled F - $a^1\Delta$ (2150 - 2270 Å) and G - $a^1\Delta$ (2070 - 2130 Å). Klein-Dunham potential energy curves are constructed for the $X_1 0^+$, $b0^+$, $A_1 0$ states as well as the previously known $B_1 0^+$ state of SeO.

The 0 - 0 and 1 - 0 bands of the $B^2\Sigma^+ - X^2\Pi_{3/2}$ subsystem of SbO have been photographed under high resolution and the rotational constants derived.

CHAPTER 1

INTRODUCTION

The development of wave mechanics greatly accelerated the spectroscopic studies of molecular structure on the basis of the spectra of molecules. Many empirical features of band spectra could be understood in terms of the validity of wave mechanics. As a matter of fact in several instances molecular spectroscopy supplied excellent confirmations of the predictions of wave mechanics and thus helped to establish its significance in understanding many atomic and molecular phenomena.

A great progress has been made during the last fifty years or so in the experimental investigation and theoretical interpretation of the electronic band spectra of molecules. From a detailed investigation of the electronic spectrum of a molecule, one can derive, precisely, the electronic, vibrational and rotational levels of that molecule. From these again, one can obtain a detailed information about the electronic structure (motion of electrons) and the vibration and rotation of the nuclei in the molecule. A knowledge of the electronic motions leads to the understanding of important properties such as chemical valence. From the vibrational frequencies and the corresponding anharmonicities,

the forces between the atoms of the molecule and the heats of dissociation can be calculated. From a study of the rotational fine structure of the electronic bands, the moments of inertia (hence the internuclear separations) and the nature of the coupling between the electronic and rotational motions of the molecule can be determined with great precision. The information thus obtained for the individual molecules by spectroscopic methods enables us to understand many of their physical and chemical properties.

1.1. Electronic Spectra of O_2, SO and SeO

For the analogous diatomic molecules O_2, SO and SeO formed of the Group VI elements of the periodic table, one expects within a first approximation similar electronic states because the outermost shells of each of the atoms O, S and Se contain four p electrons. The electronic states of O_2 differ from those of SO and SeO at least in two respects, namely, they are either even (g) or odd (u) because of the symmetry of the nuclei in O_2 and they have only symmetric rotational levels because the oxygen nucleus has zero spin. Even though the outermost electrons play a major role in determining the molecular properties mentioned above, the inner electrons and masses of the nuclei are also of considerable importance. In fact the relative positions of the electronic states and the nature of the coupling between electronic motion (orbital motion as well as spin)

and the rotation of the nuclei are dependent to a considerable extent on the electrons of the inner shells. A detailed study of the electronic spectra of analogous molecules enables one to determine the nature of coupling between the electronic motion and the rotation of the nuclei in their various electronic states and to obtain a proper correlation between these states.

Extensive investigations have been carried out on the electronic band spectrum of O_2 both in emission and absorption for a long period extending over several decades. These studies have led to great advances in our understanding of the structure of O_2 in its ground state as well as in a large number of its excited states. The number of electronic states so far observed for O_2 is at least 10 which have given rise to 14 band systems (cf. Rosen, 1970). The ground electronic state is the common lower state for 9 of these band systems. In addition, a number of Rydberg transitions (cf. Rosen, 1970) and several double electronic transitions (cf. Findlay, 1970; and the references therein) have been observed for O_2. These electronic band systems extend from 500 Å in the vacuum ultraviolet to 19 100 Å in the near infrared.

For SO, three electronic band systems all with a common ground state have been observed in the spectral region 1900 - 10 900 Å and its structure in all the four electronic states has been determined (cf. Colin, 1968, 1969).

A general spectroscopic study of the electronic spectrum of SeO in emission has been recently initiated in our laboratory and some experimental results have already been published on this spectrum (Azam & Reddy, 1973; Reddy & Azam, 1974; see section 1.2). The results obtained on the emission spectrum of SeO in the present work form a part of this systematic study and constitute a major portion of this thesis.

1.2. Previous Work on the Electronic Band Spectrum of SeO

(i) The Near Ultraviolet $B^3\Sigma^- - X^3\Sigma^-$ System (3100 - 5100 Å)

The emission spectrum of the SeO molecule was first discovered by Asundi, Jan-Khan and Samuel (1936) who observed 14 characteristic emission bands of SeO degraded to longer wavelengths in the region 3230 - 3950 Å by introducing SeO_2 into a bunsen flame. These authors proposed a tentative vibrational analysis of these bands. Later, Choong-Shin Piaw (1938) excited the spectrum of SeO by passing high power electrical discharge through SeO_2 vapor and photographed 20 double-headed bands degraded to longer wavelengths in the region 3100 - 3950 Å. He analyzed them into two systems. Subsequently, Barrow and Deutsch (1963) excited the emission spectrum of SeO in a radiofrequency electrodeless discharge through a slow stream of oxygen which passed over heated

selenium and photographed it under high resolution. These authors have carried out the rotational analysis of 9 bands and designated the system as $A^3\Sigma^- - X^3\Sigma^-$, which was later referred to as $B^3\Sigma^- - X^3\Sigma^-$ by Azam and Reddy (1973) because this system is analogous to the system $B^3\Sigma^- - X^3\Sigma^-$ in O_2 as well as in SO. The spin-spin interaction constants λ'' and λ' of the $X^3\Sigma^-$ and $B^3\Sigma^-$ states, respectively, were found by Barrow and Deutsch (1963) to be very large. The double headed nature of the bands was explained on the basis of the splitting of each band (v'-v'') into three subbands, two of which arise from $F_2 - F_2$ and $F_3 - F_3$ transitions that lie close together, and one of which arises from $F_1 - F_1$ transition which is separated by an amount $-2(\lambda'-\lambda'')$ from the former. Haranath (1965) photographed 25 additional double-headed bands of the B - X system of SeO in emission in the region 3900 - 5100 Å and assigned vibrational quantum numbers to them. These assignments were confirmed by the observed isotope heads of ^{80}SeO and ^{78}SeO.

(ii) <u>The Photographic-Infrared $b^1\Sigma^+ - X^3\Sigma^-$ System (9490 - 10 780 Å)</u>

Recently, Azam and Reddy (1973) discovered 46 new bands of SeO degraded to longer wavelengths in the region 9490 - 10 780 Å. These bands were excited in an electrodeless discharge tube containing SeO_2 powder and irradiated by a high power microwave generator. These authors assigned 42 bands as the ^SR and ^QR heads of the two subsystems

$^1\Sigma^+ - X(F_1)$ and $^1\Sigma^+ - X(F_2,F_3)$ of the forbidden transition $b^1\Sigma^+ - X^3\Sigma^-$. The separations between the corresponding bandheads of these two subsystems are found to be consistent with the expected value $\sim 2\lambda''$, λ'' being the spin-spin interaction constant of the $X^3\Sigma^-$ state, which was derived by Barrow and Deutsch (1963) from their work on the $B^3\Sigma^- - X^3\Sigma^-$ system. The vibrational assignments of Azam and Reddy (1973) were also supported by the observed isotope heads of ^{82}SeO, ^{80}SeO, ^{78}SeO and ^{76}SeO. The remaining 4 bands which were tentatively assigned to the probable forbidden transition $(a^1\Delta) - (X^3\Sigma^-)$ by them, have been, in fact, very recently assigned as the ^QQ heads of the subsystem $b^1\Sigma^+ - X^3\Sigma^-(F_2,F_3)$ by Barrow and Lemanczyk (1975), who also suggested that Hund's case (c) applies to the $X^3\Sigma^-$ state of SeO.

(iii) <u>The Far-Ultraviolet Band Systems (1800 - 2480 Å)</u>

The emission spectrum of SeO in the far-ultraviolet region excited in a radio frequency discharge through SeO_2 powder, was first observed by Haranath (1964) who photographed nearly 40 bands in the region 1800 - 2400 Å under low dispersion and analyzed the bands into four systems. Recently, in our laboratory, Reddy and Azam (1974) photographed the far-ultraviolet emission spectrum of SeO in the region 1930 - 2480 Å at medium dispersion and reanalyzed the vibrational structure of the bands. Beginning at the

longer wavelength end, the spectrum was analyzed into five band systems which were designated as $c^1\Sigma^+ - b^1\Sigma^+$, $x_2 - x_1$, $y_2 - y_1$, $C^3\Pi - X^3\Sigma^-$ and $D^3\Sigma^- - X^3\Sigma^-$. The lower state of c - b system was found to be the upper state of the infrared b - X system.

(iv) Other Bands of SeO

Kushawaha and Pathak (1972) reported several weak emission bands of SeO in the region 5250 - 6150 Å and suggested the transition $b^1\Sigma^+ - X^3\Sigma^-$ for these bands. It is now clear that this suggestion is incorrect in view of the work of Azam and Reddy (1973) discussed earlier in this section.

Carrington, Currie, Levy, and Miller (1969) studied the electron spin resonance spectrum of SeO in its $X^3\Sigma^-$ and $a^1\Delta$ states by passing oxygen through a microwave discharge cavity connected to the cavity of a spectrometer containing gaseous OCSe. These authors reported some constants of these two states.

1.3. Previous Work on the Electronic Band Spectrum of SbO

(i) Low Resolution Work

The first attempt to excite the emission spectrum of the SbO molecule was made by Mukherji (1931) who observed many characteristic bands of this molecule in the flame of an arc between antimony and carbon electrodes. All these

bands in the region 3300 - 6000 Å are degraded to longer wavelengths. Sengupta (1939) reinvestigated the spectrum of SbO in the region 3200 - 6800 Å and analyzed them into two band systems, namely $A^2\Pi - X^2\Pi_{reg}$ (4700 - 6800 Å) and $B^2\Sigma^+ - X^2\Pi_{reg}$ (3200 - 4700 Å). The latter system is analogous to the $B^2\Sigma^+ - X^2\Pi_{reg}$ systems of the NO, PO and AsO molecules. The spin-orbit splitting in the ground state $X^2\Pi_{reg}$ of SbO was found by Sengupta to be large (2272 cm^{-1}) and that of the $A^2\Pi$ state was relatively small (132 cm^{-1}).

In addition, there have been several low resolution studies of other band systems of this molecule. These are, the $C^2\Delta - X^2\Pi_{reg}$ system (2700 - 4400 Å) (Lakshman, 1960a; Shimauchi, 1960), the $D^2\Pi - X^2\Pi_{reg}$ (2780 - 3260 Å) (Lakshman, 1960a; Shimauchi, 1960), the $E^2\Sigma^+ - X^2\Pi_{reg}$ system (2450 - 2800 Å) (Sengupta, 1943; Shimauchi, 1960), the $F(^2\Delta) - X^2\Pi_{reg}$ and $G - X^2\Pi_{reg}$ systems (2500 - 2850 Å) (Shimauchi, 1960).

(ii) High Resolution Work

The first high-resolution work on SbO was that of Lakshman (1960b) who analyzed the rotational structure of the two components of the 0 - 0 band of the $B^2\Sigma^+ - X^2\Pi_{reg}$ system. The analysis was revised by Singh and Upadhyay (1967) who were able to identify the isotopic lines due to ^{121}SbO and ^{123}SbO. Subsequently, Rao and Rao (1968) have published a preliminary report on the rotational analysis of the 0 - 0 bands of the $B^2\Sigma - X^2\Pi_{reg}$ system and several

bands of the $C^2\Delta - X^2\Pi_{reg}$ and $D^2\Pi - X^2\Pi_{reg}$ systems. Rai, Upadhyay and Rai (1970) made a more detailed investigation of the rotational structure of 1 - 1 and 1 - 2 bands of the D - X system and detected the Λ-type doubling in the $X^2\Pi_{reg}$ state. Rai, Rai and Rai (1974) analyzed the rotational structure of the 2 - 0 band of the $C^2\Delta_{3/2} - X^2\Pi_{\frac{1}{2}}$ subsystem and observed a small Λ-type doubling in state C.

1.4. Present Investigations on the Emission Spectra of SeO and SbO

In the present study the emission spectra of SeO and SbO were excited by irradiating respectively SeO_2 and Sb_2O_3 contained in quartz discharge tubes by a high power microwave generator. The spectrum of SeO was investigated in a wide spectral region from far-ultraviolet (2070 Å) to the near infrared (~1.8 μm). The $B^2\Sigma^+ - X^2\Pi_{reg}$ system of SbO in the region 3200 - 4700 Å was recorded at high resolution.

A brief review of the theory applicable to the present work is given in Chapter 2.

A description of the apparatus used and of the experimental procedure adopted is presented in Chapter 3.

The rotational analysis of the b - X system of SeO shows that this band system arises from the transition $b0^+ - X0^+,1$, where X is a case (c) $^3\Sigma^-$ state. Results of this analyis are presented in Chapter 4.

In the course of the present study three new band systems of SeO have been observed for the first time. These

are a2 - X_2i (around 1.8 μm in the near infrared region), A0,1,2 - $X0^+$,1 (6730 - 8570 Å) and C2,1,0 - $X0^+$,1 (2690 - 3190 Å). Vibrational analyses have been carried out for all these three systems. In addition, reanalyses of the vibrational structure of two brief band systems of SeO which were previously observed (Haranath, 1964; Reddy & Azam, 1974) have been proposed. These brief systems are F - $a^1\Delta$ (2150 - 2270 Å) and G - $a^1\Delta$ (2070 - 2130 Å). Results of the vibrational analyses of these five band systems are presented in Chapter 5.

Klein-Dunham potential energy curves are constructed for the $X_1 0^+$, $b0^+$, $A_1 0$ and $B_1 0^+$ states of SeO. Molecular constants, potential energy curves and electron configuration of SeO are given in Chapter 6.

Finally, results of the rotational analysis of the $B^2\Sigma^+ - X^2\Pi_{reg}$ system of SbO are presented in Chapter 7.

All the results presented in Chapter 4 and a major portion of the results presented in Chapter 5 and 6 have already been published in the Journal of Molecular Spectroscopy (Verma, Azam & Reddy, 1975; Verma, Azam & Reddy, 1977; Verma & Reddy, 1977).

CHAPTER 2

THEORY

In this chapter, a brief discussion of the theory of the electronic band spectra of diatomic molecules which is mainly pertinent to the present investigations is presented. A comprehensive account of the theory can be found in Herzberg (1950, 1971), Mulliken (1930, 1931, 1932), Jarmain (1960, 1971), Nicholls and Jarmain (1956).

2.1. Electronic-, Vibrational- and Rotational-Spectral Terms

The total energy E of a diatomic molecule within the Born-Oppenheimer approximation and neglecting its translational and nuclear spin energies is represented as the sum of three parts, the electronic energy E_e, the vibrational energy E_v and the rotational energy E_r, that is

$$E = E_e + E_v + E_r.$$

Or, in term values

$$T = E/hc = T_e + G(v) + F_v(J). \qquad (2\text{-}1)$$

Here v and J are the vibrational and rotational quantum numbers respectively, and the term values T_e, $G(v)$ and $F_v(J)$ are expressed in cm^{-1} units. In Eq. (2-1), T_e for electronic states with multiplicity greater than one is represented by

$$T_e = T_o + A\Lambda\Sigma, \qquad (2\text{-}2)$$

where T_o is the electronic term value when the resultant electronic spin $\vec{S}$ of the molecule is neglected, Λ is the quantum number of the component of the total electronic orbital angular momentum in the direction of the internuclear axis, Σ is the component of the spin vector $\vec{S}$ along the same axis, and A is the spin-orbit coupling constant. Electronic states with $\Lambda = 0, 1, 2, \ldots$ are labelled Σ, $\Pi, \Delta, \ldots$, respectively. (The electronic state Σ is not to be confused with Σ, the quantized projection of the vector $\vec{S}$ in the direction of the internuclear axis). A Σ electronic state is designated Σ^- if the electronic wavefunction ψ_e changes sign upon reflection at a plane through the internuclear axis or Σ^+ if it remains unchanged. The multiplicity 2S+1 of an electronic state of a molecule is even or odd depending upon whether it has an odd or an even number of electrons. The parity of a rotational level is either positive or negative depending upon whether the total wavefunction of the molecule remains unchanged or changes sign upon reflection at the origin. For the case of non-degenerate Σ states, a Σ^+ state has the even rotational levels as positive and odd ones as negative, and the reverse is true for a Σ^- state. In the degenerate states Π, Δ, . . . etc., there are, for each J value, two degenerate levels, one positive and the other negative. This splitting of the rotational levels in states with $\Lambda \neq 0$ is called

Λ-type doubling.

In each electronic state of a molecule there may be a number of vibrational levels whose term values G(v) are expressed as

$$G(v) = \omega_e(v+\tfrac{1}{2}) - \omega_e x_e (v+\tfrac{1}{2})^2 + \omega_e y_e (v+\tfrac{1}{2})^3 + \ldots , \qquad (2\text{-}3)$$

where ω_e is the vibrational frequency (in cm^{-1}) and $\omega_e x_e$, $\omega_e y_e$, . . . are the correction terms due to the anharmonicity of the vibrations.

Each vibrational level of a given electronic state may contain a series of rotational levels. The term values of these levels in the case of a <u>singlet</u> electronic state are represented by

$$F_v(J) = B_v J(J+1) - D_v J^2(J+1)^2 + \ldots + (A-B_v)\Lambda^2, \qquad (2\text{-}4)$$

where $B_v = (h/8\pi^2 c\mu)\overline{(1/r^2)}$ is the rotational constant, $D_v = 4B_v^3/\omega^2$ is the centrifugal stretching constant and $A = h/8\pi^2 cI_A$ (not to be confused with A of Eq. (2-2)). Here μ is the reduced mass of the molecule and I_A is the moment of inertia of the electrons about the internuclear axis and hence is a constant for a given electronic state. We note that for a given electronic state both A and Λ in Eq. (2-4) are constants and it is customary to take the term $(A-B_v)\Lambda^2$ into the vibronic part of the energy. The quantities B_v and D_v can be expressed in terms of the vibrational quantum number as

$$B_v = B_e - \alpha_e(v+\tfrac{1}{2}) + \ldots ,$$

$$D_v = D_e - \beta_e(v+\tfrac{1}{2}) + \ldots , \qquad (2\text{-}5)$$

where B_e and D_e are the constants corresponding to the equilibrium internuclear separation r_e. The quantities α_e and β_e are very small compared to B_e and D_e respectively.

In the case of doublet, triplet, etc., electronic states one has two, three, etc., series of vibrational as well as rotational levels. The spacing of the rotational levels in these doublets, triplets, etc., as a function of the rotational quantum number depends on the type of coupling between different angular momenta in the molecule, such as the electronic orbital angular momentum, the electronic spin angular momentum and the angular momentum of nuclear rotation. Of the several possible couplings, we describe in the following paragraphs three cases known as Hund's case (a), case (b) and case (c).

In Hund's case (a) the electronic orbital and spin motions are coupled individually and very strongly to the internuclear axis. As a result the orbital angular momentum vector $\vec{L}$ and the spin angular momentum vector $\vec{S}$ have quantized projections Λ and Σ respectively along the internuclear axis, whose sum is represented by Ω, i.e.,

$$\Omega = \Lambda + \Sigma. \qquad (2\text{-}6)$$

For a given Λ, Ω has $2S+1$ values, i.e., the number of Σ values. In this case the molecule is a symmetric top with

the total angular momentum Ω instead of Λ along the internuclear axis. Consequently, Λ in Eq. (2-4) is to be replaced by Ω. The angular momentum $\vec{R}$ of nuclear rotation now combines with $\vec{\Omega}$ to form the resultant $\vec{J}$. For a given Ω the quantum number J has the possible values

$$J = \Omega, \Omega+1, \Omega+2, \ldots \tag{2-7}$$

Thus the first rotational level for a given multiplet component of an electronic state has $J=\Omega$. Both Ω and J have either integer or half integer values depending on whether Σ *is an integer or half an integer, i.e., whether the molecule* has an even number or odd number of electrons.

In Hund's case (b) the spin vector $\vec{S}$ is not coupled or very weakly coupled to the internuclear axis. In this case $\vec{\Lambda}$ (when it is different from zero) combines with $\vec{R}$ to *form the resultant* $\vec{N}$. *The quantum number N has the values* $\Lambda, \Lambda+1, \Lambda+2, \ldots$. The vector $\vec{N}$ in turn couples with $\vec{S}$ to form the total angular momentum $\vec{J}$ such that the quantum number J has the possible values (for a given value of N)

$$J = N+S, N+S-1, \ldots, |N-S|. \tag{2-8}$$

Therefore each rotational level with a given $N(\geq S)$ *splits* into 2S+1 components. Again J can have either integer or half interger values depending on whether the molecule has an even or odd number of electrons.

Hund's case (c) is particularly important for molecules with large atomic number for which the interaction

between $\vec{L}$ and $\vec{S}$ is stronger than their interaction with the internuclear axis. Here $\vec{L}$ and $\vec{S}$ first form a resultant $\vec{J}_a$ which is then coupled to the internuclear axis with a component $\vec{\Omega}$; and thus Λ and Σ are not defined. The vectors $\vec{\Omega}$ and $\vec{R}$ couple together to form the resultant angular momentum $\vec{J}$. Similar to Hund's case (a) the quantum number J has once again the possible values (for a given Ω)

$$J = \Omega, \Omega+1, \Omega+2, \ldots, \tag{2-9}$$

which means that in case (c) as well, the lowest rotational level of an electronic state (designated by its Ω value) has $J=\Omega$.

For a degenerate electronic state ($\Lambda\neq 0$), the two components of the Λ-type doubling of a rotational level are represented by (neglecting the terms independent of J)

$$F_i(J) = B_v J(J+1) - D_v J^2(J+1)^2 + \ldots + \phi_i(J), \tag{2-10}$$

where the subscript i stands for c or d (for details see Mulliken, 1931, pp. 94-95) and $\phi_i(J)$ is a small correction term given by

$$\phi_i(J) = \kappa_i + \delta_i J(J+1) - \mu_i J^2(J+1)^2 + \ldots, \tag{2-11}$$

where the order of κ_i is same as δ_i and $\mu_i << \delta_i$.

For a nondegenerate multiplet electronic state ($\Lambda=0$, $S>0$) the rotational levels are represented by

$$F_j(N) = B_v N(N+1) - D_v N^2(N+1)^2 + \ldots + \phi_j(N) \tag{2-12}$$

where $\phi_j(N)$ is a term representing rotational-electronic interaction. In Eq. (2-12), for a $^2\Sigma$ state each N has two components F_1 (j=1) and F_2 (j=2) corresponding to J = N+½ and N - ½ respectively. Similarly for a $^3\Sigma$ state each N has three components F_1, F_2 and F_3 corresponding to J = N+1, N and N - 1 respectively.

2.2. Rotational Selection Rules

A number of selection rules hold for the transitions between various rotational energy levels of a diatomic molecule. One type, the so called rigorous selection rules, hold strictly for electric dipole radiation of the free molecule. These are

$$\Delta J = 0, \pm 1; \quad J = 0 \nleftrightarrow J = 0 \tag{2-13}$$

$$+ \leftrightarrow -, \quad + \nleftrightarrow +, \quad - \nleftrightarrow -.$$

Another type, the approximate selection rules, depend on the coupling conditions in the molecule. For Hund's case (a) and case (b) these are

$$\Delta S = 0, \quad \Delta\Lambda = 0, \pm 1, \quad \Delta N = 0, \pm 1, \tag{2-14}$$

$$\Sigma^+ \leftrightarrow \Sigma^+, \quad \Sigma^- \leftrightarrow \Sigma^-, \quad \Sigma^+ \nleftrightarrow \Sigma^-.$$

For $\Sigma - \Sigma$ transitions $\Delta N = 0$ is forbidden. (2-15)

For Hund's case (a) $\Delta\Sigma = 0$. (2-16)

The selection rule that holds in Hund's case (c) is

$$\Delta\Omega = 0, \pm 1. \tag{2-17}$$

Also, in analogy with the selection rule (2-14) for the positive and negative Σ states, we have in case (c)

$$0^+ \leftrightarrow 0^+, \quad 0^- \leftrightarrow 0^-, \quad 0^+ \nleftrightarrow 0^- . \tag{2-18}$$

In addition, if both states have $\Omega = 0$

$$\Delta J \neq 0 \text{ is forbidden.} \tag{2-19}$$

Transitions which violate the rigorous electric dipole selection rules or the approximate selection rules are called forbidden transitions. These transitions may occur as magnetic dipole, electric quadrupole or higher multipole radiation, or may be induced by external fields such as in Raman effect or by collisions with other molecules such as in collision-induced spectra. More detailed discussion of the rotational selection rules governing specific electronic transitions of SeO and SbO is deferred to the appropriate sections in the subsequent chapters.

2.3. Vibrational Structure of Electronic Bands

For the vibrational transitions between different electronic states of a molecule there is no strict selection rule as such; however, their intensities are governed by the so called Franck-Condon Principle. If one neglects the rotational term in Eq. (2-1) and the cubic and higher order terms in Eq. (2-3), the wavenumber $\nu_{v',v''}$ resulting from a vibrational transition between an upper state T' and a lower state T'' is given by

$$\nu_{v',v''} = T' - T''$$

$$= (T_e' - T_e'') + [G'(v') - G''(v'')]$$

$$\doteq \nu_e + \omega_e'(v'+\tfrac{1}{2}) - \omega_e' x_e'(v'+\tfrac{1}{2})^2$$

$$- \{\omega_e''(v''+\tfrac{1}{2}) - \omega_e'' x_e''(v''+\tfrac{1}{2})^2\}. \qquad (2\text{-}20)$$

Here ν_e $(= T_e' - T_e'')$ is the system origin which is a constant for a given system. The separation between the terms G(v') and G(v'') of a given electronic state (omitting again the cubic and higher order terms in Eq. (2-3) is given by

$$\Delta G(v+\tfrac{1}{2}) = G(v+1) - G(v)$$

$$= \omega_e - 2\omega_e x_e (v+1)$$

$$= (\omega_e - \omega_e x_e) - 2\omega_e x_e (v+\tfrac{1}{2}). \qquad (2\text{-}21)$$

The second difference of the vibrational terms is given by

$$\Delta^2 G(v+1) = \Delta G(v+3/2) - \Delta G(v+\tfrac{1}{2})$$

$$= -2\omega_e x_e, \qquad (2\text{-}22)$$

which is independent of v.

2.4. Potential Energy Curves

The Schröedinger wave equation for the rotation and vibration of a diatomic molecule has the form

$$(\hbar^2/2\mu)\nabla^2\psi + (E-U)\psi = 0, \qquad (2\text{-}23)$$

where μ is the reduced mass of the molecule and U is the effective potential energy. Obviously the solution of Eq.

(2-23) depends upon the nature of the potential function U. Although the exact form of U for a diatomic molecule is not known, several empirical functions are proposed by various authors for U, based upon different models of the molecule. One of the most commonly-used empirical potential functions is due to Morse (1929) and is given as

$$U(r) = D_e[1 - \exp(-\beta (r-r_e)^2)], \qquad (2-24)$$

where D_e is the dissociation energy referred to the minimum of the potential and $\beta [= (2\pi^2 c\mu/D_e h)^{\frac{1}{2}}\omega_e]$ is a function of the molecular constants. These empirical functions are quite adequate for many of the electronic states of diatomic molecules. However, a more accurate method of computing the potential energy curves from a knowledge of the actual energy levels of the molecule may be essential. Such a method becomes particularly important for highly perturbed states. Once the potential energy is known for an electronic state, its Schröedinger equation can be integrated numerically to yield the wavefunctions of various vibrational and rotational energy levels, which in turn may be used to calculate the intensity factors and r-centroids for various bands of the electronic band system.

One of the most commonly-used numerical methods to construct the internuclear potential energy curves is the Rydberg-Klein-Rees (RKR) method (Rydberg, 1931; Klein, 1932; Rees, 1947). In this method, the auxiliary function of a diatomic molecule in an electronic state is

written as (Klein, 1932)

$$S(U,k) = (1/2\pi^2\mu)^{\frac{1}{2}} \int_0^{I'} [U-E(I,k)]^{\frac{1}{2}} dI. \qquad (2\text{-}25)$$

Here $I = h(v+\frac{1}{2})$, (2-26)

$$k = [J(J+1)h^2]/8\pi^2\mu, \qquad (2\text{-}27)$$

$$E(I,k) = \omega_e(v+\tfrac{1}{2}) - \omega_e x_e (v+\tfrac{1}{2})^2 + \ldots + B_e J(J+1)$$
$$- D_v J^2(J+1)^2 + \ldots - \alpha_e J(J+1)(v+\tfrac{1}{2}) + \ldots, \qquad (2\text{-}28)$$

and $I = I'$ when $U = E$. (2-29)

In terms of the turning points r_{min} and r_{max} of the potential energy curve, S(U,k) can be expressed as

$$S(U,k) = (\tfrac{1}{2}) \int_{r_{min}(U)}^{r_{max}(U)} \int_{V_{eff}}^{U} dr\, dE. \qquad (2\text{-}30)$$

By integrating this equation with respect to r or E and then by differentiating S(U,k) with respect to U and k we obtain the following expressions for the quantities f and g for the nonrotating (k=0) molecule vibrating with energy U:

$$f(U) = \left|\frac{\partial S}{\partial U}\right|_{k=0}$$
$$= (1/2)(r_{max}-r_{min}) = (1/8\pi^2\mu)^{\frac{1}{2}} \int_0^{I'} [U-E(I,k)]^{-\frac{1}{2}} dI, \qquad (2\text{-}31)$$

$$g(U) = \left|\frac{\partial S}{\partial k}\right|_{k=0}$$
$$= (\tfrac{1}{2})[(1/r_{min})-(1/r_{max})] = (1/8\pi^2\mu)^{\frac{1}{2}} \int_0^{I'} \frac{\partial E}{\partial k} [U-E(I,k)]^{-\frac{1}{2}} dI. \qquad (2\text{-}32)$$

Putting $I = h(v+\frac{1}{2}) = hV$ in Eqs. (2-31) and (2-32), we have

$$f(U) = N\int_0^{V'} [U - (\omega_e V - \omega_e x_e V^2 + \ldots)]^{-\frac{1}{2}} dV, \qquad (2\text{-}33)$$

$$g(U) = \frac{1}{N}[B_e \int_0^{V'} \{U - (\omega_e V - \omega_e x_e V^2 + \ldots)\}^{-\frac{1}{2}} dV$$

$$- \alpha_e \int_0^{V'} V\{U - (\omega_e V - \omega_e x_e V^2 + \ldots)\}^{-\frac{1}{2}} dV]. \qquad (2\text{-}34)$$

Here, when U, ω_e, $\omega_e x_e$, B_e, etc. are expressed in cm^{-1}, N is given by $N = (h/8\pi^2\mu c)^{\frac{1}{2}} = r_e B_e^{\frac{1}{2}}$. Then the functions f and g are in units of cm and cm^{-1} respectively. In terms of f and g the turning points r_{min} and r_{max} are given by

$$r_{min} = [(f/g)+f^2]^{\frac{1}{2}} - f,$$

$$r_{max} = [(f/g)+f^2]^{\frac{1}{2}} + f = r_{min} + 2f. \qquad (2\text{-}35)$$

It can be seen from Eqs. (2-35) that the evaluation of the integrals f and g (Eqs. (2-33) and (2-34)) for different values of U corresponding to various energy levels enables one to calculate the turning points r_{min} and r_{max}. Thus the potential energy curves can be mapped by using the actual experimental points.

It must be pointed out, however, that there are certain difficulties in the evaluation of the integrals f and g. At the upper limit of integration where U=E, there is a singularity and hence numerical integration cannot be used

for the entire range. In the literature different methods to overcome this difficulty are suggested by several authors. We summarize in the following paragraphs the method given by Jarmain (1971). This author has shown (Jarmain, 1960) that his 'Modified Klein-Rydberg-Rees Method' produces a potential which is mathematically identical with that of Dunham (1932) if Dunham's small correction terms are neglected. Consequently he named the potential 'Klein-Dunham potential', which is basically the same as the RKR except some variations in approximate numerical methods.

For each energy level, at the upper limit of integrations for f and g, Jarmain (1971) fits a function of the form

$$y = ax^{-p} \qquad (2\text{-}36)$$

for the last three ordinates. In this expression $x = 0$ at $V = V'$. If the size of the subdivision for V is H and the ordinates are labelled y_0, y_1 and y_2 respectively from the top, we have

$$y_1 = aH^{-p} \quad \text{and} \quad y_2 = a(2H)^{-p},$$

and hence

$$a = y_2(2H)^p, \qquad (2\text{-}37)$$

and

$$p = \ln (y_1/y_2)/\ln 2. \qquad (2\text{-}38)$$

The contribution to the f integral from the last two subdivisions of integration is obtained as

$$[h/(8\pi^2\mu)^{\frac{1}{2}}]\int_{-2H}^{0} y_2(2H)^{p_x-p}dx$$

$$= 2Hy_2h/(8\pi^2\mu)^{\frac{1}{2}}(1-p). \qquad (2\text{-}39)$$

However, in the g integral we have $\partial E/\partial k|_{k=0} = (8\pi^2\mu/h^2)B_v$. For integration near the upper limit B_v is assumed to be of the form $B_v = Ax^2 + Bx + C$. The constants A, B and C are evaluated from the points $(2H, B_2)$, (H, B_1) and $(0, B_0)$. The approximate contribution to g(U) at the end points is then given by

$$[(8\pi^2\mu)^{\frac{1}{2}}/h]\int_{-2H}^{0} y_2(2H)^{p_x-p}B_v dx$$

$$= [(8\pi^2\mu)^{\frac{1}{2}}/h]\,2Hy_2\left[\frac{2(B_2-2B_1+B_0)}{3-p} + \frac{(-B_2+4B_1-3B_0)}{2-p} + \frac{B_0}{1-p}\right]. \qquad (2\text{-}40)$$

Obviously, the turning points are functions of energy. In the present numerical solution of the Schrödinger equation, the potential energy is required at equally spaced values of r. This inversion of the function was achieved by using a five point Lagrangian interpolation which was set up to reject any double valued function of r.

In most of the cases the vibrational intervals are not observed experimentally up to the dissociation limit. If the levels are observed up to a particular level v, say v_{max}, the calculation of the vibrational wave functions up to v_{max} requires that extensions should be added to each side

of the potential to a considerably higher energy. Here these extensions on the left (repulsive part) and right (attractive part) are made by fitting the Morse function (Eq. 2-24).

On the repulsive side, the Morse function is fitted to the three uppermost points on the Klein-Dunham potential in its inverted form. Corresponding to the three points, three values of the parameter β in the Morse function are obtained by using the experimental values of D_e and r_e. Finally, the Morse function with the average value of β replaces the segment of the Klein-Dunham potential encompassing the three points.

As the limit on the attractive side of the potential is not very sensitive to r, it is possible to make a satisfactory fit of the Morse function by means of a semi-iterative method, by using just one point and the slope at that point on the Klein-Dunham curve. At first β is calculated from the point and slope from the relation

$$\beta = (\tfrac{1}{2})\frac{U'(r)}{[D_e U(\infty)]^{\frac{1}{2}} - U(r)}, \qquad (2\text{-}41)$$

by using the experimental value of D_e. Then, an effective value of r_e is obtained by using that point and the expression

$$r_e = \frac{\ln[1-\{U(r)/D_e\}^{\frac{1}{2}}]}{\beta} + r. \qquad (2\text{-}42)$$

With the extensions on both sides the potential curve is complete.

The accuracy of the calculated vibrational wave-functions, in the present work, is tested by the orthogonality test or "noise factor" given by (Jarmain, 1951)

$$\text{Noise factor} = \max_{v_1 \neq v_2} [\int \psi_{v_1} \psi_{v_2} dr]^2. \qquad (2\text{-}43)$$

2.5. Franck-Condon Factors and r-Centroids

The intensity of an emission band from a unit volume of a gas containing $N_{v'}$ molecules in the vibrational state v' is expressed as (Herzberg, 1950)

$$I_{v'v''} = N_{v'} h\nu_{v'v''} A_{v'v''}, \qquad (2\text{-}44)$$

where the Einstein coefficient for emission $A_{v'v''}$ is given by (neglecting rotation)

$$A_{v'v''} = (64\pi^4/3hc^3)\nu^3_{v'v''} p_{v'v''}. \qquad (2\text{-}45)$$

Here the relative vibrational transition probability $p_{v'v''}$ is represented by

$$p_{v'v''} = \bar{R}_e^2(\bar{r}_{v'v''}) \left| \int \psi_{v'} \psi_{v''} dr \right|^2$$

$$= \bar{R}_e^2(\bar{r}_{v'v''}) q_{v'v''}, \qquad (2\text{-}46)$$

where the electronic transition moment $\bar{R}_e^2(\bar{r}_{v'v''})$ is a slowly varying function of r and the Franck-Condon factor $q_{v'v''}$ is

given by

$$q_{v'v''} = \left| \int \psi_{v'} \psi_{v''} \, dr \right|^2 . \qquad (2\text{-}47)$$

The quantity $\bar{r}_{v'v''}$, defined by the expression

$$\bar{r}_{v'v''} = \int \psi_{v'} r \psi_{v''} \, dr / \int \psi_{v'} \psi_{v''} \, dr , \qquad (2\text{-}48)$$

is known as r-centroid which represents an average value of the internuclear separation for the transition between the states v' and v''.

CHAPTER 3

APPARATUS AND EXPERIMENTAL TECHNIQUE

The emission spectra of the free radicals SeO and SbO were excited in electrodeless discharge tubes by means of a microwave generator and were photographed or recorded with two optical spectrographs and an infrared spectrometer. In this chapter, a description of the apparatus and the experimental procedure is presented. Also given is a brief account of the mechanism of the electrical discharges.

3.1. Apparatus for the Excitation of the Spectra of SeO and SbO

The emission spectrum of SeO was excited in an electrodeless quartz discharge tube 45 cm long and 2.5 cm in diameter containing 20-30 gm of selenium dioxide (SeO_2) powder. The spectrum of SbO was also excited in a similar tube containing 30-40 gm of antimony trioxide (Sb_2O_3) powder. These chemicals (SeO_2 and Sb_2O_3) were supplied by the British Drug House Ltd., England. The discharge tube which was connected through a series of traps to an evacuation system is schematically shown in Fig. 1. The spiral glass tubing T_1 and two liquid nitrogen traps T_2 (shown one only in Fig. 1) prevented the contamination of the pumping system which consists of a Franklin/rotary pump and an oil diffusion pump. Condensation of SeO_2 vapour on the window W of the discharge

Electric

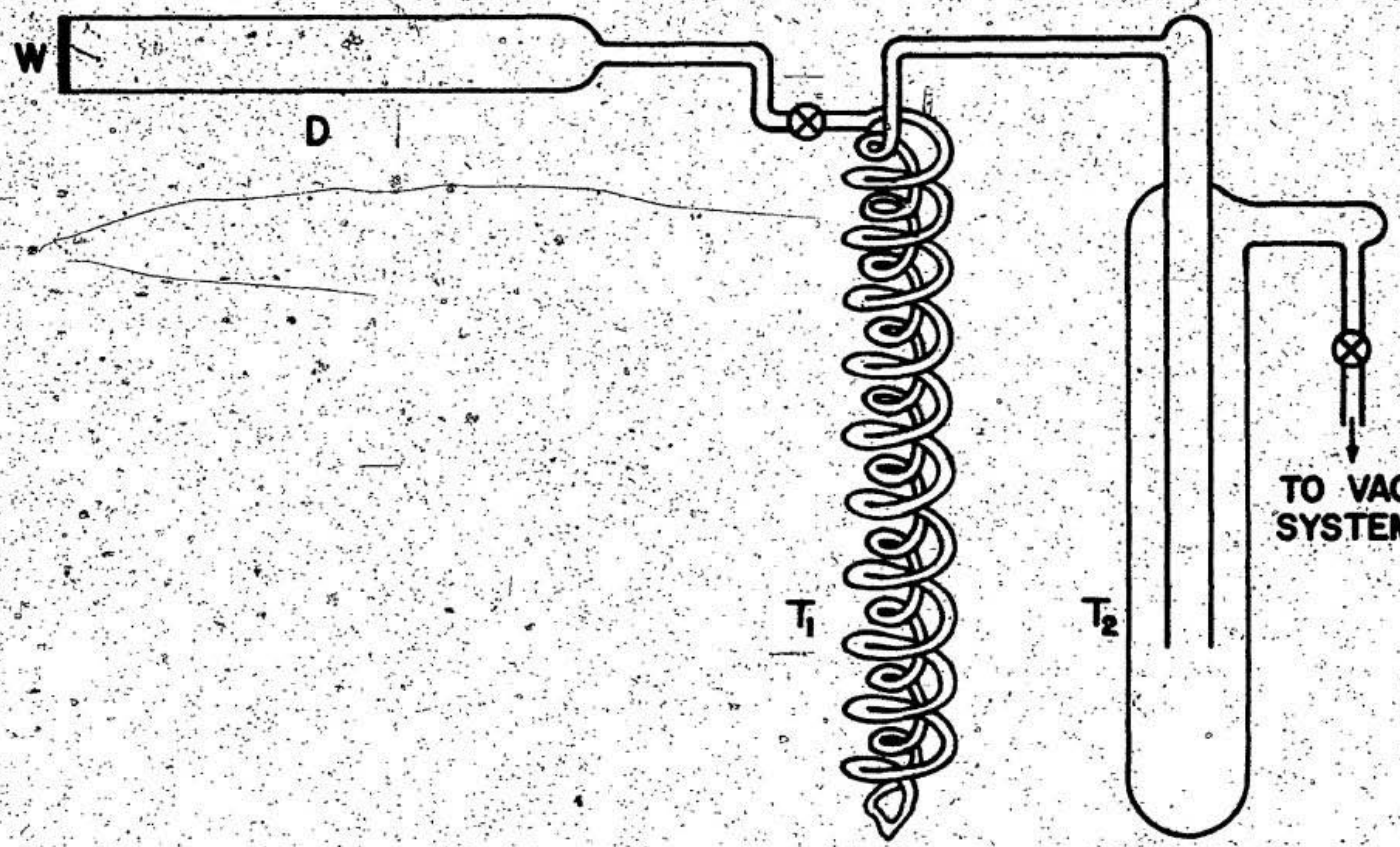

Fig. 1. Discharge tube and the accompanying accessories: D-quartz discharge tube, W-quartz window, T_1-spiral glass tubing, T_2-liquid nitrogen trap.

tube was prevented by an electrical heater 4 cm in diameter and 7.5 cm long.

The spectra of both SeO and SbO were produced by irradiating the discharge tube with radiation from a Raytheon Model PGM-100 microwave generator which consists of a fixed-frequency, air-cooled, cw-type magnetron oscillator. The magnetron has a full-wave rectified power supply unit with a magnetic regulator which keeps the average anode current constant. Thus, the variations in the magnetron impedance with load and life are overcome and a constant power output is achieved. A cross-sectional view of the experimental arrangement of the microwave generator is shown in Fig. 2. The generator is fitted with a wave guide G which is connected to a horn H. The metallic reflector R focuses the microwave radiation on the discharge tube D. The filter unit F provides microwave power output with a modulation of about 10% in the detected R.F. envelope. The model PGM-100 generator, with its filter in, has an output power supply in the range 250-800 W at a frequency of 2450 ± 25 MHz. The wavelength of the microwave radiation in the waveguide is 14.8 cm. To overcome the hazards of the microwave radiation, the horn, the discharge tube and the reflector were shielded in a rectangular radiation cage C which consists of a metallic frame 26" x 22" x 20" enclosed by a copper screen of mesh size 2.0 mm x 1.5 mm. A photograph of the microwave generator, radiation cage, vacuum

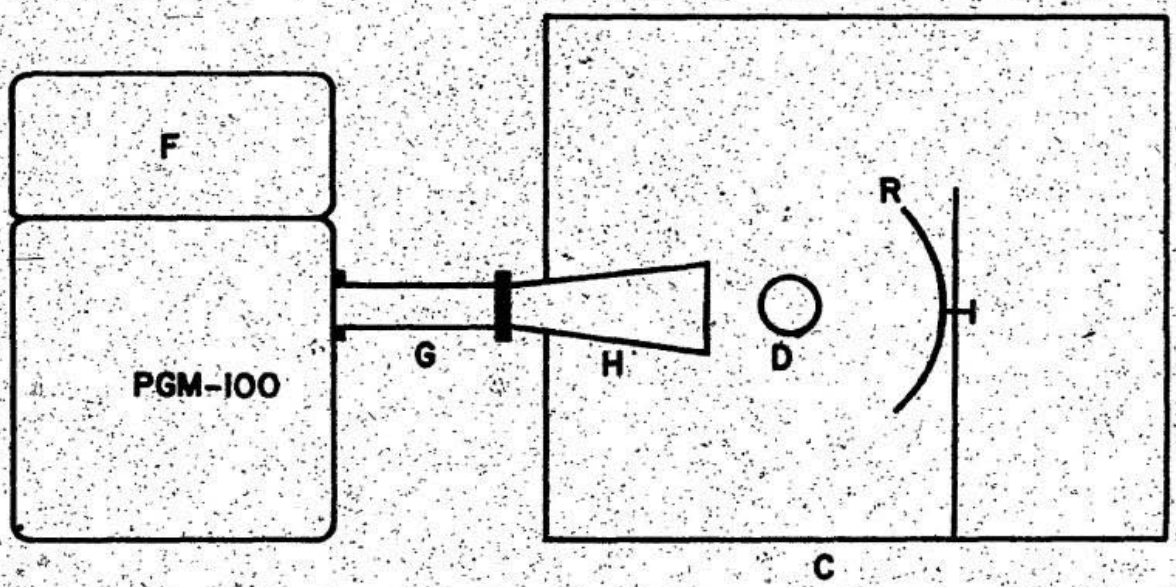

Fig. 2. A cross-sectional view of the experimental arrangement: PGM-100-microwave generator, F-filter unit, G-rectangular waveguide, H-horn, D-discharge tube, R-metallic reflector, C-microwave radiation cage.

system and other accessories is shown in Fig. 3.

3.2. Mechanism of Electrical Discharges

In an electrical discharge tube, free electrons are first accelerated by an electric field produced by a device such as a microwave power generator. The translational kinetic energy of these free electrons is then transformed into the internal energy of the atoms and molecules in the discharge tube due to collisions. Consequently, the atoms and molecules are excited to their higher energy states. For molecules this internal energy could be electronic, vibrational and rotational in nature whereas it is only electronic for atoms. Higher energy states of atoms and molecules are inherently unstable and consequently, the excited atoms and molecules give up their energy by dropping into lower states with the emission of electromagnetic radiation of energy $h\nu$ corresponding to the energy difference between the upper and lower states. As long as the discharge tube is subjected to the electric field, the process of collisions between the electrons and the atoms and/or molecules is continued and the emission of radiation is maintained.

One of the important methods of obtaining emission spectra of free radicals (i.e., species having a short lifetime in gaseous phase) is by way of electrical discharges. In fact, the physical existence of diatomic free radicals such as CH, NH, OH, C_2, He_2, etc., as well as of the

Figure 3

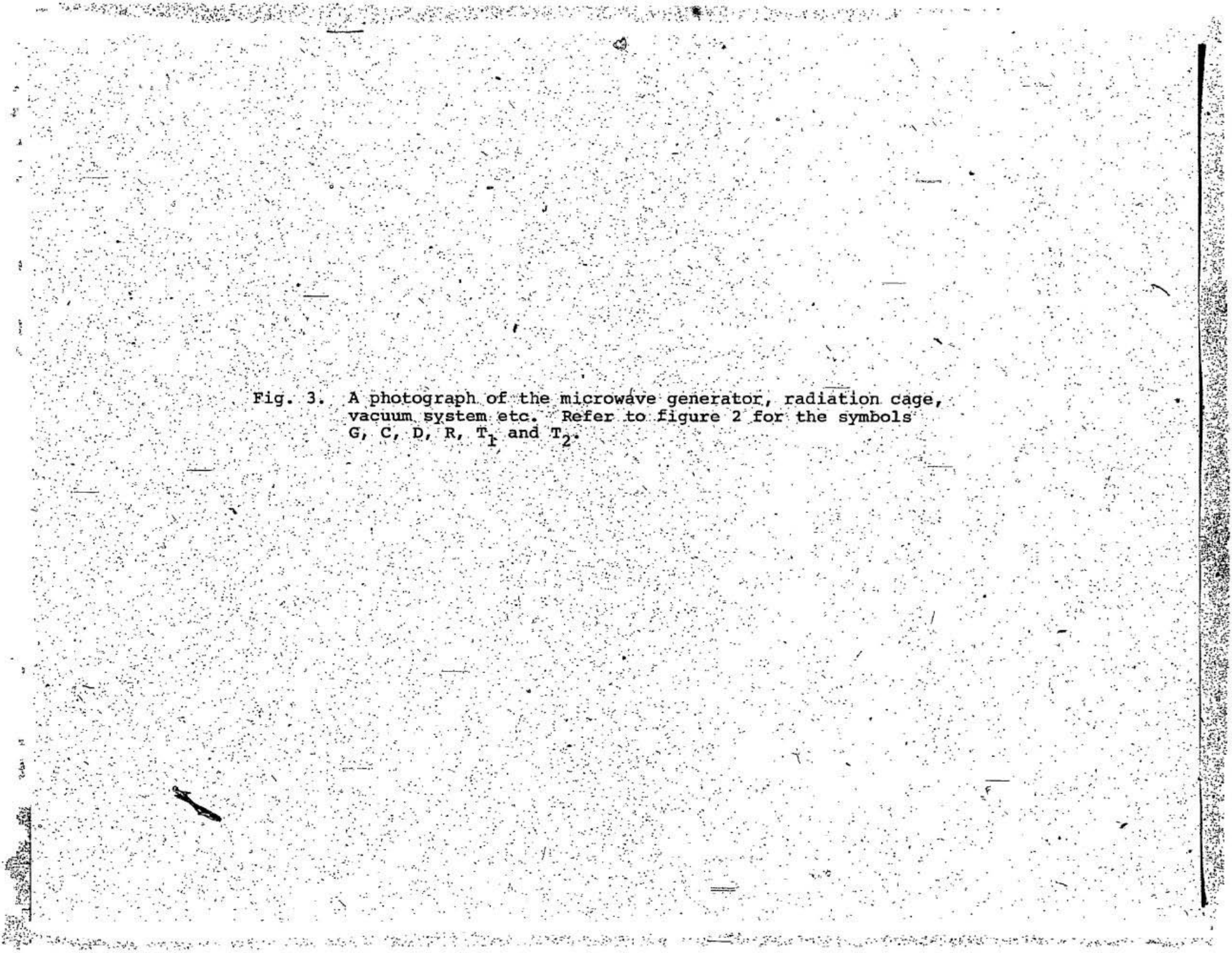

Fig. 3. A photograph of the microwave generator, radiation cage, vacuum system etc. Refer to figure 2 for the symbols G, C, D, R, T_1 and T_2.

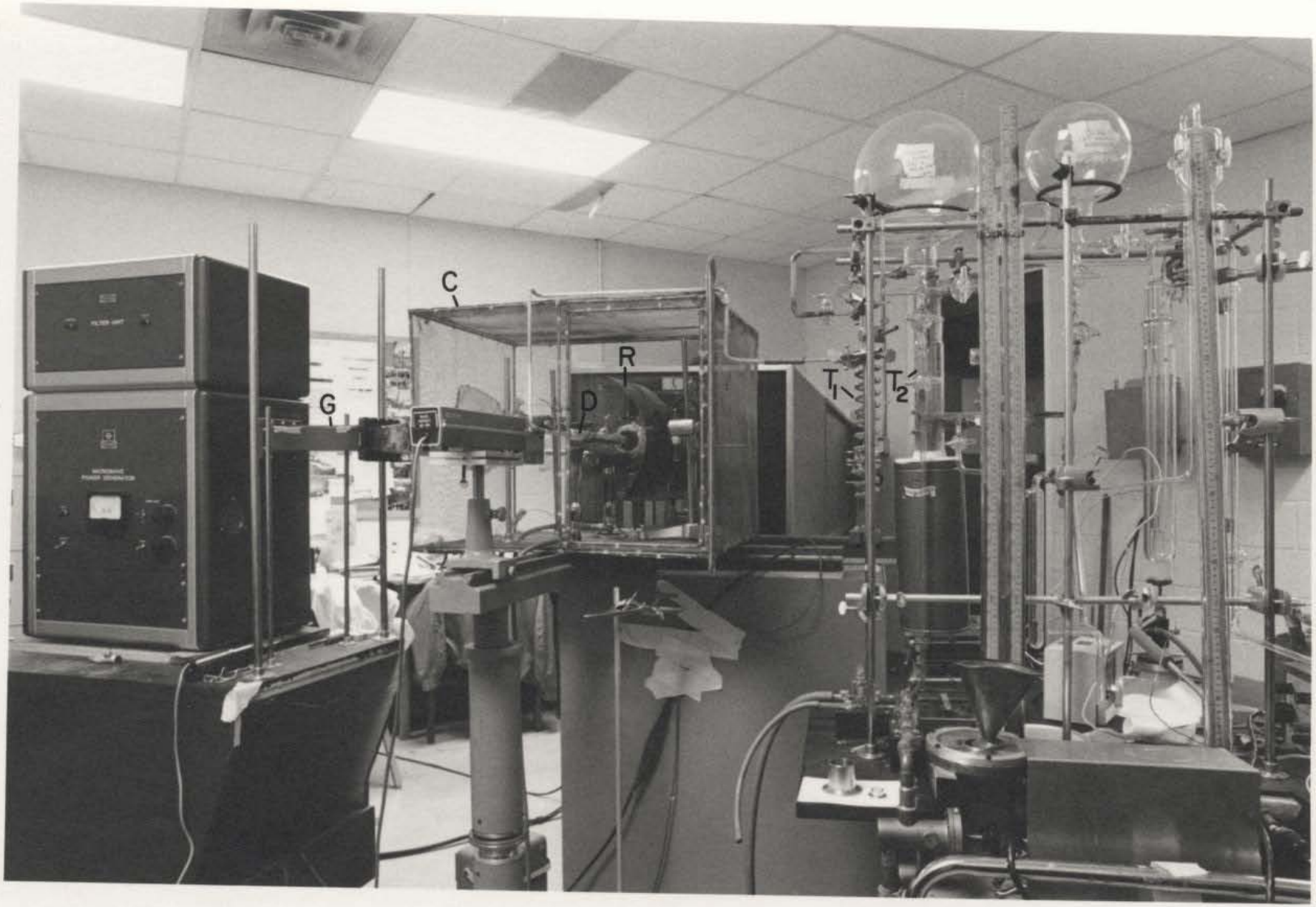
C
R
G
D
T1
T2

molecular ions N_2^+, CO^+, CO_2^+, etc., has been firmly established as a result of the identification of their spectra (cf. Herzberg, 1971). Molecules such as SeO and SbO which are the subject of the present investigation belong to this type of free radical. The characteristic emission spectrum of SeO or SbO obtained under continuous evacuation of the discharge tube shows clearly that SeO_2 or Sb_2O_3 in the discharge tube gives rise to SeO or SbO, oxygen and some free selenium or free antimony. The presence of atomic lines of oxygen and selenium or antimony in the recorded emission spectra shows the existence of atomic oxygen and selenium or antimony in the discharge. No known emission bands of O_2 and Se_2 or Sb_2 have been observed with the present method of excitation.

3.3. Spectrographs and Spectrometer

A very large part of the present work has been carried out with a 2 m Bausch and Lomb dual grating spectrograph and a 3.4 m Jarrell-Ash Ebert grating spectrograph. The a-X system of the SeO molecule which occurs in the near infrared region 6500-5500 cm^{-1} has been recorded with a Perkin-Elmer Model 112G single-beam double-pass grating spectrometer. These three instruments are described briefly in this section.

(i) The 2 m Bausch and Lomb Dual Grating Spectrograph

A schematic diagram of the optical arrangement of the spectrograph is shown in Fig. 4. Light from a source enters the spectrograph through the variable slit VS and, after being reflected by a plane mirror M, is incident on the spherical mirror SM having a numerical aperture f/15.5. It is then dispersed by the plane grating G_1 or G_2 which can be set into position by means of a rotatable turret T, and is again incident on the spherical mirror SM which then focuses it on the photographic plate P. The plate holder can take one 10" x 4" or two 10" x 2" photographic plates. Gratings G_1 and G_2 have a ruled width of 128 mm and a groove length of 102 mm each and have 1200 and 600 grooves/mm respectively. The blaze wavelengths of these gratings in the first order are 1.0 μm and 2.5 μm respectively.

(ii) The 3.4 m Jarrell-Ash Ebert Grating Spectrograph

The optical lay out of this spectrograph is shown in Fig. 5. Light entering through the slit S passes over the plane grating G and is incident on the upper part of the large concave mirror M having diameter of 16", a radius of curvature of 21' 10" and a numerical aperture of f/35. The mirror M renders the light parallel and reflects it back to the grating. The light dispersed by the grating consists of parallel group of rays for each wavelength, the separate groups at diverging angles in accordance with the dispersion

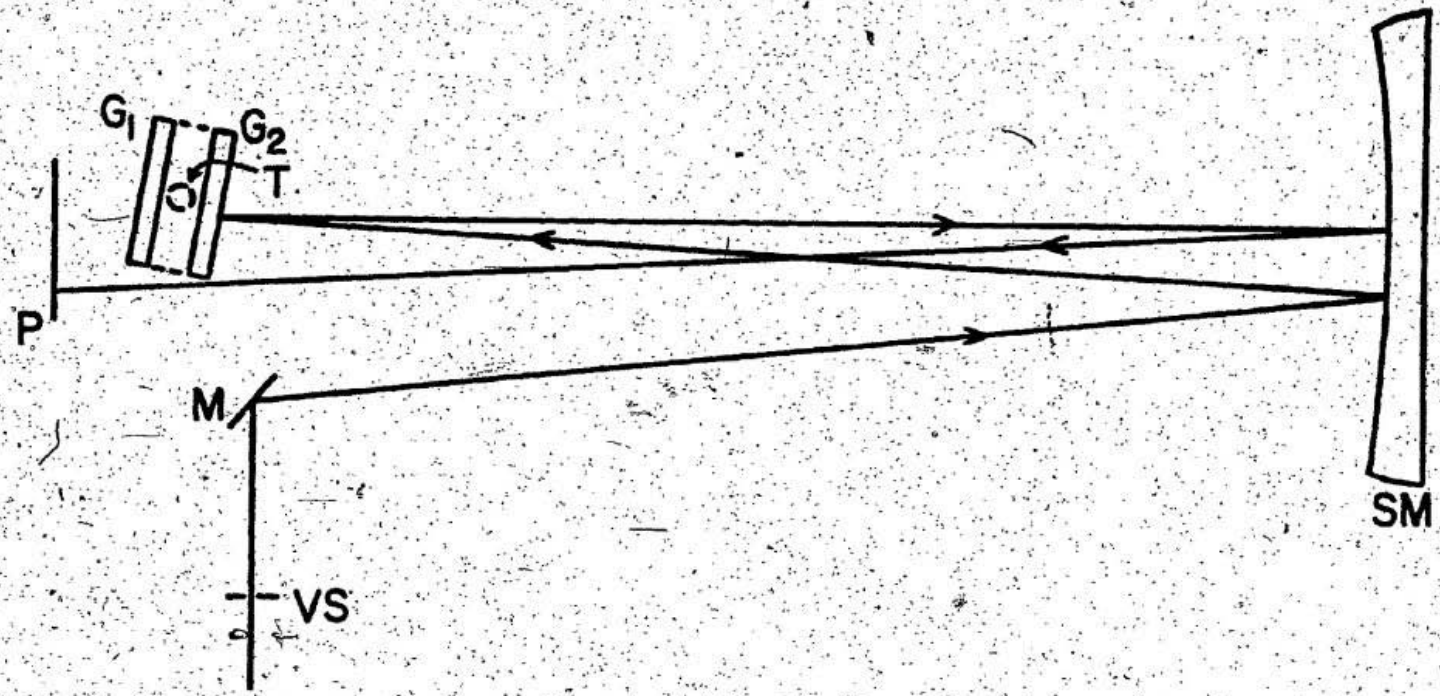

Fig. 4. A schematic diagram of the optical arrangement of the 2 m Bausch and Lomb dual grating spectrograph. VS:Variable Slit, M:Plane Mirror, SM:Spherical Mirror, P:Photographic Plate, G_1 and G_2:Two gratings with 1200 grooves/mm and 600 grooves/mm, T:turret axis.

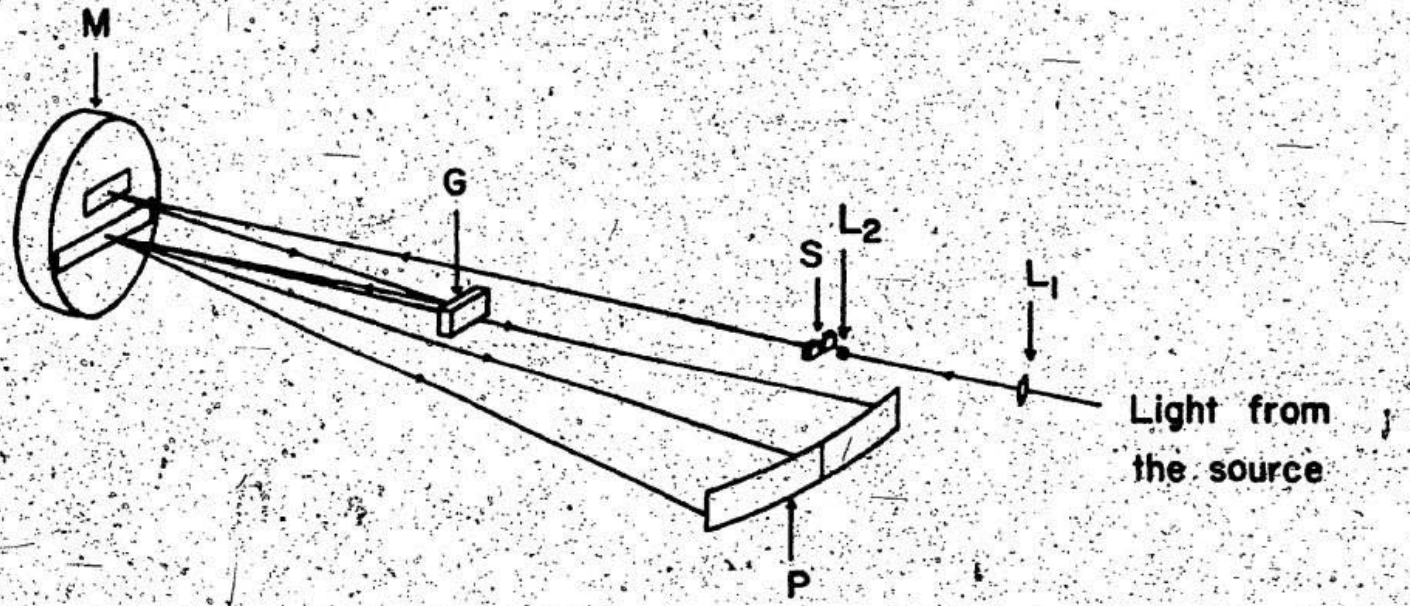

Fig. 5. Optical layout of the 3.4 m Jarrell-Ash Ebert grating spectrograph. L_1 and L_2:Collimating Quartz Lenses, S:Adjustable Slit, M:Concave Mirror, G:Plane Grating, P:Plate Holder.

of the grating. These rays strike the lower part of the mirror which now focuses them on the photographic plate P. Just as in the 2 m Bausch and Lomb spectrograph, the mounting is achromatic and thus makes it possible to change the wavelength range by merely rotating the grating. The spectrograph can be equipped with either an MIT echelle grating blazed at 57 000 Å and having 7 620 grooves/inch or a Bausch and Lomb special plane grating blazed at 14 000 Å and having 1 200 grooves/mm. Each of these gratings has a ruled width of 186 mm and a groove length of 63 mm. The plate holder takes either one 20" x 2" or two 10" x 2" photographic plates.

(iii) The Perkin-Elmer Model 112 G Grating Spectrometer

A schematic representation of the optical arrangement of this spectrometer is shown in Fig. 6. Light from the discharge tube enters the slit S_1 of the spectrometer which is a single-beam double-pass instrument fitted with a Bausch and Lomb 300 grooves/mm plate grating G blazed at 3.0 μm. The detector D is a PbS cell mounted on a ceramic or brass support which serves as a heat sink and was operated at room temperature. The original Perkin-Elmer 13 Hz mechanical chopper was replaced by an American Time Products model L-40 400 Hz tuning fork chopper which is small enough to fit between mirrors M_2 and M_3 (Fig. 6) and chops the radiation after it is once dispersed by the grating. A schematic

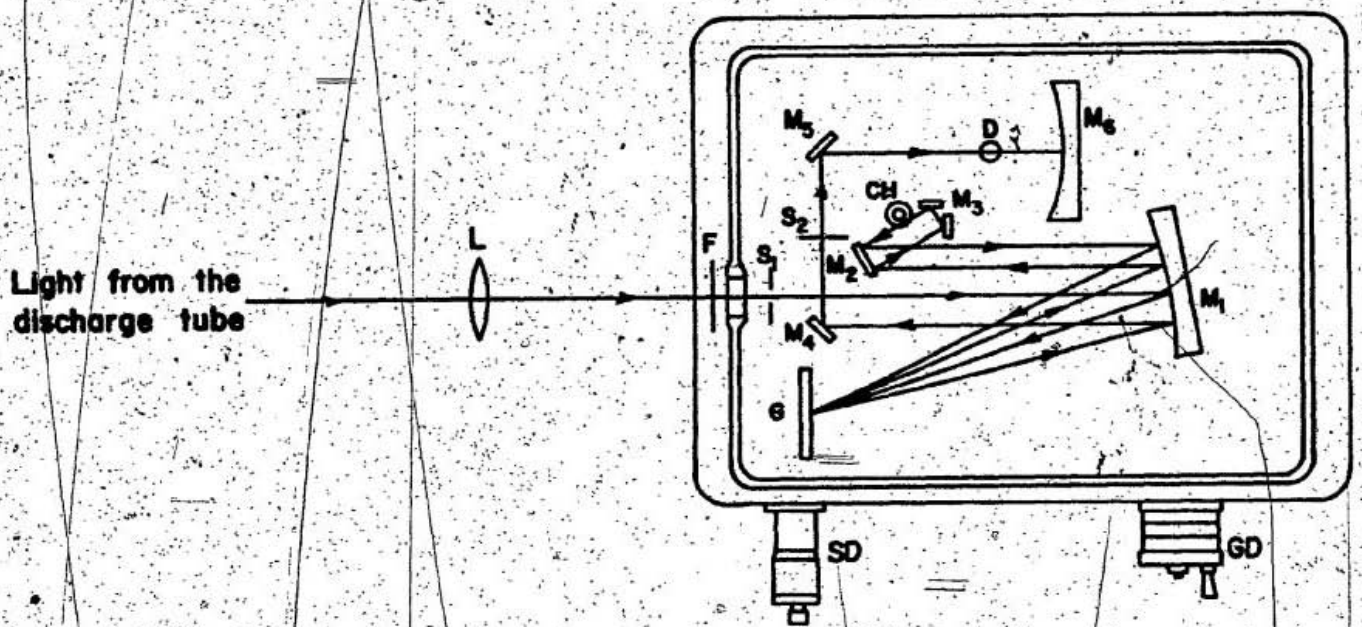

Fig. 6. Optical layout of the Perkin-Elmer Model 112 G spectrometer. L-Focusing Lens, F-Filter, S_1-Entrance Slit, SD-Slit Drive, M-Off-axis Paraboloid Mirror, M_2, M_3, M_4, M_5-Plane Mirrors, CH-400 Hz Tuning Fork Chopper, S_2-Exit Slit, M_6-Spherical Mirror, D-Lead Sulphide Detector, G-Plane Grating, GD-Grating Drive.

diagram of the detection-amplification system of the spectrometer used in the present work is shown in Fig. 7 (cf. Prasad, 1976). The signal is amplified by Brower Laboratories model 261 preamplifier and model 131 lock-in voltmeter coupled with their model 500 frequency programmer. The reference signal is supplied by the power supply unit for the tuning fork and the phasing adjustment is contained in the lock-in voltmeter. The energy received by the detector is converted into an electrical signal which is proportional to the intensity. The spectrum was recorded on a Leeds and Northrup model S 60 000 type G strip chart recorder.

3.4. Experimental Procedure

An empty discharge tube was first aligned with respect to the slit and the optic axis of the spectrograph or spectrometer with the help of a He-Ne laser. Requisite amount of SeO_2 or Sb_2O_3 powder was spread uniformly in the tube which was then connected to the evacuation system. When the vacuum obtained was of the order of 10^{-6} torr, the discharge tube was heated in its central portion with a bunsen burner. It was then irradiated with microwave radiation from the generator. The position of the metallic reflector with respect to the discharge tube and the waveguide (Fig. 2) was adjusted so that the standing wave ratio (VSWR) in the waveguide be minimum when the microwave radiation was on (cf. Ali, 1969). A tesla coil was used to

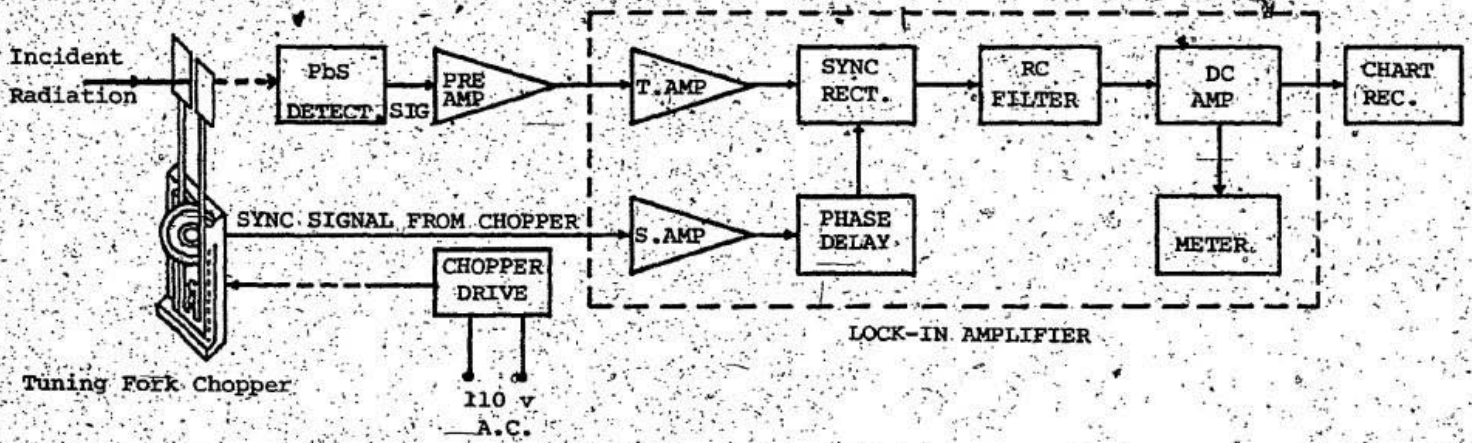

Fig. 7. Block diagram of the signal detection-amplification system with a tuning fork chopper.

start the discharge initially.

It was found necessary that a small portion in the center of the discharge tube should be cleared of the SeO_2 powder by heating it, before the SeO discharge was excited. Once the discharge started in the center, it extended slowly to the entire tube. The discharge tube was continuously evacuated during the experiment although it was found desirable to switch off the oil diffusion pump in the evacuation system a few minutes after the discharge was started.

Similar procedure was adopted for the excitation of SbO as well. The only difference was that for the excitation of SeO the discharge tube was heated only at the beginning, whereas for SbO a constant heating was required. In addition, a small quantity of argon as a carrier gas in the discharge tube was found to be helpful in the excitation of SbO.

The spectra in different optical regions were photographed with Kodak SWR, 103a-O, I-N, and I-Z plates. The I-N plates were hypersensitized by bathing them in cold water at 40° F and methyl alcohol for durations of 3 min and 2 min respectively. The I-Z plates were hypersensitized similarly by using a solution of two parts of 28% ammonia diluted with 100 parts of cold water and then methyl alcohol. Kodak SWR plates were developed in a 1:1 diluted Kodak D-19 developer for 2 min and fixed in Kodak fixer for 4 min.

Kodak 103a-O, I-N and I-Z plates were developed in undiluted Kodak D-19 developer for 4 min and fixed in Kodak fixer for 10 to 15 min.

Spectral lines from iron and copper dc arcs were used as standards for the wavelength calibration in the optical region (NBS monograph 108 and atlas of copper lines, Adam Hilger Ltd.). The near infrared region was calibrated with the emission lines of mercury (Humphreys, 1953; Plyler et al., 1955; Zaidel, 1970) and absorption peaks of atmospheric water vapour (I.U.P.A.C. Tables of Wavenumbers 1961).

3.5. Measurement of Spectra

All the spectra in the photographic region were measured on a linear comparator model M1205C supplied by Gaertner Optical Company, Chicago, U.S.A. The least count of this comparator is 0.001 mm. However, readings can be estimated correct to 0.0001 mm. Once the positions of the standard iron or copper lines and the bandheads or rotational lines were measured, a polynomial

$$\lambda_{air} = a_0 + a_1 d + a_2 d^2 + \ldots \qquad (3\text{-}1)$$

was fitted by the least squares method using the d and λ values of the standard lines to find the constants a_0, a_1, a_2, . . . etc. The accuracy of these constants was tested by recalculating the wavelengths of the same lines from the fitted polynomial and the best fit was accepted. The wavelengths of the bandheads or rotational lines were calculated

from the equation (3-1). Edlen's formula (1953) for the refractive index, n, of air, i.e.,

$$n = 1 + 6432.8 \times 10^{-8} + \frac{2949810}{146 \times 10^{8} - \nu^2} + \frac{25540}{41 \times 10^{8} - \nu^2}, \qquad (3\text{-}2)$$

$$\text{where} \quad \nu(\text{cm}^{-1}) = \frac{10^8}{n\lambda_{air}(\text{Å})}$$

was used to convert the wavelengths in air, λ_{air}, to vacuum wavenumbers ν. An iterative method was employed to do the computation on an IBM 370 computer and the iteration was continued until the absolute difference between the successive values of ν was $\leq 10^{-10}$ cm^{-1}.

The procedure adopted for the determination of the wavenumbers ν of the bandheads of SeO in the near infrared region is as follows: The distances of the standard emission and absorption peaks were measured from a reference line on the recorded charts. The wavenumbers ν of these lines were expressed as a polynomial function of d in the form

$$\nu = A + Bd + Cd^2 + Dd^3 + \ldots \qquad (3\text{-}3)$$

The constants A, B, C, D, . . . were first obtained by a non-linear least squares fit of the above polynomial. A fifth order fit was found to be satisfactory. These constants were used in turn to obtain wavenumbers against positions at intervals of 1 cm by means of a computer program. A calibration chart giving the wavenumbers at these intervals was then drawn. Finally, the wavenumbers of the bandheads were inferred by making use of this calibration chart.

CHAPTER 4

ROTATIONAL ANALYSIS OF THE b-X SYSTEM OF SeO

4.1. Introduction

In the analogous molecules O_2, SO, S_2, SeO, . . . etc., the lowest electron configuration consists of a number of closed shells and two electrons in a π shell which give rise to the molecular states $X^3\Sigma^-$, $a^1\Delta$, and $b^1\Sigma^+$, all of which are even for homonuclear molecules. For O_2, the $b^1\Sigma^+ - X^3\Sigma^-$ transition has been observed in absorption (Babcock & Herzberg, 1948) and for SO, this transition was observed in emission (Colin, 1968). For S_2, although several allowed electronic transitions involving all the three states arising from its lowest electron configuration are observed (Barrow & du Parcq, 1965; Barrow & du Parcq, 1968; Maeder & Miescher, 1948; Barrow, du Parcq & Ricks, 1969), the corresponding forbidden transition $b^1\Sigma^+ - X^3\Sigma^-$ has not yet been observed. The $b^1\Sigma^+ - X^3\Sigma^-$ system of SeO was first observed in emission in the spectral region 9490 - 10 780 Å by Azam and Reddy (1973) who have reported the vibrational analysis of this system. In this chapter a rotational analysis of the b - X system of SeO will be presented. The present analysis shows that this band system arises from the $bO^+ - XO^+$, 1 transition (where X is a case (c) $^3\Sigma^-$ state). The

rotational constants of the 0 - 0 bands of the subsystems $b0^+ - X_1 0^+$ and $b0^+ - X_2 1$ are determined. The observed isotope shifts of the rotational lines of $^{78}Se^{16}O$ from those of $^{80}Se^{16}O$ are found to be in agreement with the calculated values. Klein-Dunham potential energy curves for $b0^+$ and $X_1 0^+$ states are constructed from the observed data and are given in Chapter 6. Franck-Condon factors and r-centroids are calculated for the $b0^+ - X_1 0^+$ subsystem and the intensity distribution in the rotational structure of the 0 - 0 bands is briefly discussed.

Attempts to photograph the band system with the 3.4 m Jarrell-Ash Ebert spectrograph in the fifth order of the grating blazed at 57 000 Å, were not successful owing to inherent weakness of the bands. Finally, the spectra were photographed on the 2 m littrow type Bausch and Lomb spectrograph both in the first order of a 1200 grooves/mm plane reflectance grating blazed at 10 000 Å and in the third order of a 600 grooves/mm plane grating blazed at 25 000 Å. These gratings gave the reciprocal dispersions of 2.93 cm^{-1}/mm and 0.87 cm^{-1}/mm at 10 450 Å, respectively. The slit width of the spectrograph was maintained at 50 um. Hypersensitized Kodak I-Z plates were used to photograph the spectra. Exposure times varied from 10 hours for the first-order spectra to 22 hours for the third order spectra. Spectral lines from a dc iron arc, photographed in the third and fifth orders, were used as wavelength standards. The measurements of the sharp rotational lines were estimated to be accurate to about 0.02 cm^{-1};

however, this accuracy was not obtained for blended lines.

4.2. A $^3\Sigma^-$ Electronic State in Hund's case (b) and case (c)

A $^3\Sigma^-$ state can be described by either Hund's case (b) or Hund's case (c) depending upon the strength of the coupling of the electronic orbital angular momentum $\vec{L}$ and the total electron spin $\vec{S}$ with the internuclear axis. The splitting in a $^3\Sigma$ state has been discussed by several authors (Kramers, 1929; Van Vleck, 1929; Hebb, 1936; Schlapp, 1937; and Kovacs, 1962). A multiplet structure of the ordinary kind, due to magnetic interaction between the total spin $\vec{S}$ (S=1 for a triplet state) and the electronic orbital angular momentum along the internuclear axis $\vec{\Lambda}$, does not arise in Σ states obviously because the latter is zero for them. The main contributions to the splitting in a $^3\Sigma$ state are:

(i) The spin-spin interaction of the uncompensated electrons which is equivalent to an interaction between $\vec{S}$ and the figure axis;

(ii) the interaction between the uncompensated spins and the magnetic field set up by the rotation of the molecule as a whole;

(iii) without rotation the precession of $\vec{L}$ for a Σ state is perpendicular to the internuclear axis. But in a rotating molecule this precession is no longer uniform (rotational distortion) and on the average a non-zero magnetic moment

results along $\vec{N}$ which couples with $\vec{S}$ in the same way as $\vec{N}$.

Taking the above three contributions into account, the triplet components of a $^3\Sigma$ state in Hund's case (b) coupling are given by (Schlapp, 1937; Herzberg, 1950; Townes & Schawlow, 1955)

$$F_1(N) = B_v N(N+1) - D_v N^2(N+1)^2 + (2N+3)\, B_v - \lambda_v - \{(2N+3)^2 B_v^2 + \lambda_v^2 - 2\lambda_v B_v\}^{\frac{1}{2}} + \gamma_v(N+1), \tag{4-1a}$$

$$F_2(N) = B_v N(N+1) - D_v N^2(N+1)^2, \tag{4-1b}$$

$$F_3(N) = B_v N(N+1) - D_v N^2(N+1)^2 - (2N-1)\, B_v - \lambda_v + \{(2N-1)^2 B_v^2 + \lambda_v^2 - 2\lambda_v B_v\}^{\frac{1}{2}} - \gamma_v N. \tag{4-1c}$$

In these expressions F_1, F_2, and F_3 refer to the levels with $J = N+1$, $J = N$, and $J = N-1$ respectively, and λ and γ are respectively the spin-spin and spin-rotation interaction constants. Normally, terms involving λ in the above equations arise from the first contribution and also from the L uncoupling. The terms involving γ are due to contributions (ii) and (iii), the third one being dominant.

In the case of light molecules the values of λ in the ground state $^3\Sigma^-$ are small (cf. Barrow & Yee, 1974). However, as atomic number increases, λ begins to assume large values (more precisely, $\lambda_v >> B_v$) so that for heavier molecules the coupling in the $^3\Sigma^-$ state approximates to Hund's case (c).

Therefore, as the spin-rotation constant γ remains always small, the F_1 levels separate to form the levels of an $\Omega = 0^+$ state, while the F_2 and F_3 levels converge to form the levels of an $\Omega = 1$ state. More specifically, the F_2 and F_3 levels correlate with $\Omega = 1^-$ and 1^+ respectively. The term values of the rotational levels of a case (c) $^3\Sigma^-$ state are represented by the following expressions:

For $\Omega = 0^+$, $\quad F_1(J) = B_v J(J+1) - D_v J^2(J+1)^2$. (4-2a)

For $\Omega = 1$, $\quad F_2, F_3(J) = B_v J(J+1) - D_v J^2(J+1)^2 + 2\lambda_v$. (4-2b)

A schematic energy level diagram showing a transition of a $^3\Sigma^-$ state from Hund's case (b) to case (c) is given in Fig. 8. It is to be noted that in Schlapp's (1937) notation the minimum of the F_2 levels of a case (b) $^3\Sigma$ state is taken as zero whereas in case (c) notation, as written here, the minimum of the $\Omega = 0^+$ levels is taken as zero. For the state $\Omega = 1$ a doubling occurs which is similar to the Λ-type doubling in Hund's case (a) and is called Ω-type doubling. In case (c) limits the Ω-type doubling in the 1 component appears as a difference in the effective B values,

$$q_v = B_v(1^+) - B_v(1^-) \qquad (4\text{-}3)$$

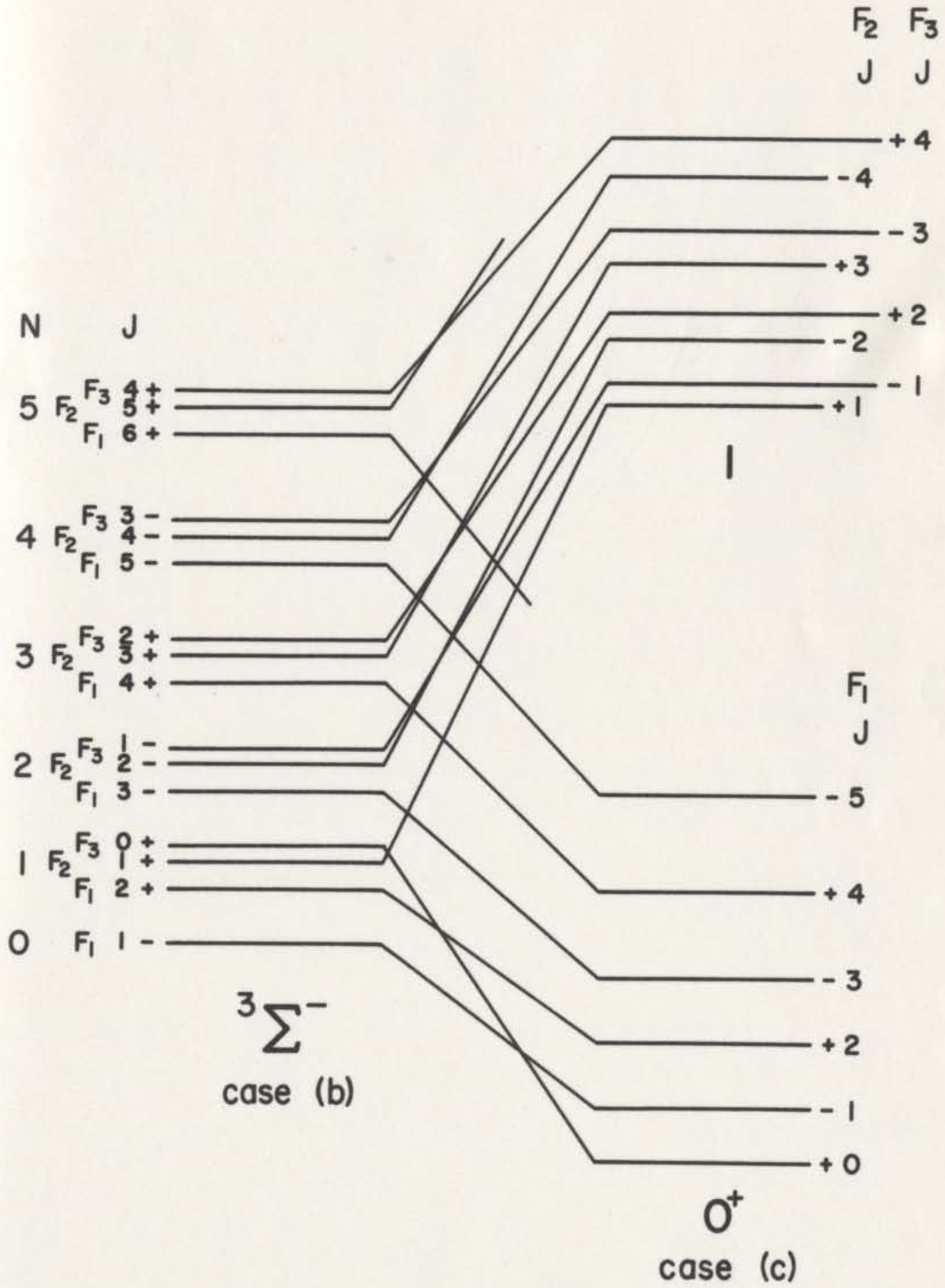

Fig. 8. A schematic energy level diagram showing a transition of a $^3\Sigma^-$ state from Hund's case (b) to case (c).

4.3. Results

A. Vibrational Structure

The vibrational structure of the intense bands of the $\Delta v = 0$ sequence of the $bO^+ - XO^+, 1$ system of SeO is shown in Fig. 9. The new measurements of the bandheads of both $\Delta v = 0$ and $+1$ sequences agree essentially with the data reported earlier by Azam and Reddy (1973). The bands which have been assigned by them to the subsystems $b^1\Sigma^+ - X^3\Sigma^-(F_1)$ and $b^1\Sigma^+ - X^3\Sigma^-(F_2,F_3)$ are now designated as the R heads of $bO^+ - XO^+$ and $bO^+ - X1$, respectively. Particularly the bands with heads at 9518.4, 9439.1, 9356.8 and 9276.0 cm^{-1} (the first two of which are shown in Fig. 9) which have been tentatively assigned by them to the a - X system are now assigned as the Q heads of $bO^+ - X1$ (Barrow & Lemanczyk, 1975). The vacuum wavenumbers, vibrational quantum numbers and the R and Q head assignments of the bands of the $bO^+ - XO^+, 1$ system of ^{80}SeO are given in Table 1. The vibrational constants of states b and X are given in Table 3.

B. Rotational Structure

The rotational structure of the 0 - 0 bands of the b - X system of SeO are shown in Fig. 10. The line-spacings in the structure and the number of branches in the bands indicate that they arise from $\Omega = 0^+ - \Omega = 0^+, 1$ transition. The branches resulting from the electric dipole selection rules $\Delta\Omega = 0, \pm1$; $\Delta J = 0, \pm1$ $(J=0 \not\leftrightarrow J=0)$; and $+ \leftrightarrow +$ $-$ for a

Figure 9

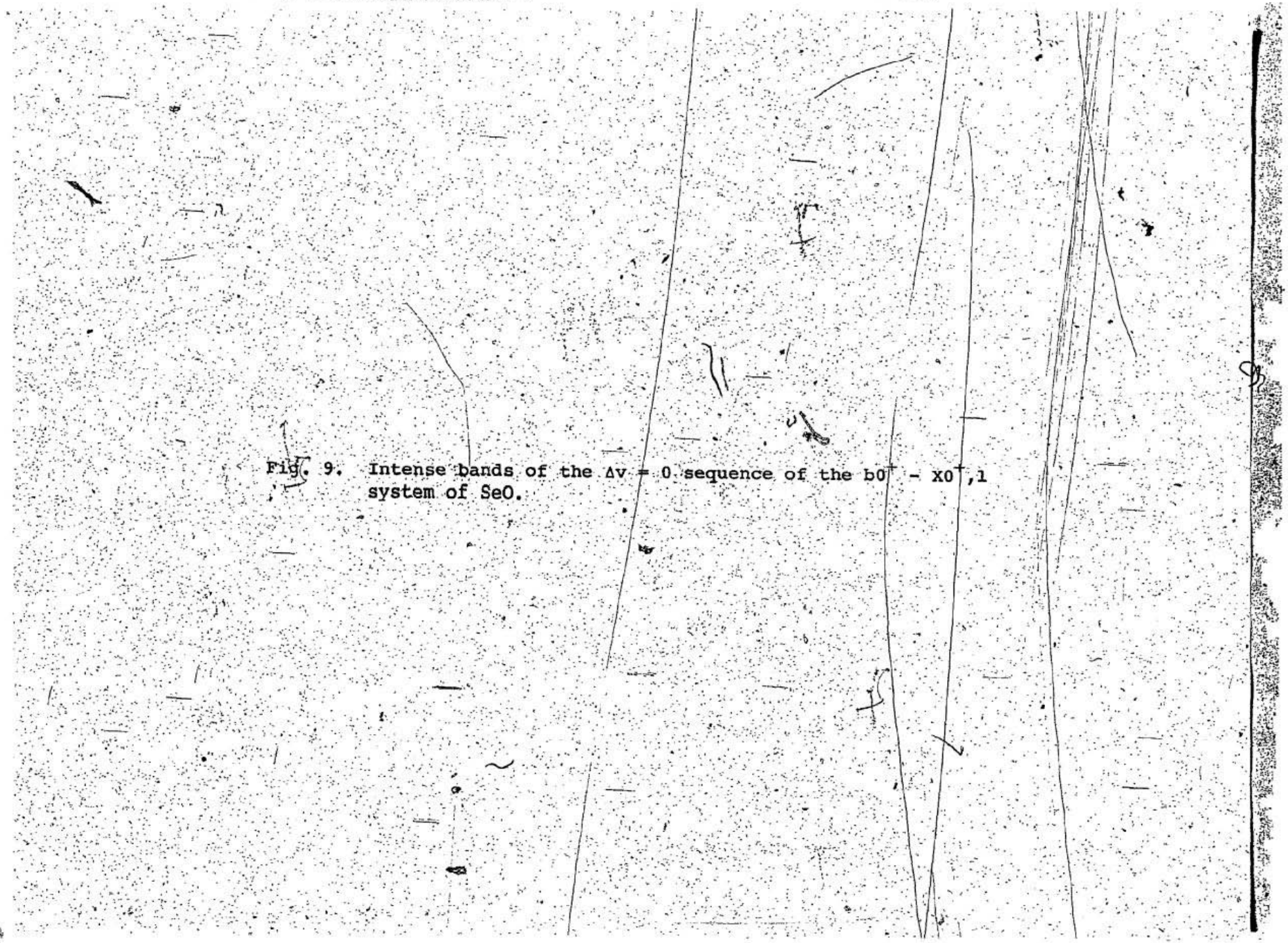

Fig. 9. Intense bands of the $\Delta v = 0$ sequence of the $b0^+ - X0^+,1$ system of SeO.

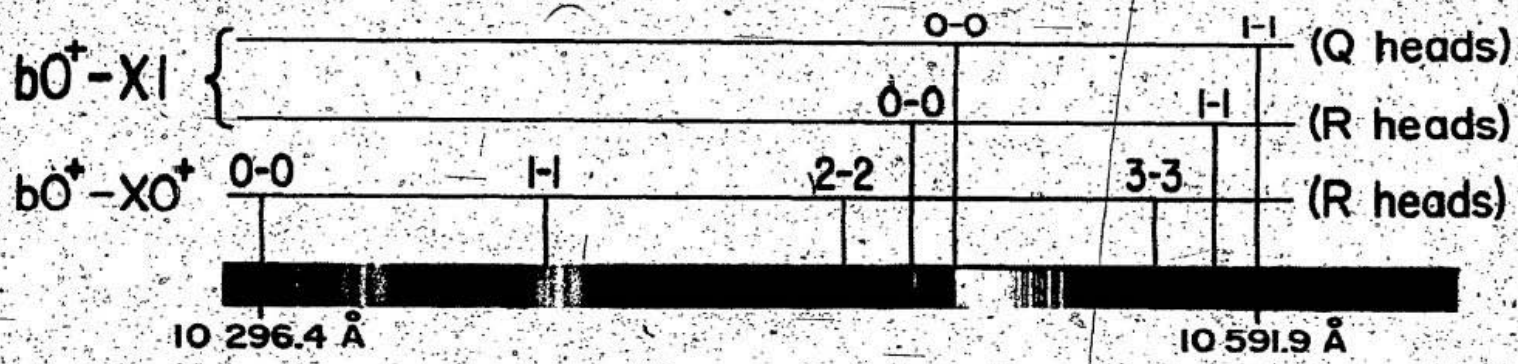
$b0^+ - X1$
0-0
1-1
(Q heads)
0-0
1-1
(R heads)
$b0^+ - X0^+$
0-0
1-1
2-2
3-3
(R heads)
10 296.4 Å
10 591.9 Å

TABLE 1

Bandheads of the $bO^+ - XO^+,1$ system of ^{80}SeO in the region 9490 - 10 780 Å

ν_{obs} (vacuum) (cm^{-1})	v'-v''	Head
	Subsystem $bO^+ - X_1O^+$	
10 530.3	1-0	R
10 440.1	2-1	R
10 348.7	3-2	R
10 255.9	4-3	R
10 161.9	5-4	R
10 066.4	6-5	R
9969.6	7-6	R
9871.0	8-7	R
9773.4	9-8	R
9710.0	0-0	R
9629.7	1-1	R
9548.3	2-2	R
9465.4	3-3	R
9381.4	4-4	R
9296.8	5-5	R

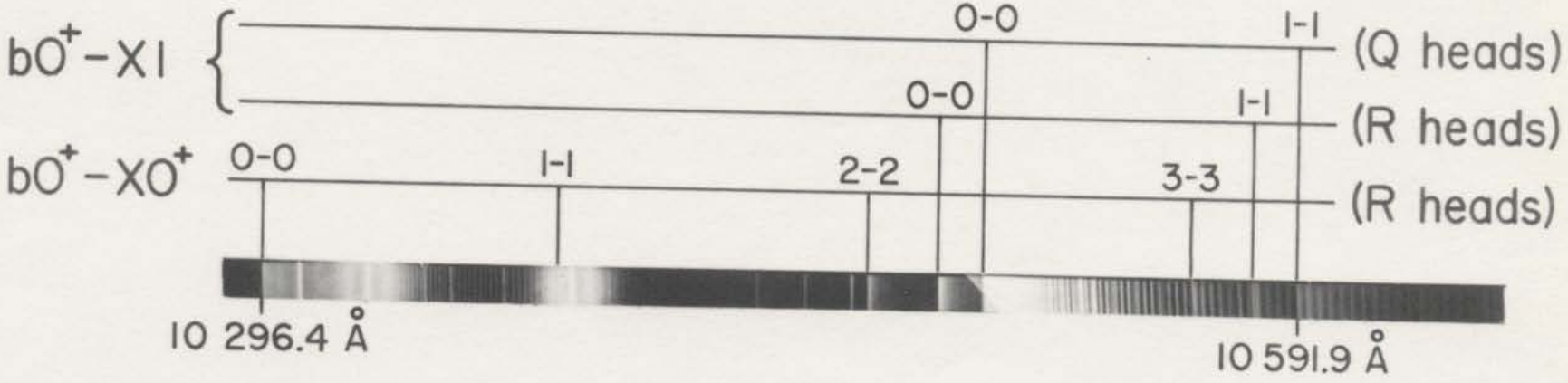
bO+ - X1
0-0
1-1
(Q heads)
0-0
1-1
(R heads)
bO+ - XO+
0-0
1-1
2-2
3-3
(R heads)
10 296.4 Å
10 591.9 Å

Figure 10

Fig. 10. Rotational structure of the 0-0 bands of the $b0^+ - X0^+,1$ system of SeO:
(a) The P and R branches of $b0^+ - X0^+$.
(b) The P and R branches of $b0^+ - X1^+$ and the Q branch of $b0^+ - X1^-$.

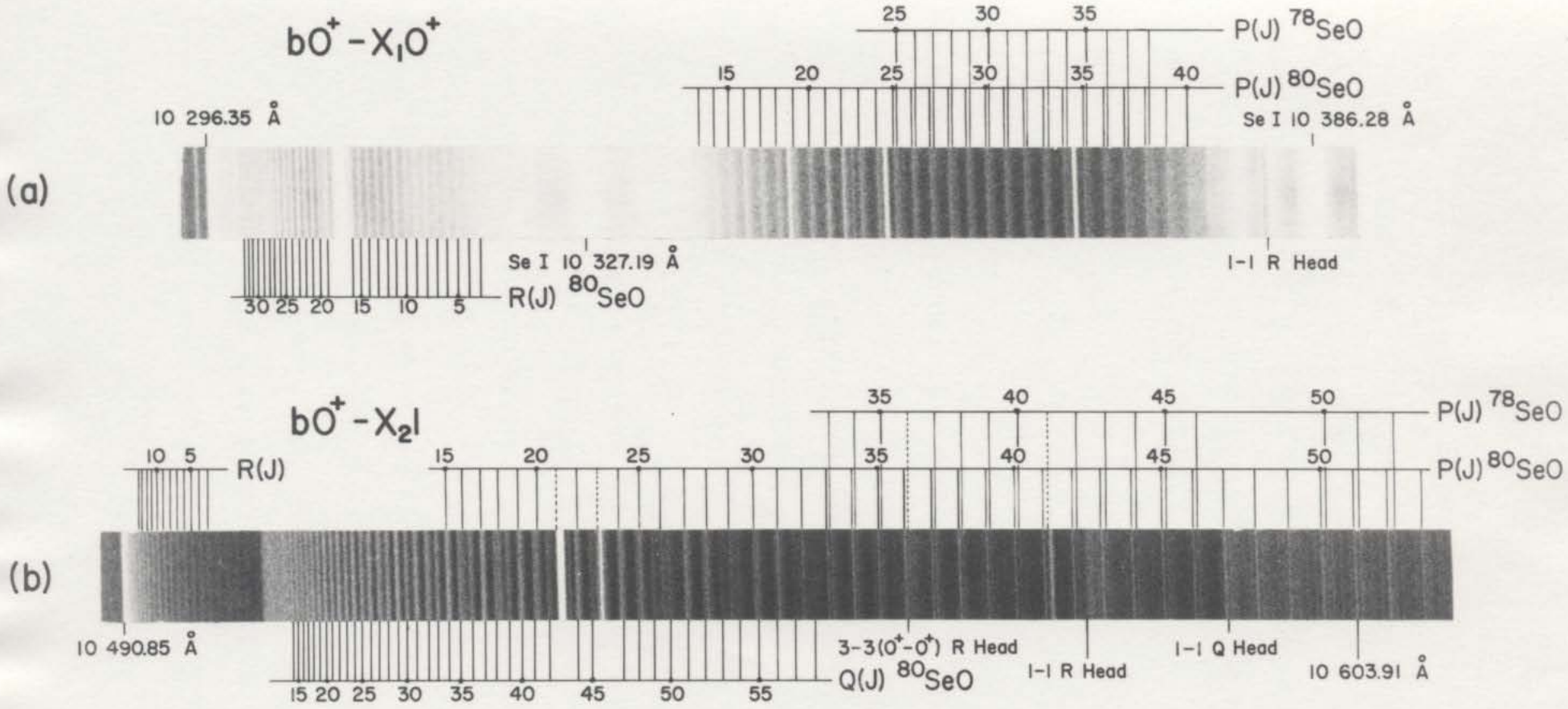
(a)
$bO^+ - X_1O^+$
10 296.35 Å
Se I 10 327.19 Å
30 25 20 15 10 5
R(J) ^{80}SeO
25 30 35
P(J) ^{78}SeO
15 20 25 30 35 40
P(J) ^{80}SeO
Se I 10 386.28 Å
I-I R Head
(b)
$bO^+ - X_2I$
10 5
R(J)
15 20 25 30 35 40 45 50
P(J) ^{80}SeO
35 40 45 50
P(J) ^{78}SeO
10 490.85 Å
15 20 25 30 35 40 45 50 55
Q(J) ^{80}SeO
3-3(0^+-0^+) R Head
I-I R Head
I-I Q Head
10 603.91 Å

band of the $bO^+ - XO^+$, 1 system of SeO are shown in Fig. 11. The $bO^+ - X_1O^+$ subsystem which has only R and P branches is analogous to a $^1\Sigma - {}^1\Sigma$ transition and the $bO^+ - X_21$ subsystem consisting of R, Q, and P branches is analogous to a $^1\Sigma - {}^1\Pi$ transition. Vacuum wavenumbers and J assignments of the rotational lines are listed in Table 2.

(i) $\underline{bO^+ - X_1O^+}$ Subsystem

Although the rotational analysis of a band of a $0^+ - 0^+$ subsystem is expected to be straight forward, some difficulty was experienced in locating the null gap in the present case because of the presence of a very strong SeI line at 10 327.19 Å [see Fig. 10(a)]. The approximate position of the null gap of the 0 - 0 band of this subsystem was initially estimated from the known value of B_o'' of the ground state (Barrow et al., 1963) and a rough value of B_o' calculated from the separation between the R and Q heads in the 0 - 0 band of the $0^+ - 1$ subsystem [Fig. 10(b)]. Although this estimation facilitated to some extent the process of assigning the J values to the rotational lines of the P and R branches, correct J numbering was finally made from a plot of the combination differences $\Delta_2F(J)$ against $(J+\frac{1}{2})$ which, when extended, passes through the point $J = -\frac{1}{2}$ as shown in Fig. 12. The lower - and upper - state rotational constants were obtained from the combination relation (Herzberg, 1950)

$$\Delta_2F(J) = 4B_o(J+\tfrac{1}{2}) - 8\,D_o(J+\tfrac{1}{2})^3, \qquad (4-4)$$

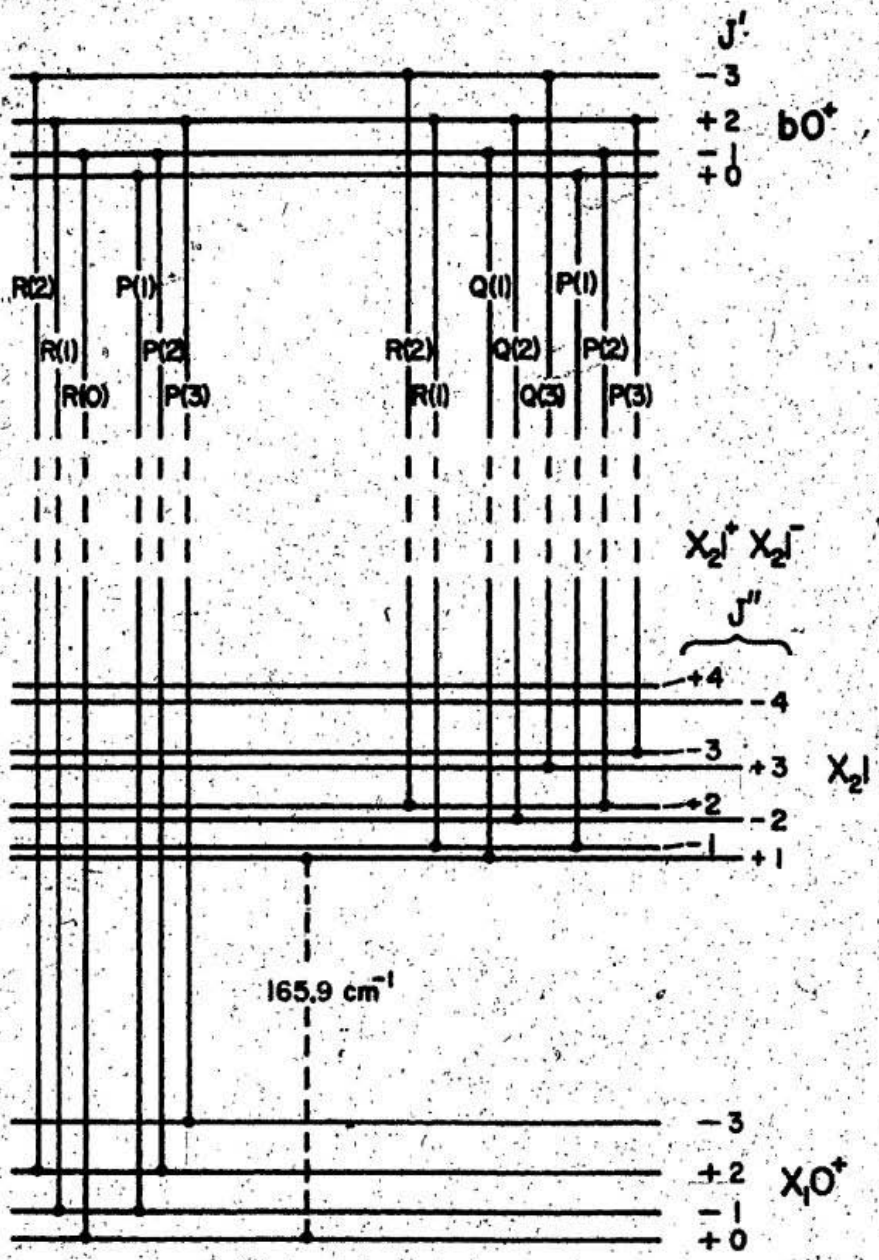

Fig. 11. A schematic energy level diagram for a band of the $b0^+ - X0^+,1$ system of SeO.

TABLE 2

Vacuum wavenumbers (cm^{-1}) of the rotational lines of the 0-0 bands of the $bO^+ - XO^+, 1$ system of ^{80}SeO

J	$bO^+ - X_1O^+$		$bO^+ - X_2 1$		
	R(J)	P(J)	R(J)	Q(J)	P(J)
3	9688.91		9523.09		
4	9689.77		9523.71		
5	9690.63		9524.32		
6	9691.45		9524.93		
7	9692.26		9525.53		
8	9693.01		9526.05		
9	9693.71		9526.55		
10	9694.54		9527.00		
11	9695.30		9527.43		
12	9695.98	9673.19	9527.80		
13	9696.68	9672.10	9528.12		
14	9697.36	9670.92		9515.66*	9503.98*
15	9698.01	9669.80		9515.21*	9502.77*
16	9698.66	9668.62		9514.81*	9501.38*
17	†	9667.41		9514.35*	9499.87*
18	†	9666.22		9513.90*	9498.44*
19	9700.53	9664.94		9513.38*	9496.74*
20	9701.09	9663.76		9512.85*	9495.29*
21	9701.63	9662.49		9512.33*	†
22	9702.17	9661.23		9511.76*	9491.85*
23	9702.68	9659.92		9511.13*	†
24	9703.19	9658.57		9510.52*	9488.46*
25	9703.68	9657.31		9509.88*	9486.74*
26	9704.16	9655.93		9509.19*	9484.97
27	9704.60	9654.60		9508.42*	9483.03*
28	9705.03	9653.20		9507.70*	9481.26*
29	9705.43	9651.79		9506.90*	9479.27

TABLE 2 (Continued)

J	$bo^+ - X_1o^+$ R(J)	$bo^+ - X_1o^+$ P(J)	$bo^+ - X_21$ R(J)	$bo^+ - X_21$ Q(J)	$bo^+ - X_21$ P(J)
30	9705.82	9650.42		9506.16*	9477.34*
31	9706.19	9648.94		9505.34*	9475.35
32	9706.56	9647.48		9504.26*	9473.31
33	9706.88	9645.95		9503.60	9471.25
34		9644.49		9502.52*	9469.15
35		9643.00		9501.75*	9467.00
36		9641.44		9500.77	9464.82
37		9639.89		9499.70*	9462.63
38		9638.32		9498.77	9460.39
39		9636.73		9497.70*	9458.09
40		9635.12		9496.65*	9455.74
41				9495.55*	9453.39
42				9494.48	9451.03
43				†	9448.60
44				9492.07*	9446.17
45				9490.85	9443.64
46				†	9441.12
47				9488.17*	9438.57
48				9486.74	9435.97
49				9485.71	9433.33
50				9484.39	9430.60
51				9482.72*	9427.90
52				9481.49*	9425.31
53				9480.11	9422.44
54				9478.69	
55				9477.07*	
56				9475.60*	
57				9473.98	
58				9472.44	

* Blended line
† Superposed by atomic line

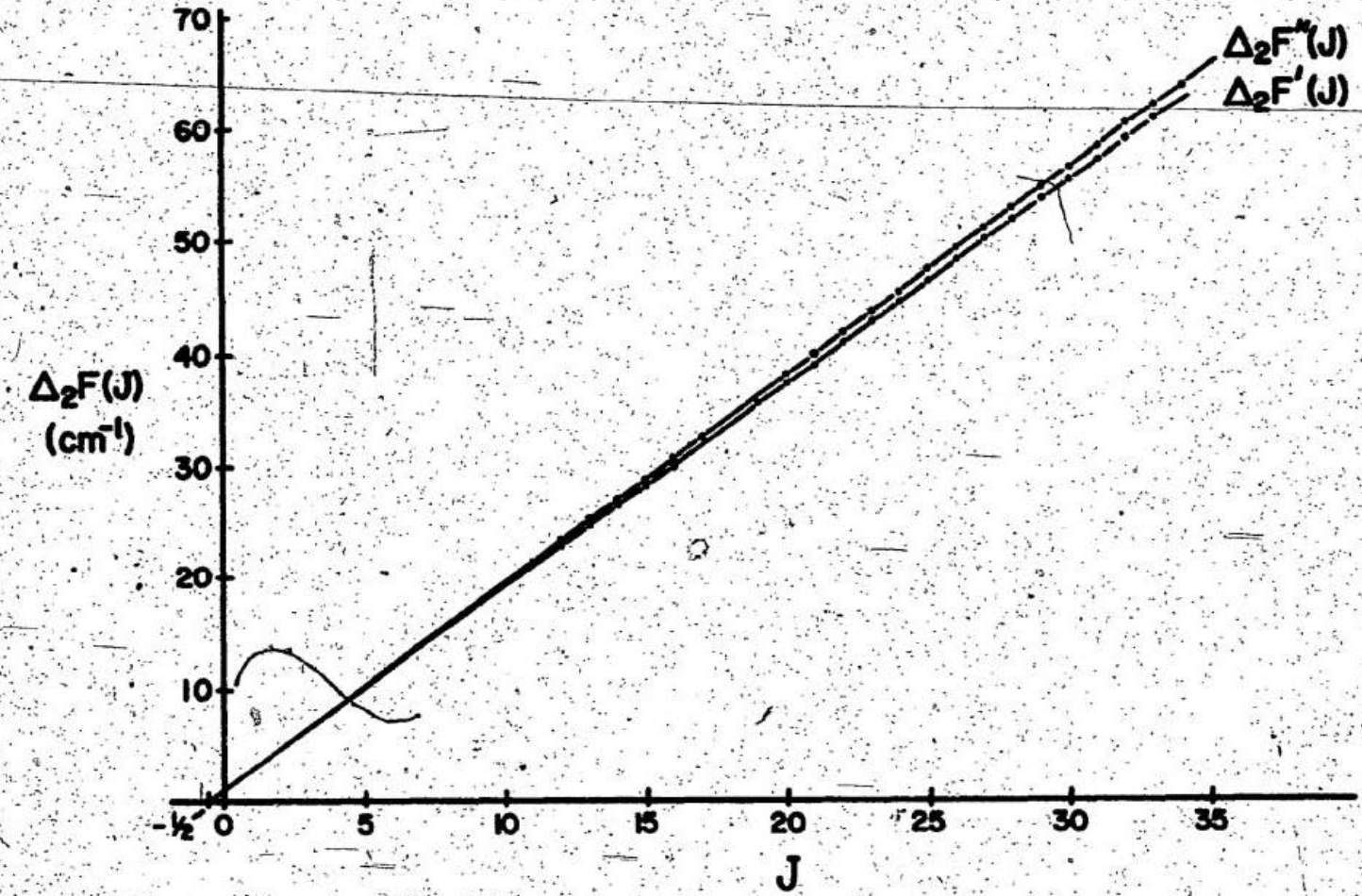

Fig. 12. $\Delta_2F(J)$ curves for the lower and upper states of the 0-0 band of the $b0^+ - X0^+$ subsystem of ^{80}SeO.

where

$$\Delta_2 F''(J) = R(J-1) - P(J+1),$$

and

$$\Delta_2 F'(J) = R(J) - P(J).$$

The measured values of $\Delta_2 F''(J)$ and $\Delta_2 F'(J)$ were used to obtain linear least squares fits of the quantities $\Delta_2 F(J)/(J+\frac{1}{2})$ against $(J+\frac{1}{2})^2$ which are shown in Fig. 13. The values of the rotational constants B_o and D_o of both bO^+ and $X_1 O^+$ states derived, respectively, from the intercepts and slopes of these fits are given in Table 3. The value of ν_o for this band was then found by fitting the measured R lines to the equation (Herzberg, 1950)

$$R(J) = \nu_o + (2B_o' - 4D_o') + (3B_o' - B_o'' - 12D_o')J + (B_o' - B_o'' - 13D_o' + D_o'')J^2 - 2(3D_o' - D_o'')J^3 - (D_o' - D_o'')J^4, \qquad (4\text{-}5)$$

and is given in Table 3.

(ii) $bO^+ - X_2 1$ Subsystem

In the 0 - 0 band of the system $bO^+ - X_2 1$, R and P branches occur for the $0^+ - 1^+$ component while Q branch occurs for the $0^+ - 1^-$ component [see Figs. 10(b) and 11]. For the former component the assigned J numberings of the R and P branches do not overlap with each other and hence it was not possible to form the combination differences $\Delta_2 F(J)$

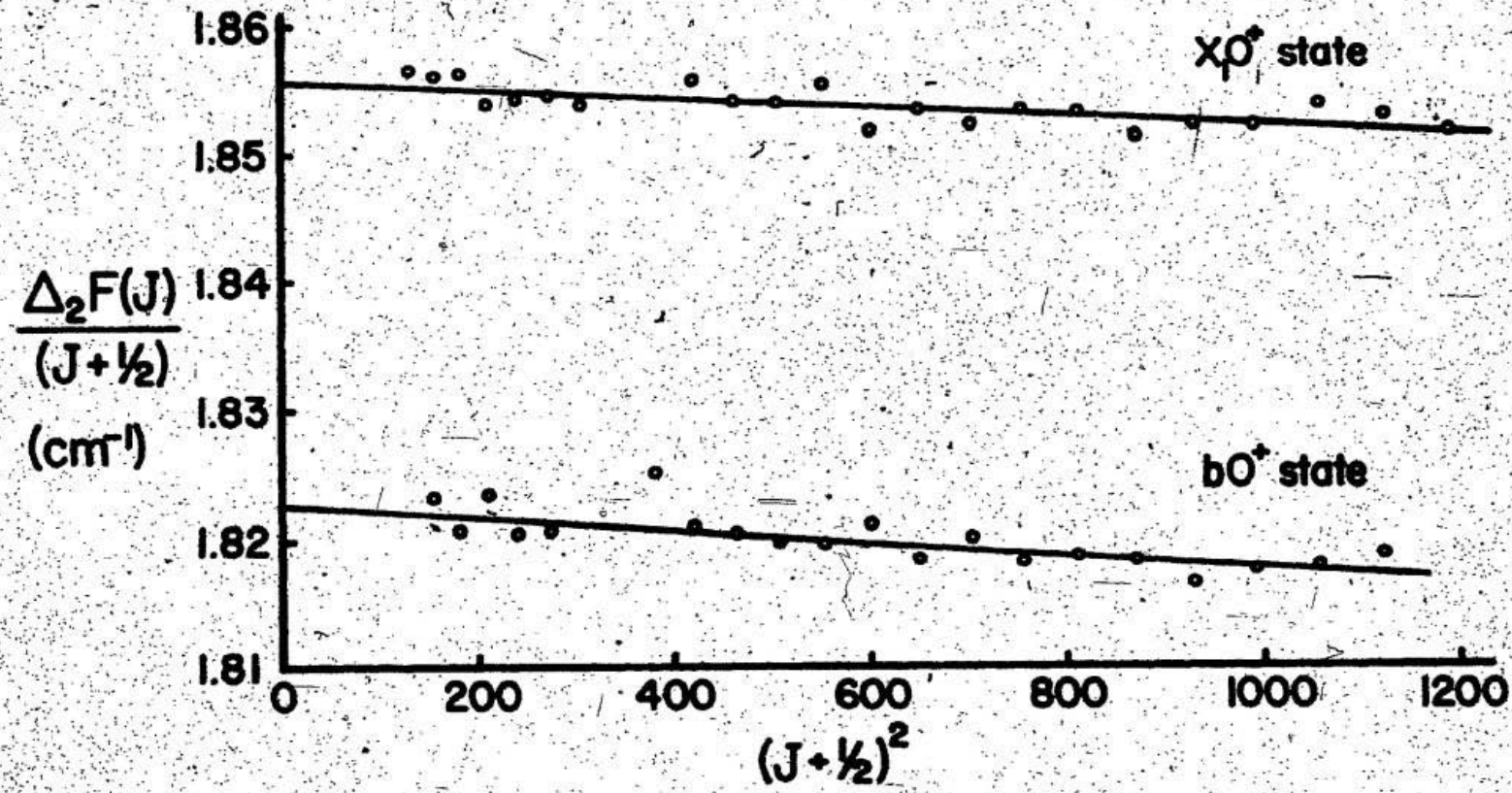

Fig. 13. Plots of $\Delta_2 F(J)/(J+\frac{1}{2})$ against $(J+\frac{1}{2})^2$ for the $X_1 0^+$ and $b0^+$ states.

TABLE 3

Molecular constants of the $bO^+ - XO^+,1$ system of ^{80}SeO

	bO^+	X_1O^+	$X_2 1^+$	$X_2 1^-$
$T_e(cm^{-1})$	9725.55	914.69[a]	165.9_1	165.9
$\omega_e(cm^{-1})$	838.83	914.69[a]	915.43[a]	915.43[a]
$\omega_e x_e(cm^{-1})$	5.11	4.52[a]	4.52[a]	4.52[a]
$B_o(cm^{-1})$	0.4560 ±0.0002	0.4639 ±.0001	0.4745 ±.0005	0.4697 ±.0008
$D_o(cm^{-1})$	8×10^{-7}	4×10^{-7}	—	—
$I_o(gcm^2)$	61.48×10^{-40}	60.41×10^{-40}	59.05×10^{-40}	59.66×10^{-40}
$r_o(\text{Å})$	1.667	1.652	1.634	1.642

Estimated separation $T_e(1^+) - T_e(1^-) = 0.0096\ cm^{-1}$

ν_o of the 0 - 0 band of $bO^+ - X_1O^+ = 9686.4\ cm^{-1}$

ν_o of the 0 - 0 band of $bO^+ - X_2 1^- = 9519.1\ cm^{-1}$

[a]Barrow and Deutsch (1963)

for them. The method of using the combination differences $\Delta_1 F(J)$ by including the Q(J) lines arising from the $0^+ - 1^-$ component was not adopted because of the so-called combination defects. Finally, the following procedure was adopted for the analysis of the P and Q branches: If one neglects the stretching constants D_o' and D_o'', the P and Q lines of a 0 - 0 band can be represented by the relations (Herzberg, 1950)

$$P(J) = \nu_o - (B_o' + B_o'') J + (B_o' - B_o'') J^2, \qquad (4\text{-}6a)$$

$$Q(J) = \nu_o + (B_o' - B_o'') J + (B_o' - B_o'') J^2. \qquad (4\text{-}6b)$$

Using the value of B_o' (of the bO^+ state) determined from the $bO^+ - XO^+$ subsystem, the ν_o value for the 0 - 0 band of $0^+ - 1^-$ component and B_o'' for the $X_2 1^-$ and $X_2 1^+$ substates were derived by fitting the measured P and Q lines to equations (4-6a) and 4-6b), and the values of these constants are given in Table 3. As most of the Q branch consists of blended lines, the value of B_o'' of the 1^- state is considered to be less precise. It may be mentioned here that a fit of the measured P and Q lines to the fourth order equation in J containing D_o' and D_o'' terms was not satisfactory because of insufficient data. The values of B_o'' of the 0^+ and 1 states obtained in the present work are in excellent agreement with those derived by Barrow and Deutsch (1963) from the analysis of the $B^3\Sigma^- - X^3\Sigma^-$ system (the values

obtained by them are: $B_o''(0^+) = 0.4638\ cm^{-1}$, $B_o(1^+) = 0.4745\ cm^{-1}$, $B_o(1^-) = 0.4688\ cm^{-1}$). Finally, the estimated separation between the $T_e(1^+)$ and $T_e(1^-)$ levels is also given in Table 3.

(iii) Isotope Effect

In addition to the rotational lines of ^{80}SeO, several lines have been observed in the 0 - 0 band, at longer wavelengths of the subbands of the $0^+ - 0^+$ and $0^+ - 1^+$ components. These lines were assigned to the P branches of the ^{78}SeO molecule (see Fig. 10). A densitometer trace of the rotational structure of the P branches of both ^{80}SeO and ^{78}SeO is shown in Fig. 14. Isotope shifts for the lines of ^{78}SeO from those of ^{80}SeO were calculated from the following equation by using the molecular constants of ^{80}SeO:

$$\Delta\nu(^{80}Se^{16}O - {}^{78}Se^{16}O) = \nu_{v'J'v''J''}(^{80}Se^{16}O) - \nu_{v'J'v''J''}(^{78}Se^{16}O) = \Delta\nu_{vib} + \Delta\nu_{rot} \qquad (4\text{-}7)$$

where

$$\Delta\nu_{vib} = (1-\rho)\{\omega_e'(v'+\tfrac{1}{2}) - \omega_e''(v''+\tfrac{1}{2})\} - (1-\rho^2)\{\omega_e'x_e'(v'+\tfrac{1}{2})^2 - \omega_e''x_e''(v''+\tfrac{1}{2})^2\}, \qquad (4\text{-}7a)$$

and

$$\Delta\nu_{rot} = (1-\rho^2)\{B_e'J'(J'+1) - B_e''J''(J''+1)\} - (1-\rho^3)\{\alpha_e'(v'+\tfrac{1}{2})J'(J'+1) - \alpha_e''(v''+\tfrac{1}{2})J''(J''+1)\} - (1-\rho^4)\{D'J'^2(J'+1)^2 - D''J''^2(J''+1)^2\}, \qquad (4\text{-}7b)$$

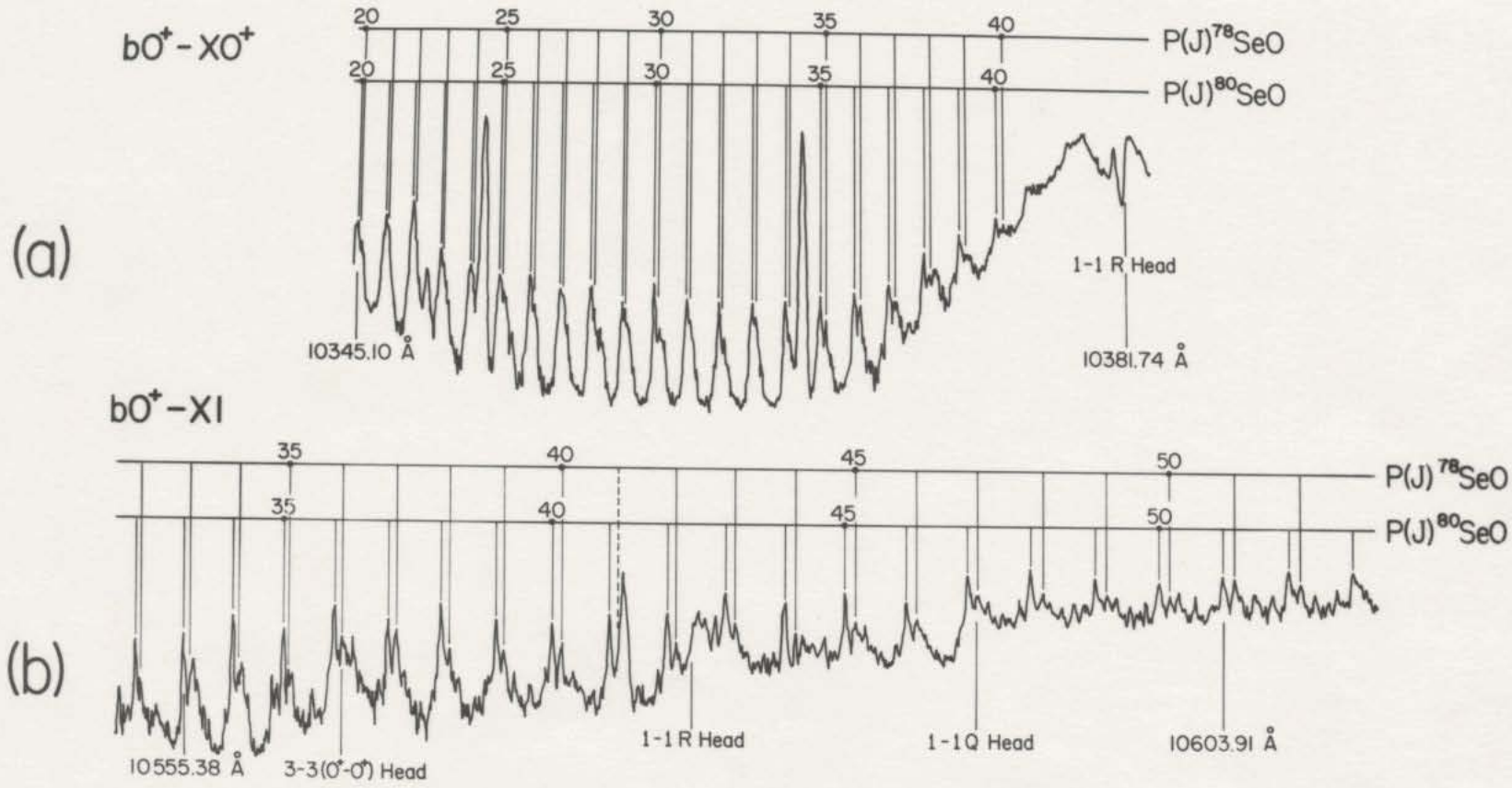

Fig. 14. Isotope effect in the 0-0 band of SeO: (a) the $b0^+ - X_1 0^+$ component, (b) the $b0^+ - X_2 1$ component. Only part of the densitometer trace of the P branch lines of ^{80}SeO and ^{78}SeO is shown in each case.

ρ being equal to $\{\mu(^{80}Se^{16}O) / \mu(^{78}Se^{16}O)\}^{\frac{1}{2}}$. (Note $\mu_A(^{80}Se^{16}O) = 13.3275$ a.m.u., $\mu_A(^{78}Se^{16}O) = 13.2707$ a.m.u. The values of B_e and α_e are taken from Chapter 6). The observed and calculated isotope shifts are listed in Table 4. The close agreement between them confirms the correctness of the J numbering.

(iv) Rotational Intensity Distribution

The relative intensities of the rotational branches in $^1\Sigma^\pm - ^3\Sigma^\mp$ electric dipole transitions have been first calculated by Schlapp (1932). Although his intensity formulae have been shown to be in agreement with the observed intensities in the spectra of atmospheric O_2 (Schlapp, 1937; Tilford et al., 1965) and of NF (Douglas & Jones, 1966) an error in the relative phases of the two transition moments used by Schlapp (1932) was pointed out by Watson (1968) who gave corrected expressions for the intensity distribution of the rotational lines in $^3\Sigma^\mp - ^1\Sigma^\pm$ transitions. The observed intensities in the $b^1\Sigma^+ - X^3\Sigma^-$ system of SO by Colin (1968) are found to be in approximate agreement with Watson's formulae (1968). However, the relative intensities of the rotational branches of the present $bO^+ - XO^+$, 1 system of SeO do not seem to agree with either Schlapp's or Watson's formulae presumably because of the fact that these formulae have been derived for transitions involving Hund's case (b) triplet states. Although intensity calculations for

TABLE 4

Isotope shifts (cm^{-1}) in the rotational lines of the 0 - 0 bands of the $b0^+ - X0^+,1$ system of SeO

$\Delta\nu(^{80}SeO - ^{78}SeO)$ $b0^+ - X_1O^+$ subsystem			$\Delta\nu(^{80}SeO - ^{78}SeO)$ $b0^+ - X_2l^+$ subsystem		
Line	obs.	calc.	Line	obs.	calc.
P(28)	0.21	0.22	P(33)	0.26	0.26
P(29)	0.23	0.23	P(34)	0.28	0.27
P(30)	0.24	0.23	P(35)	0.28	0.28
P(31)	0.24	0.24	P(37)	0.30	0.29
P(32)	0.24	0.24	P(38)	0.31	0.30
P(33)	0.25	0.25	P(39)	0.31	0.31
P(34)	0.25	0.26	P(40)	0.32	0.31
P(35)	0.28	0.26	P(42)	0.33	0.33
P(36)	0.28	0.27	P(43)	0.33	0.34
P(37)	0.28	0.28	P(44)	0.34	0.35
P(38)	0.29	0.28	P(45)	0.35	0.36
P(39)	0.30	0.29	P(46)	0.36	0.36
P(40)	0.31	0.30	P(50)	0.40	0.40
			P(51)	0.40	0.41
			P(52)	0.42	0.42

pure case (c) (to which the ground state of SeO belongs) are not available, Kovacs (1969, p. 179) has given the formulae for the intensity distribution in the rotational branches of $^1\Sigma^{\pm} - {}^3\Sigma^{\mp}$ transitions, which include the departure from Hund's case (b) by the introduction of the spin-spin interaction constant. It is found that the observed relative intensities* of the rotational branches of the 0 - 0 band of the $bO^+ - XO^+$, 1 system of SeO are in approximate agreement with the formulae given by Kovacs.

4.4. Franck-Condon Factors and r-Centroids

From the observed data, the internuclear potential energy curves are derived for bO^+ and X_1O^+ states by Klein-Dunham method (described in Chapter 2) and are given in Chapter 6. These potentials are used to calculate the vibrational wavefunctions, Franck-Condon factors and r-centroids of the $bO^+ - XO^+$ subsystem. The results are summarized in Table 5. The fact that only $\Delta v = 0$ and +1 sequences are observed for the $bO^+ - XO^+$ subsystem (Azam & Reddy, 1973) agrees very well with the values of the Franck-Condon factors given in Table 5. The maximum value of the noise-factor (cf. Chapter 2) in these calculations is 0.58×10^{-11}.

4.5. Discussion

The triplet separation $2\lambda_{SO}$ (see section 4.2) for the ground states of SeO and other diatomic molecules of the

* as determined by the peak heights of the densitometer traces.

TABLE 5

Franck-Condon factors and r-centroids (Å) for the $b^4\Sigma^- - X^2\Pi$ subsystem of SeO[a]

v' \ v''	0	1	2	3	4	5	6	7	8
0	0.9660 1.659	0.0324 1.875	0.0012 1.894						
1	0.0334 1.462	0.8980 1.668	0.0643 1.884	0.0039 1.899					
2	0.0002 0.870	0.0684 1.479	0.8260 1.676	0.0968 1.892	0.0084 1.904				
3		0.0008 0.937	0.1070 1.498	0.7500 1.684	0.1280 1.901	0.0145 1.913			
4			0.0019 1.015	0.1450 1.516	0.6720 1.691	0.1570 1.910	0.0227 1.922		
5				0.0039 1.099	0.1840 1.532	0.5930 1.697	0.1850 1.918	0.0329 1.931	
6					0.0070 1.162	0.2230 1.548	0.5120 1.703	0.2100 1.927	0.0450 1.940
7						0.0119 1.221	0.2600 1.564	0.4340 1.708	0.2300 1.936
8							0.0188 1.273	0.2940 1.580	0.3580 1.711
9								0.0277 1.317	0.3240 1.594

[a] For each band, the upper number is the Franck-Condon factor and the lower one is the r-centroid.

Group VI elements are summarized in Table 6. It is seen from this table that in the series of molecules O_2, SO, S_2, . . . , Te_2, there is a rapid increase in the value of λ. For molecules O_2, SO and S_2 the values of λ are small (λ_o = 1.98, 5.28, 11.84 cm^{-1} respectively). On the other hand, the λ_o values for SeO, Se_2, . . ., and Te_2 vary from 83.65 cm^{-1} (for SeO) to $\leq$1115 cm^{-1} (for Te_2). The large triplet separation between $F_1(0^+)$ and F_2, F_3 (1) levels for these heavier molecules is attributed to the case (c) character of their ground states.

For the molecules in this series, the lowest Π state above the ground state is a $^3\Pi$ state (cf. Chapter 6) and the corresponding Π-Σ separation decreases as the nuclear charge increases, thus producing a larger splitting. This type of interaction might be larger for heteronuclear than for homonuclear molecules because of the selection rule which, for homonuclear molecules, prevents the interaction of the $^3\Sigma_g^-$ state with the lowest $^3\Pi_u$ state.

From the experimental information about the molecules of this group, it is found that λ_v in the ground state increases with the vibrational quantum number v at least at low values. On the other hand, the ground state atoms $^3P_2 + {}^3P_2$ yield both 0^+ and 1 molecular states so that, if states of like Ω do not cross, λ_v should reach a maximum at some large value of v and then decrease to zero at the dissociation limit. However, due to lack of experimental data

TABLE 6

Triplet separations $2\lambda_o$ for the ground electronic states of the diatomic molecules of the Group VI elements

Molecule	$2\lambda_o$ (cm^{-1})	Reference
O_2	3.9690	Babcock and Herzberg (1948) Welch and Mizushima (1972) Townes and Schawlow (1955) Bowers et al. (1959)
SO	10.558	Powell and Lide (1964) Daniel and Dorain (1966) Carrington et al. (1967)
S_2	23.68	Barrow and Ricks (unpublished) Barrow and Ketteringham (1963)
SeO	167.3	Present work
SeS	205.0 ± 7.5	Ahmed and Barrow (1974)
Se_2	512	Gouedard and Lehmann (1976) Greenwood and Barrow (1976)
TeO	679 ± 15	Barrow and Hitchings (1972)
TeS	≥1084*	Mohan and Majumdar (1961)
TeSe	1547.2	Ahmed et al. (1975)
Te_2	≤2230†	Yee and Barrow (1972)

* The quoted numerical value is the minimum limit and the actual value may be more than that by a few cm^{-1}.

† The quoted numerical value is the maximum limit and the actual value may be less than that by a few cm^{-1}.

on λ_v at very large values of v (i.e., in the vicinity of dissociation limit)- for any of these molecules it is not possible to arrive at a definite conclusion.

CHAPTER 5

NEW EMISSION BAND SYSTEMS OF SeO

In this chapter we report the first observation of three emission band systems of the SeO molecule and their vibrational analyses. Also included in this chapter are the reanalyses of two brief band systems of SeO which have been previously observed (Haranath, 1964; Reddy & Azam, 1974). The band systems observed for the first time are a2 - $X_2$1 (in the near infrared region 6470 - 5540 cm^{-1}); A0, 1, 2 - XO^+; 1 (6730 - 8570 Å) and C2, 1, 0 - XO^+, 1 (2690 - 3190 Å). The two brief band systems are F - a (2150 - 2270 Å) and G - a (2070 - 2130 Å). Details of these five band systems form the rest of this chapter.

5.1. The a2 - $X_2$1 System

(i) Introduction

Prior to the present work the only molecule (among the diatomic molecules of the Group VI elements) for which the forbidden transition $a^1\Delta - X^3\Sigma^-$ has been observed is O_2 (Herzberg & Herzberg, 1947). As mentioned in Chapter 4, Azam and Reddy (1973) tentatively assigned four bands at 9518.4, 9439.1, 9356.8, and 9276.0 cm^{-1} to the probable transition $a^1\Delta - X^3\Sigma^-$ of SeO, but these bands have now been

assigned as the Q heads of the subsystem $b^1\Sigma^+ - X^3\Sigma^-$ (F_2, F_3) (i.e., $bO^+ - X_2 1$ in case (c) notation). Thus the $a^1\Delta - X$ system of SeO remains to be observed.

On theoretical considerations Raftery et al. (1972) have shown that in the absence of configuration mixing, the three states arising from the lowest electronic configuration $\ldots \pi^2$ have the following energies:

$$^3\Sigma^- : \quad E = (J^0 - K^2)_{\pi\pi}$$

$$^1\Delta : \quad E = J^0_{\pi\pi}$$

$$^1\Sigma : \quad E = (J^0 + K^2)_{\pi\pi}.$$

This implies that the $^1\Delta$ state lies halfway between the $^1\Sigma^+$ and $^3\Sigma^-$ states. This theoretical result is in approximate agreement with the experimental observations in the case of O_2 and the hydrides and halides of the Group V elements (which have $\ldots \pi^2$ as the ground electronic configuration), as evidenced from Table 7. This table lists the T_e values for $a^1\Delta$ and $b^1\Sigma^+$ states of some of these molecules. The ratio of T_e values for $a^1\Delta$ and $b^1\Sigma^+$ states appears to be 0.55±0.05. If the same ratio is assumed for the corresponding states of SeO, the T_e value for its $a^1\Delta$ state is estimated to be about 5350±500 cm^{-1} because T_e for $b^1\Sigma^+$ of SeO is 9725.6 cm^{-1} (cf. Chapter 4). Our attempt in search of a characteristic emission spectrum of the SeO molecule in the near infrared region has indeed yielded positive results. Brief experimental details and results

TABLE 7

T_e values for the $^1\Delta$ and $^1\Sigma^+$ states and their ratios for molecules with .... π^2 ground electronic configuration

Molecule	$T_e(a\,^1\Delta)$	$T_e(b\,^1\Sigma^+)$	$T_e(a\,^1\Delta)/T_e(b\,^1\Sigma^+)$	Reference
NH	11 900*	20 100*	0.59	O'Neil and Shaeffer (1971)
PH	7640*	15 150*	0.50	Jordan (1964)
NF	11 435+	18 905+	0.605	Jones (1967)
AsF	7053.5	13 647.6	0.517	Chatalic et al. (1973)
O_2	7918.6	13 195.2	0.600	Rosen (1970)
S_2	5500c	9100c	0.60	Colin (1968)

* Calculated values.

\+ Values of T_o.

c Estimated values.

of this work are given in the following paragraphs.

The emission spectra of SeO in the region 6470 - 5540 cm^{-1} were recorded with a Perkin-Elmer model 112 G single-beam double-pass grating spectrometer equipped with a lead sulphide detector at room temperature. The second order of the plane grating with 300 grooves/mm and blazed at 3.0 μm was used to record the spectra. Higher orders of the grating were removed by means of a Perkin-Elmer 203 - 1104 filter. Emission lines of mercury in different overlapping orders and absorption peaks of atmostpheric water vapour were used as wavelength standards. Different slit widths in the range 100 - 500 μm were used.

(ii) Vibrational Structure

A recorder trace of the spectrum in the region 6470 - 5540 cm^{-1} is shown in Fig. 15. It consists of five characteristic bands of SeO in two groups which are degraded to longer wavelengths. The group of bands at low and high wavenumbers are assigned as the $\Delta v = 0$ and $\Delta v = +1$ sequences respectively. Vacuum wavenumbers (cm^{-1}) of the bands and their vibrational assignments are given in Table 8. Both Q and R heads are observed for the 0 - 0 band whereas only R heads are observed for the three bands in the $\Delta v = +1$ sequence. The band system is assigned to the transition $a2 - X_2 1$. It is to be noted that the selection rule $\Delta\Omega = 0, \pm 1$ forbids the transition $a2 - X_1 0^+$. The upper

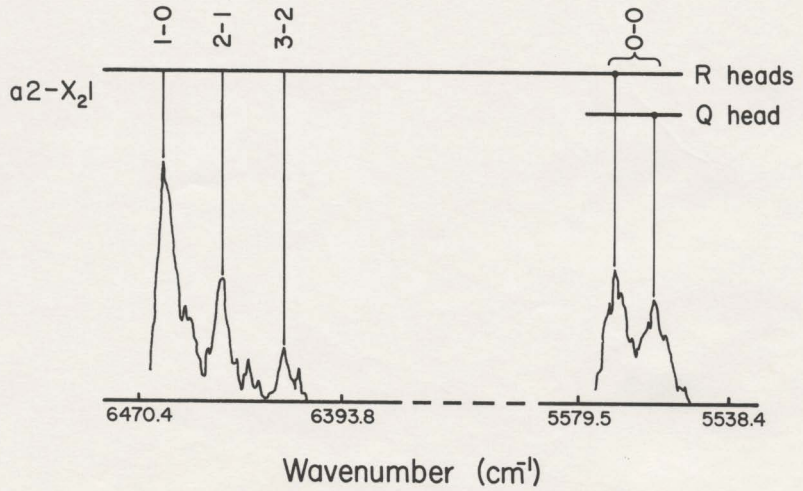

Fig. 15. A recorder trace of the a2 - $X_2$1 system of SeO.

TABLE 8

Bandheads of the a2 - $X_2$1 system

(All bands are degraded to longer wavelengths)

ν_{obs} (vacuum) (cm^{-1})	v' - v''
64 60.9	1-0 R
64 39.8	2-1 R
64 17.1	3-2 R
55 77.6	0-0 R
55 66.2	0-0 Q

state vibrational interval, $\Delta G'(\frac{1}{2}) = 883.3\ cm^{-1}$. Even though no further vibrational constants could be obtained from the analysis of this system, it has been assigned to the transition $a2 - X_2 1$ because of the proximity of the occurrence of the system in the spectral region predicted on theoretical considerations. The present interpretation must, however, be confirmed by a detailed rotational analysis of this band system.

(iii) Approximate Rotational Constant of State a

The separation between the head (ν_{vertex}) and origin (ν_o) of a band can be expressed in terms of the rotational constants B_v of the upper and lower states by the relation (Herzberg, 1950)

$$\nu_{vertex} - \nu_o = - \frac{(B_v' + B_v'')^2}{4(B_v' - B_v'')} \qquad (5\text{-}1)$$

The quantity ν_{vertex} can be replaced by ν_R for the bands degraded to longer wavelengths. If ν_o is approximated by the value of ν_Q and B_v'' is known, it is then possible to estimate the value of B_v' approximately. The value of the separation ($11.4\ cm^{-1}$) between the R and Q heads of the 0 - 0 band (Table 8) and $B_o''(X_2 1) = 0.4745\ cm^{-1}$ (Chapter 4) are substituted in Eq. (5-1) and a value of $0.45_6\ cm^{-1}$ for B_o' of $a^1\Delta$ state is obtained. This value is in reasonable agreement with $B_o = 0.461\ cm^{-1}$ (for $a^1\Delta$) obtained by Carrington et al. (1969) from a study of the gas phase electron spin

resonance spectrum of SeO.

5.2. The AO, 1, 2 - XO^+, 1 System

(i) Introduction

This is a weak but straightforward band system of the SeO molecule. All the thirty-four bandheads, observed in the spectral region 6730 - 8570 Å, are degraded to shorter wavelengths. It is revealed through vibrational analysis that this system arises from a transition $^3\Pi_{reg}$ - X. As the T_e value of the upper state lies immediately below the known $B\,^3\Sigma^-$ state, this state has been labeled A $^3\Pi_{reg}$ state. Apart from deriving the vibrational constants of the system, it was possible to estimate an approximate value of the rotational constant B for the A state from the observed separations of the P and Q heads of some bands.

The A - X system of SeO was photographed on the Bausch and Lomb spectrograph in the first order of the 600 grooves/mm grating. The slit width was maintained at 100 μm which gives a reciprocal linear dispersion of about 8.1 Å/mm at 8000 Å. The exposure times varying between four and five hours were necessary to photograph the spectra on hypersensitized Kodak I-N plates. Kodak K-26 filter was used to remove higher order spectra. The error in the measurement of good bandheads is less than 0.05 Å; however, it is considerably more for the diffuse bandheads.

(ii) Vibrational Analysis

The spectrograms of the emission bands of the A - X system of SeO in the region 6730 - 8570 Å are shown in Fig. 16. The bands are degraded to shorter wavelengths and are generally weak. As discussed below, the A - X system arises most probably from the transition $A\ ^3\Pi_{reg}$ - X. Even though it is not possible to identify the ground electronic state vibrational intervals $\Delta G(\frac{1}{2})$ and $\Delta G(3/2)$ from the observed bands of this system, the separations between the prominent band heads at 13 805 cm^{-1} (7242 Å), 12 931 cm^{-1} (7731 Å) and 12 064 cm^{-1} (8287 Å) (Fig. 16) which are 874 and 867 cm^{-1}, respectively, are identified as the vibrational intervals $\Delta G(7/2)$ and $\Delta G(9/2)$ of the ground state of SeO (cf. Barrow & Deutsch, 1963; Azam & Reddy, 1973). The separation between the band heads at 13 495 cm^{-1} (7408 Å) and at 13 323 cm^{-1} (7504 Å), which is 172 cm^{-1} corresponds approximately to the interval between $\Omega = 1$ and $\Omega = 0^+$ levels of the ground electronic state. The separation between the band heads at 13 805 cm^{-1} (7242 Å) and 13 495 cm^{-1} (7408 Å), which is 310 cm^{-1}, is identified as the spin-splitting between the neighboring components $^3\Pi_0$ and $^3\Pi_1$ of the $A\ ^3\Pi$ state. These and similar observations prompted us to attribute the present band system of SeO to the transition $A\ ^3\Pi_{reg}$ - X. As the separation between the $X_1 0^+$ and $X_2 1$ sublevels is moderately large for SeO, the following five subsystems of the A - X system which arise from the

Figure 16

Fig. 16. The emission spectrum of the A0,1,2 - $X0^+$,1 system of SeO in the region 6730 - 8570 Å. The P heads are marked for all the bands. The Q heads are also marked whenever possible to identify them without ambiguity.

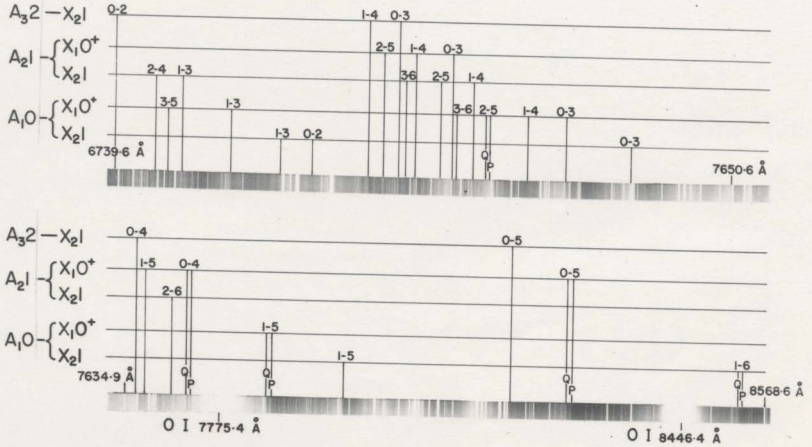
$A_3 2 - X_2 1$
$A_2 1 - \{X_1 0^+, X_2 1$
$A_1 0 - \{X_1 0^+, X_2 1$
0-2
1-4 0-3
2-5 1-4 0-3
3-6 2-5 1-4
3-6 2-5 1-4 0-3
2-4 1-3
3-5 1-3
1-3 0-2
0-3
Q P
6739·6 Å
7650·6 Å
$A_3 2 - X_2 1$
$A_2 1 - \{X_1 0^+, X_2 1$
$A_1 0 - \{X_1 0^+, X_2 1$
0-4
1-5 0-4
2-6
0-5
0-5
1-5
1-5
1-6
Q P
7634·9 Å
8568·6 Å
O I 7775·4 Å
O I 8446·4 Å

selection rule $\Delta\Omega = 0, \pm 1$ are expected to occur:

$A_1O - X_1O^+$; $A_1O - X_2 1$; $A_2 1 - X_1O^+$; $A_2 1 - X_2 1$; and $A_3 2 - X1$.

A schematic energy level diagram showing these five subsystems is given in Fig. 17.

Table 9 lists the bandhead measurements $\lambda(\mathring{A})$ and $\nu(cm^{-1})$, the visual estimates of their relative intensities and the vibrational quantum numbers assigned to the bands, of all the observed five subsystems of the A - X system. For some bands, both P and Q heads were identified. In Fig. 16 P heads are marked for all the bands, Q heads are also marked whenever they are well defined without ambiguity. The separations between these heads vary from 10 to 14 cm^{-1} and are too large to be accounted on the basis of isotope effect. Deslandres vibrational schemes for the P heads of the $A_1O - XO^+,1$ and $A_2 1 - XO^+,1$ subsystems are shown in Tables 10 and 11, respectively. For both states A and X the vibrational constants ω_e and $\omega_e x_e$ are calculated by the linear least squares fit of the data to the Eq. (2-21). The system origins ν_e were calculated from Eq. (2-20). The derived vibrational constants (in cm^{-1}) are listed below:

$A_1O - X_1O^+$:

$\nu_e = 16131$

$\omega'_e = 994$ $\qquad \omega'_e x'_e = 6.5$

$\omega''_e = 908$ $\qquad \omega''_e x''_e = 4.0$

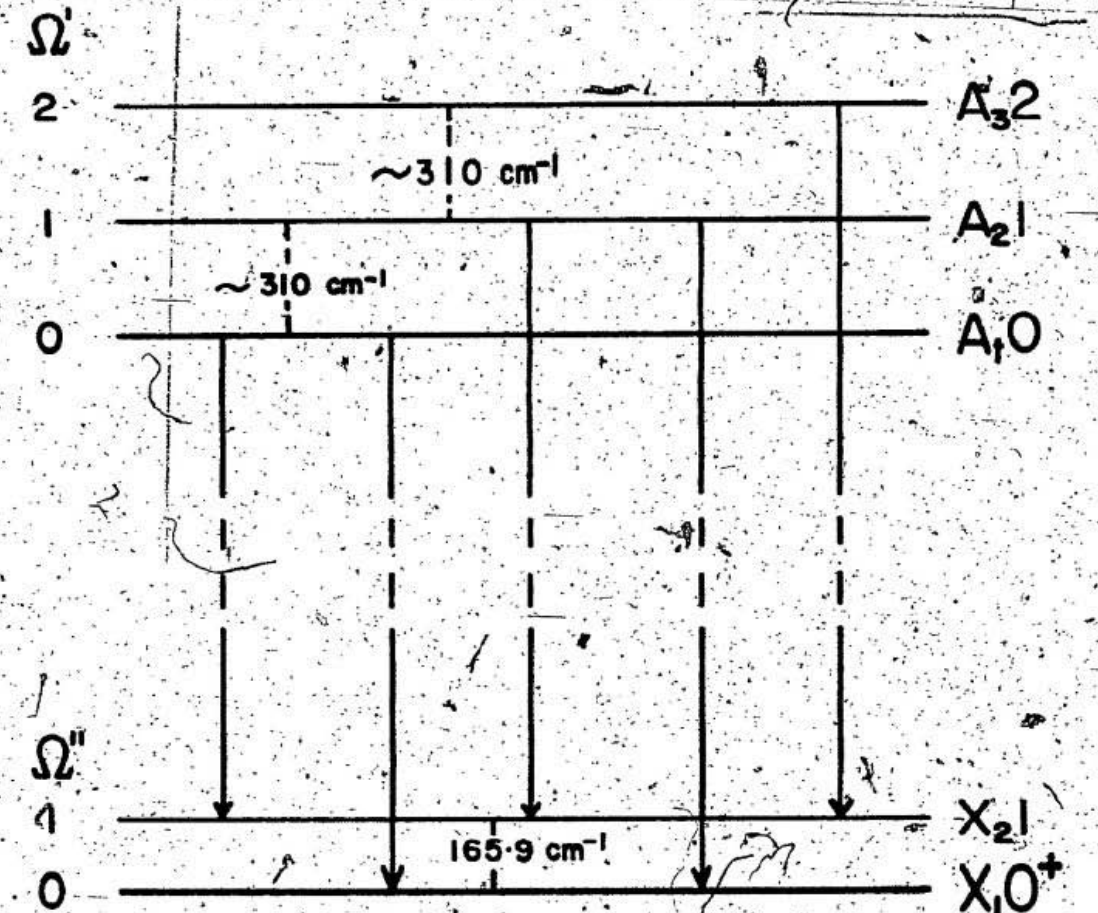

Fig. 17. A schematic energy level diagram showing the subsystems of the A0,1,2 - X0⁺,1 system of SeO, allowed by the selection rule $\Delta\Omega = 0, \pm 1$.

TABLE 9

Bandheads of the AO,1,2 - XO^+,1 system in the region 6720 - 8600 Å

(All bands are degraded to shorter wavelengths)

λ(air) Å	ν_{obs} (vacuum) cm^{-1}	Relative Intensity[a]	v'-v''	$\nu_{obs} - \nu_{calc}$ cm^{-1}
		Subsystem $A_1O-X_1O^+$		
7849.2	12 736	m	1-5 (P)	-2
7842.1	12 748	m	1-5 (Q)	
7408.1	13 495	s	0-3 (P)	0
7350.7	13 600	vw	1-4 (P)	-2
7296.0	13 702	w	2-5 (P)	+2
7289.0	13 716	w	2-5 (Q)	
7245.8	13 797	w	3-6 (P)	0
6905.1	14 478	m	1-3 (P)	+2
6819.5	14 659	w	3-5 (P)	0
		Subsystem A_1O-X_2		
8536.6	11 711	vw	1-6 (P)	
8529.6	11 721	m	1-6 (Q)	
7954.4	12 568	w	1-5 (P)	
7503.6	13 323	m	0-3 (P)	
7443.8	13 430	vw	1-4 (P)	
7033.8	14 213	vw	0-2 (P)	
6986.7	14 309	vw	1-3 (P)	

TABLE 9. (Continued)

λ (air) (Å)	ν_{obs} (vacuum) (cm^{-1})	Relative Intensity[a]	v'-v''	$\nu_{obs}-\nu_{calc}$ (cm^{-1})
		Subsystem $A_2 1-X_1 0^+$		
8286.6	12 064	m	0-5(P)	-5
8280.1	12 074	m	0-5(Q)	
7730.9	12 931	m	0-4(P)	+1
7724.4	12 942	s	0-4(Q)	
7663.2	13 046	m	1-5(P)	+3
7241.7	13 805	s	0-3(P)	-1
7185.8	13 913	m	1-4(P)	+3
7133.6	14 014	w	2-5(P)	+3
		Subsystem $A_2 1-X_2 1$		
7701.2	12 981	vw	2-6(P)	0
7271.3	13 748	w	1-4(P)	+1
7222.9	13 841	vw	2-5(P)	+1
7171.9	13 939	vw	3-6(P)	-1
6836.1	14 624	m	1-3(P)	0
6795.3	14 712	vw	2-4(P)	0
		Subsystem $A_3 2-X_2 1$		
8197.7	12 195	w	0-5(P)	
7650.6	13 067	m	0-4(P)	
7167.4	13 948	m	0-3(P)	
7116.9	14 047	m	1-4(P)	
6739.6	14 834	w	0-2(P)	

[a] Abbreviations used: s, m, w and vw denote strong, medium, weak and very weak, respectively.

TABLE 10

Vibrational scheme of the P heads of the subsystems A_1O-XO^+, 1

v' \ v''	2	3	4	5	6	Mean $\Delta G'_{v+\frac{1}{2}}$
0	14212(1) 890	13495(0^+) 172 13323(1) 983 986				983(0^+) 986(1)
1		14478(0^+) 878	13600(0^+) 864	12736(0^+) 168 12568(1) 857	11711(1)	966(0^+)
2		14309(1)		13702(0^+) 957		957(0^+)
3				14659(0^+) 862	13797(0^+)	
Mean $\Delta G''_{v+\frac{1}{2}}$	890(1)	878(0^+)	864(0^+)	862(0^+) 857(1)		

TABLE 11

Vibrational scheme of the P heads of the subsystems $A_2 1\text{-}XO^+, 1$

v' \ v''	3		4		5		6	Mean $\Delta G'_{v+\frac{1}{2}}$
	13805(0^+)	874	12931(0^+)	867	12064(0^+)			
0								
			982		982			982(0^+)
			13913(0^+)	867	13046(0^+)			
1			165					
	14624(1)	876	13748(1)					
					968			968(0^+)
			964					964(1)
					14014(0^+)			
2					173			
			14712(1)	871	13841(1)	860	12981(1)	
							958	958(1)
3								
							13939(1)	
Mean $\Delta G''_{v+\frac{1}{2}}$		874(0^+)		867(0^+)				
		876(1)		871(1)		860(1)		

$A_2 1 - X_1 0^+$:

$$\nu_e = 16442$$

$$\omega_e' = 996 \qquad \omega_e'x_e' = 7.0$$

$$\omega_e'' = 906 \qquad \omega_e''x_e'' = 3.5$$

$A_3 2 - X_2 1$: $\Delta G'(\frac{1}{2}) = 980$

$$\omega_e'' = 908 \qquad \omega_e''x_e'' = 3.5$$

For the subsystems $A_1 0 - X_2 1$ and $A_2 1 - X_2 1$ the vibrational constants could not be derived because of insufficient data. The bandheads of the subsystems for which the vibrational constants were derived, were calculated from Eq. (2-20) and the values of $(\nu_{obs.} - \nu_{cal})$ are listed in Table 9. These differences range from 0 to 5 cm^{-1}. The vibrational constants of the ground electronic state derived from the present work are in a reasonable agreement with those obtained previously from the B - X system ($\omega_e'' = 914.69$ cm^{-1}, $\omega_e''x_e'' = 4.52$ cm^{-1}) (Barrow & Deutsch, 1963) and from the b - X system ($\omega_e'' = 909.5$ cm^{-1}, $\omega_e''x_e'' = 4.4$ cm^{-1}) (Azam & Reddy, 1973).

(iii) Estimation of Rotational Constant

A rough estimate of the rotational constant B_v' of state A was made from the separation of the observed P and Q heads by using the relation

$$\nu_P - \nu_Q = - \frac{(B'_v + B''_v)^2}{4(B'_v - B''_v)}$$

and the ground state rotational constant B_v'' obtained by Barrow and Deutsch (1963). The derived values in cm^{-1} of B_v' are:

$$B_0'(A_21) = 0.47_0$$

$$B_1'(A_1O) = 0.46_7$$

$$B_2'(A_1O) = 0.46_3$$

(iv) Discussion

The $A^3\Pi_{reg} - X^3\Sigma^-$ system has also been observed for the SO molecule (Colin, 1968). However, in SeO, the vibrational frequency of the A state is larger than the ground state frequency whereas in SO, the reverse is true. This difference may be explained on the basis of the fact that in SO both the $A\ ^3\Pi$ and $X^3\Sigma^-$ states dissociate into the ground-state atoms $S(^3P)$ and $O(^3P)$ whereas in SeO the ground state dissociates into $Se(^3P) + O(^3P)$ but the $A^3\Pi$ state dissociates into $Se(^1D) + O(^3P)$ which is about 9576 cm^{-1} above the ground-state atoms.

In the absence of a large number of observed vibrational levels of an electronic state, the best available estimate of the dissociation energy comes from a linear extrapolation of the vibrational levels. As pointed out by Barrow and Deutsch (1963), for O_2, SO and S_2, this procedure gives dissociation energies which are too large by a factor of about 5/4. Assuming the same correction factor for SeO,

the dissociation energies ($D_e = (4/5)\ \omega_e^2/4\omega_e x_e$) of states A and X are 30 401 cm^{-1} and 37 020 cm^{-1}, respectively. The value of T_e for A is 16 131 cm^{-1}. Thus for SeO, ($D_e + T_e$) of state A minus D_e of state X gives a value of 9512 cm^{-1}, which is in good agreement with the value of 9576 cm^{-1}, the term value of $Se(^1D) + O(^3P)$ above the ground-state atoms.

5.3. The C2, 1, O - $^1XO^+$, 1 System,

(i) Introduction

This transition occurs in the region 2690 - 3190 Å and consists of 40 bands, all degraded to longer wavelengths. The analysis suggests that the bands arise from the transition $^3\Pi_{inv}$ - X. The upper state $^3\Pi_{inv}$ of this transition is labeled $C^3\Pi_{inv}$ because it lies immediately above the $B^3\Sigma^-$ state (Choong, 1938; Barrow & Deutsch, 1963). Also, in the same region, eight new bands of the known B - X system have been observed.

This spectrum was photographed on the Bausch and Lomb spectrograph in the first order of the 1200 g/mm grating. Kodak 103a-O plates were used to photograph the spectra. Due to large variation in the intensity of the spectrum, several plates were exposed with different exposure times ranging from 2 min around 3000 Å to 40 min around 2700 Å while the slit width of the spectrograph was maintained at 70 μm. The reciprocal dispersion obtained with the grating was 4.1 Å/mm at 3000 Å. The accuracy of measurements of

spectra is better than 0.03 Å for sharp heads but it is ~0.08 Å for diffuse heads.

(ii) Vibrational Structure

The first order spectrograms of the C - X system are given in Fig. 18. In the first instance, the analysis of this system appeared somewhat complex on account of the overlapping of the B - X system and the diffuse nature of the bands in the shorter-wavelength region. A preliminary vibrational analysis of the bands which occur in characteristic groups in Fig. 18 (for example, bands at 35 313, 34 407, 35 510, 32 619, and 31 742 cm^{-1}) showed that the lower state vibrational quanta $\Delta G''_{v+\frac{1}{2}}$ (906, 897, 891, and 877 cm^{-1}, respectively) of this system are in close agreement with those of the ground state of SeO, as obtained from earlier work (Barrow & Deutsch, 1963; Azam & Reddy, 1973). The close proximity of these separations suggested that the lower state of the new system is the ground state of SeO. The nature of the upper and the lower states of this system became more clear from the observation of the wavenumber separations between bandheads of certain characteristic group. An example of such a characteristic group of bands is the 0 - 2 group of bandheads at 33 510 cm^{-1} (2984.2 Å), 33 437 cm^{-1} (2989.9 Å), 33 352 cm^{-1} (2997.4 Å), and 32 274 cm^{-1} (3005.4 Å). Here, the separations between the first and third bandheads and the second and fourth bandheads are

Figure 18

Fig. 18. The emission spectrum of SeO in the region 2690 - 3190 Å. Bands marked * were previously assigned to the B-X system by Choong (1938) and Barrow and Deutsch (1963).

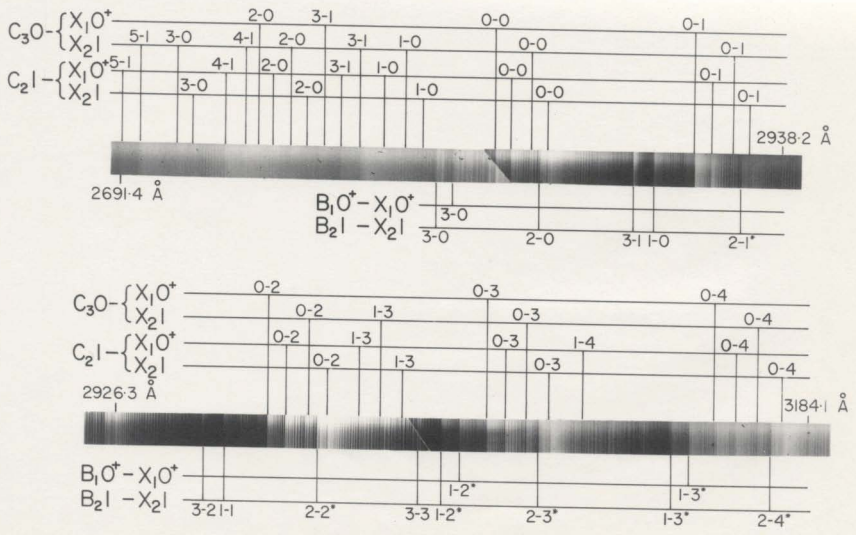
C3O- {X1O+ / X2I
C2I- {X1O+ / X2I
2-0
3-1
0-0
0-1
5-1
3-0
4-1
2-0
3-1
1-0
0-0
0-1
5-1
4-1
2-0
3-1
1-0
0-0
0-1
3-0
2-0
1-0
0-0
0-1
2938·2 Å
2691·4 Å
B1O+ - X1O+
B2I - X2I
3-0
3-0
2-0
3-1
1-0
2-1*
0-2
0-3
0-4
0-2
1-3
0-3
0-4
0-2
1-3
0-3
1-4
0-4
0-2
1-3
0-3
0-4
2926·3 Å
3184·1 Å
3-2
1-1
2-2*
3-3
1-2*
1-2*
2-3*
1-3*
1-3*
2-4*

158 and 163 cm^{-1}, respectively. The fact that these separations are in close agreement with the interval 165.9 cm^{-1} between $\Omega = 0^+$ and $\Omega = 1$ components (cf. Chapter 4) of the ground states of SeO further supports the view that the lower state of the C - X system is the ground state. Also, in the 0 - 2 group of bands, the separations between the first and the second bandheads and the third and the fourth bandheads are 73 and 78 cm^{-1}, respectively. This observation and the fact that there are as many as four bandheads with the same v' - v'' values indicate that the upper state could be a $^3\Pi$ state. Attempts to analyze the system on the basis of the transition $^3\Pi_{reg}$ - X were not successful but all the bands of the system could be analyzed on the assumption that the C state is a $^3\Pi_{inv}$ state. In the following paragraphs we present the results of the vibrational analysis of the C - X system on the basis of the transition $^3\Pi_{inv}$ - X.

Due to moderately large separation between $X_1 0^+$ and $X_2 1$ sublevels of the ground state, the following subsystems of the C - X system are expected to occur on account of the selection rule $\Delta\Omega = 0, \pm 1$:

$C_1 2 - X_2 1$; $C_2 1 - X_1 0^+$; $C_2 1 - X_2 1$;

$C_3 0 - X_1 0^+$; and $C_3 0 - X_2 1$.

In the observed spectrum, the subsystem $C_1 2 - X_2 1$ has not been identified. A shematic diagram of the expected five subsystems of the C - X system is shown in Fig. 19.

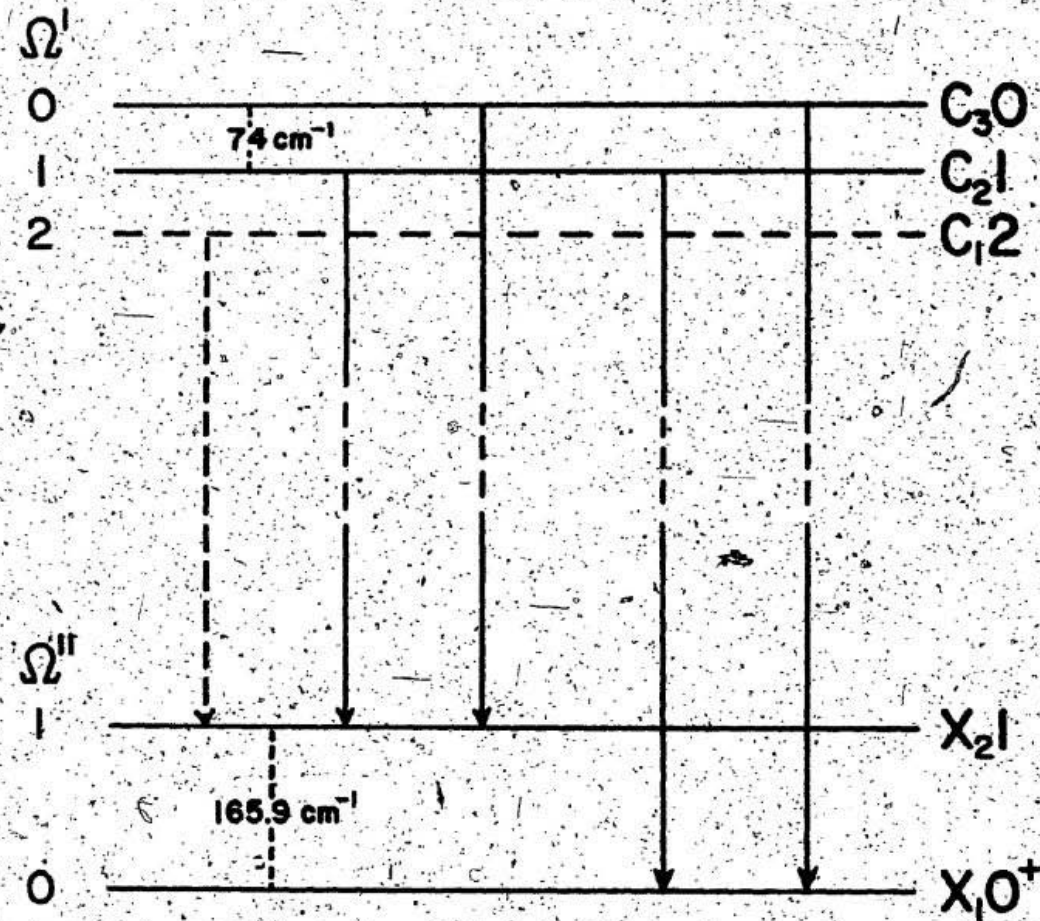

Fig. 19. A schematic energy level diagram showing the allowed subsystems in the C2,1,0 - X0⁺,1 system of SeO. In the present work the subsystem $C_1 2$ - X1 has not been identified.

The data of the bandheads (λ ($\overset{0}{A}$) and ν (cm^{-1})), the visual estimates of their relative intensities, and the vibrational quantum numbers of all the observed four subsystems of the C - X system are listed in Table 12. The Deslandres vibrational schemes for the subsystems $C_2 1 - XO^+, 1$ and $C_3 O - XO^+, 1$ are shown in Tables 13 and 14, respectively. The vibrational constants ω_e and $\omega_e x_e$ of the upper and ground states were calculated by the least squares method using Eq. (2-21) and ν_e was calculated from Eq. (2-20). The constants obtained from the vibrational analysis are listed below in cm^{-1}. For the subsystem $C_3 O - X_1 O^+$, the vibrational constants could not be derived due to insufficient data.

$C_3 O - X_2 1$:

$$\nu_e = 35\,323$$

$$\omega_e' = 581 \qquad \omega_e' x_e' = 3.5$$

$$\omega_e'' = 914 \qquad \omega_e'' x_e'' = 3.9$$

$C_2 1 - X_1 O^+$:

$$\nu_e = 35\,405$$

$$\omega_e' = 586 \qquad \omega_e' x_e' = 4.2$$

$$\omega_e'' = 914 \qquad \omega_e'' x_e'' = 4.1$$

$C_2 1 - X_2 1$:

$$\nu_e = 35\,238$$

$$\omega_e' = 583 \qquad \omega_e' x_e' = 4.0$$

$$\omega_e'' = 911 \qquad \omega_e'' x_e'' = 3.8$$

TABLE 12

Bandheads of the C 2,1,0-XO^+,1 system[a] in the region 2690 - 3190 Å

λ(air) Å	ν_{obs} (vacuum) (cm^{-1})	Relative Intensity[b]	v'v''	$\nu_{obs} - \nu_{calc}$ (cm^{-1})
		Subsystem $C_2 1 - X_2 1$		
3173.0	31 506	w	0-4	0
3086.5	32 389	m	0-3	+2
3033.1	32 960	w	1-3	-2
3004.4	33 274	m	0-2	-1
2925.6	34 171	m	0-1	0
2850.2	35 075	m	0-0	+1
2803.9	35 654	vw	1-0	+5
2760.1	36 221	vw	2-0	+5
2718.1	36 780	w	3-0	+5
		Subsystem $C_2 1 - X_1 O^+$		
3187.0	31 666	m	0-4	-1
3100.4	32 245	w	1-4	0
3071.5	32 547	m	0-3	-1
3018.0	33 125	m	1-3	-1
2989.9	33 437	m	0-2	-1
2911.8	34 334	s	0-1	-1
2836.9	35 240	m	0-0	-1
2791.0	35 820	vw	1-0	+1
2773.5	36 045	w	3-1	+2
2747.4	36 388	w	2-0	0
2731.5	36 600	w	4-1	+5
2691.5	37 144	w	5-1	+5

TABLE 12 (Continued)

λ(air) Å	ν_{obs} (vacuum) (cm^{-1})	Relative Intensity[b]	v'-v''	$\nu_{obs}-\nu_{calc}$ (cm^{-1})
		Subsystem $C_3O-X_2^1$		
3165.6	31 580	m	0-4	+1
3079.5	32 463	m	0-3	+2
3025.8	33 039	w	1-3	+4
2997.4	33 352	s	0-2	0
2918.9	34 250	s	0-1	0
2843.6	35 156	m	0-0	-1
2797.8	35 732	vw	1-0	+1
2780.8	35 951	w	3-1	0
2754.3	36 297	w	2-0	-1
2738.7	36 504	w	4-1	0
2712.4	36 857	w	3-0	-1
2698.2	37 051	w	5-1	+1
		Subsystem $C_3O-X_1O^+$		
3149.4	31 742	w	0-4	
3064.8	32 619	m	0-3	
2983.3	33 510	s	0-2	
2905.6	34 407	m	0-1	
2830.9	35 313	m	0-0	
2768.5	36 110	vw	3-1	
2742.3	36 456	vw	2-0	

[a] All bands are degraded to longer wavelengths.

[b] Abbreviations used: s, m, w and vw denote stong, medium, weak and very weak, respectively.

TABLE 13

Vibrational scheme of the subsystem $C_2 1\text{-}XO^+, 1$

v' \ v''	0		1		2		3		4	Mean $\Delta G'_{v+\frac{1}{2}}$
	35240 (0^+)	906	34334 (0^+)	897	33437 (0^+)	890	32547 (0^+)	881	31666 (0^+)	
0	165		163		163		158		160	
	35075 (1)	904	34171 (1)	897	33274 (1)	885	32389 (1)	883	31506 (1)	
	580						578		579	579 (0^+)
	579						571			575 (1)
	35820 (0^+)						33125 (0^+)	880	32245 (0^+)	
1	166						165			
	35654 (1)						32960 (1)			
	568									568 (0^+)
	567									567 (1)
	36388 (0^+)									
2	167									
	36221 (1)									
	559									559 (1)
			36045 (0^+)							
3										
	36780 (1)									
	–		555							555 (0^+)
	–		–							
	–		36600 (0^+)							
4			–							
			–							544 (0^+)
			544							
			–							
			37144 (0^+)							
5			–							
Mean $\Delta G'_{v+\frac{1}{2}}$		906 (0^+)		897 (0^+)		890 (0^+)		881 (0^+)		
		904 (1)		897 (1)		885 (1)		883 (1)		

TABLE 14

Vibrational scheme of the subsystems C_3O-XO^+, 1

v'' / v'	0		1		2		3		4	Mean $\Delta G'_{v+\frac{1}{2}}$
	35313 (0^+)	906	34407 (0^+)	897	33510 (0^+)	891	32619 (0^+)	877	31742 (0^+)	
0	157		157		158		156		162	
	35156 (1)	906	34250 (1)	898	33352 (1)	889	32463 (1)	883	31580 (1)	
	–		–		–		–			
	576						576			576 (1)
	–						–			
1	–						–			
	35732 (1)						33039 (1)			
	–									
	565									565 (1)
	36456 (0^+)									
2	159									
	36297 (1)									
	–									
	560									560 (1)
	–		36110 (0^+)							
3	–		159							
	36857 (1)	906	35951 (1)							
			–							
			553							553 (1)
			–							
4			–							
			36504 (1)							
			–							
			547							547 (1)
			–							
5			–							
			37051 (1)							
Mean $\Delta G''_{v+\frac{1}{2}}$		906 (0^+)		897 (0^+)		891 (0^+)		877 (0^+)		
		906 (1)		898 (1)		889 (1)		883 (1)		

The bandheads were calculated from Eq. (2-20) and the differences $\nu_{obs} - \nu_{calc}$ are listed in Table 12. These differences vary from 0 to 5 cm^{-1}. The ground state vibrational constants derived from the analysis of the C - X system are in reasonably good agreement with those obtained from the analysis of the B - X and b - X systems, as given in section 5.2. The difference between the ν_e^o values of the $C_2 1 - X_1 0^+$ and $C_2 1 - X_2 1$, which is 167 cm^{-1}, represents the separation between the $\Omega = 0^+$ and $\Omega = 1$ substates of the ground state of SeO and is consistent with the value (165.9 cm^{-1}) obtained in Chapter 4.

5.4. Extension of the Known B - X System

In the region 2800 - 3040 Å, eight new bands degraded to longer wavelengths have been observed. These bands could not be fitted into the C - X system but it was possible to include them in the Deslandres vibrational scheme of the known B - X system. Seven of these bands belong to the $B_1 0^+ - X_1 0^+$ subsystem and one belongs to the $B_2 1 - X_2 1$ subsystem. These new bands together with a few other bands previously analyzed (Choong, 1938; Barrow & Deutsch, 1963) are shown in Fig. 18. The wavelengths (Å), wavenumbers (cm^{-1}), visual estimate of the intensities, and the vibrational quantum numbers of the new bands are listed in Table 15.

TABLE 15

New bands of the B-X system[a]

λ (air) Å	ν_{obs} (vacuum) (cm^{-1})	Relative Intensity[b]	v'-v''
	Subsystem $B_1O^+-X_1O^+$		
3039.0	32 895	m	3-3
2967.3	33 691	s	1-1
2959.2	33 784	m	3-2
2890.3	34 588	s	1-0
2882.6	34 681	s	3-1
2847.4	35 109	s	2-0
2809.1	35 588	w	3-0
	Subsystem B_2l-X_2l		
2815.1	35 513	w	3-0

[a]All bands are degraded to longer wavelengths.

[b]Abbreviations used: s, m and w denote strong, medium and weak, respectively.

5.5. The F - a and G - a Systems

This section describes two brief band systems of the SeO molecule in the far ultraviolet region. One of the systems occurs in the region 2150 - 2270 Å and the other in the region 2070 - 2130 Å. Actually these bands were first observed under low dispersion by Haranath (1964) and later reinvestigated under medium dispersion by Reddy and Azam (1974a). But none of these researchers could assign these bands to a system having connection with any of the known states of SeO. In section 5.1, the observation of the $a^1\Delta$ state of SeO from the analysis of the a - X system is described. From this knowledge, it is now possible to do a vibrational analysis of these bands, in terms of two brief systems both having the $a^1\Delta$ state as their common lower state. The exact nature of the upper states is not known. However, from their T_e values, these are assigned as F - $a^1\Delta$ and G - $a^1\Delta$ systems, respectively.

These bands were photographed on the 2 m Bausch and Lomb spectrograph in the third order of the 1200 grooves/mm grating with Kodak SWR plates. The exposure times varied between three and four hours. A 5 cm clorine filter was used to remove the second order spectrum and SWR plates are not sensitive to the first order spectrum. Copper lines were used as wavelength standards. The reciprocal linear dispersion at 2100 Å is 1.29 Å/mm in the third order spectrum.

The spectrograms of the F - $a^1\Delta$ and G - $a^1\Delta$ systems are given in Fig. 20. All the bands belonging to both systems are degraded to shorter wavelengths. Some bands of the G - a system have diffuse heads. The wavelengths λ (air, $\mathring{A}$), the wavenumbers ν (vacuum, cm^{-1}), the visual estimate of the relative intensities and the vibrational quantum numbers for the bands of these systems are given in Table 16. Deslandres' vibrational scheme for the G - a system is given in Table 17. The $\Delta G(\frac{1}{2})$ values for the $a^1\Delta$ state obtained from the analysis of the F - a and G - a systems are 874 and 870 cm^{-1}, respectively. These are in reasonable agreement with the previous value (883 cm^{-1}) obtained from the near infrared system considering the fact that at 2100 $\mathring{A}$, one angstrom equals 23 cm^{-1}. However, the confirmation of the present interpretation, namely, that the common lower state of the two band systems is $a^1\Delta$ must come from rotational analyses of these systems. The vibrational constants for these systems in cm^{-1} are as follows:

F - $a^1\Delta$ system:

$$\nu_{00} = 46\ 082$$

$$\Delta G'(\tfrac{1}{2}) = 953$$

$$\Delta G''(\tfrac{1}{2}) = 874$$

G - $a^1\Delta$ system:

$$\nu_e = 47\ 829$$

$$\omega_e'' = 971 \qquad \omega_e'x_e' = 12.5$$

$$\omega_e'' = 875 \qquad \omega_e''x_e'' = 2.5$$

Figure 20

Fig. 20. The emission band systems G - $a^1\Delta$ and F - $a'^1\Delta$ of SeO.

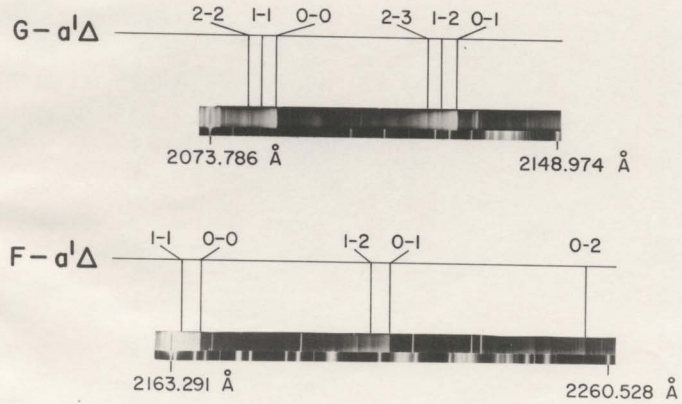
G – a¹Δ
2-2
1-1
0-0
2-3
1-2
0-1
2073.786 Å
2148.974 Å
F – a¹Δ
1-1
0-0
1-2
0-1
0-2
2163.291 Å
2260.528 Å

TABLE 16

Bandheads of the F-$a^1\Delta$ and G-$a^1\Delta$ systems[a]

λ(air) (Å)	ν_{obs} (vacuum) (cm^{-1})	Relative Intensity[b]	v'-v''
	F-$a^1\Delta$		
2165.7	46 160	s	1-1
2169.3	46 082	s	0-0
2206.8	45 300	m	1-2
2211.3	45 208	m	0-1
2254.2	44 348	m	0-2
	G-$a^1\Delta$		
2082.4	48 006	w	2-2
2084.9	47 950	w	1-1
2088.2	47 874	s	0-0
2120.4	47 146	m	2-3
2123.2	47 085	m	1-2
2126.7	47 004	s	0-1

[a]All bands are degraded to shorter wavelengths.

[b]Abbreviations used: s, m and w denote strong, medium and weak, respectively.

TABLE 17

Vibrational scheme of the G-$a^1\Delta$ system

v	v'' 0		1		2		3	Mean $\Delta G'_{v+\frac{1}{2}}$
0	47874	870	47004					
			946					946
1			47950	865	47085			
					921			921
2					48006	860	47146	
Mean $\Delta G''_{v+\frac{1}{2}}$		870		865		860		

The vibrational constants for the upper states F and G appear to be nearly equal. However, as these states are separated by ~1800 cm^{-1}, they can not be assigned as the components of the same electronic state.

CHAPTER 6

MOLECULAR CONSTANTS, ELECTRON CONFIGURATIONS AND POTENTIAL ENERGY CURVES OF SeO

In this chapter, molecular constants derived for all the observed electronic states of SeO are summarized. Also included here are the electron configurations for the ground and low-lying excited states of SeO and the potential energy curves for its states X_1O^+, bO^+, A_1O and B_1O^+ calculated by Klein-Dunham method.

6.1. Summary of Molecular Constants

In Chapter 1, the known electronic transitions of the SeO molecule, before the present research project was undertaken, have been described. Now that several new electronic band systems of this molecule are observed and analyzed during the course of the present work, it is considered worthwhile to summarize all the existing data on this molecule. Table 18 lists the term values of the electronic states, derived molecular constants and the observed electronic transitions of SeO. In this table a mixed case (b) - case (c) notation is used for the electronic states and the term values T_e are represented with respect to the minimum in the $\Omega = 0^+$, i.e., $^3\Sigma_0^-$ component of the ground state. For

TABLE 18

Molecular Constants (in cm^{-1}) of the SeO Molecule

State	T_e	ω_e	$\omega_e x_e$	B	α_e	r (Å)	λ	Observed Transition	Reference
G	53457*	971	12.5					G-a	Present Work
$c^1\Sigma_o^+$	53258	954	13.0					c-b	Reddy and Azam (1974)
F	51665*	$\Delta G(\frac{1}{2})$=953						F-a	Present Work
$E_2\,^3\Sigma_1^-$	51588	955	9.3				~36	E_2-X_2	Reddy and Azam (1974)
$E_1\,^3\Sigma_o^-$	51528	955	8.5					E_1-X_1	"
D	50870	1034	9.3					D-X	"
$C_3\,^3\Pi_o$	35489	581	3.5					C_3-X_2	Present Work
$C_2\,^3\Pi_1$	35405	586	4.2					C_2-X_1	"
$B_2\,^3\Sigma_1^-$	34012.18*	$\Delta G(\frac{1}{2})$=517.7		B_o=0.3391		r_o=1.931 Å	λ_o=51	B_2-X_2	Barrow & Deutsch (1963)

TABLE 18 (Continued)

State	T_e	ω_e	$\omega_e x_e$	B	α_e	$r(\AA)$	λ	Observed Transition	Reference
$B_1\,^3\Sigma_o^-$	34081.75*	522.3	3.9	B_o=0.3332				B_1-X_1	Barrow & Deutsch (1963)
$A_3\,^3\Pi_2$	16758	$\Delta G(\frac{1}{2})$=980						A_3-X_2	Present Work
$A_2\,^3\Pi_1$	16442	996	7.0	(B_o= 0.476)				A_2-X_1	"
$A_1\,^3\Pi_o$	16131	994	6.5	(B_1= 0.467)				A_1-X_1	"
$b\,^1\Sigma_o^+$	9725.55	838.83	5.11	B_o=0.4560		r_o=1.667		b-X	Present Work, Azam and Reddy (1973)
$a\,^1\Delta$	5577.6*	$\Delta G(\frac{1}{2})$=883.3		B_o=0.461				a-X_2	Present Work
$X_2\,^3\Sigma_1^-$	165.9	915.43	4.52	B_e=0.4704	0.0033	r_e=1.640	λ_o=86.4	—	Barrow and Deutsch (1963) and Present Work
$X_1\,^3\Sigma_o^-$	0	914.69	4.52	B_e=0.4655	0.0032			—	"

*ν_{oo} value

†Carrington et al. (1972)

the states for which the vibrational constants ω_e and $\omega_e x_e$ could not be derived, their $\Delta G(\frac{1}{2})$ values are given. A schematic energy level diagram of SeO is given in Fig. 21. It is to be noted that the states designated C and D earlier by Reddy and Azam (1974) will hereafter be referred to as D and E, respectively. In Fig. 21, for state $C\,^3\Pi_{inv}$, the $C_1\,^3\Pi_2$ component and the transition $C_1\,^3\Pi_2 - X_2 1$ are shown with dotted lines although this transition has not been observed experimentally.

6.2. Electron Configurations

The electron configurations of the O and Se atoms are

$$O:\ K\ 2s^2 2p^4\ ;\quad Se:\ KLM\ 4s^2 4p^4$$

In standard notation (Mulliken, 1932; Herzberg, 1950) the lowest electron configuration of the SeO molecule is written as

$$KKLM\ (z\sigma)^2\ (y\sigma)^2\ (w\pi)^4\ (x\sigma)^2\ (v\pi)^2\ :\ {}^3\Sigma^-,\ {}^1\Delta,\ {}^1\Sigma^+. \qquad (6\text{-}1)$$

The three states resulting from configuration (6-1) are attributed to the $X\,^3\Sigma^-$, $a\,^1\Delta$ and $b\,^1\Sigma^+$ states. As pointed out earlier in this thesis, the states of the forbidden transitions $a\,^1\Delta - X\,^3\Sigma^-$ and $b\,^1\Sigma^+ - X\,^3\Sigma^-$ belong to this configuration.

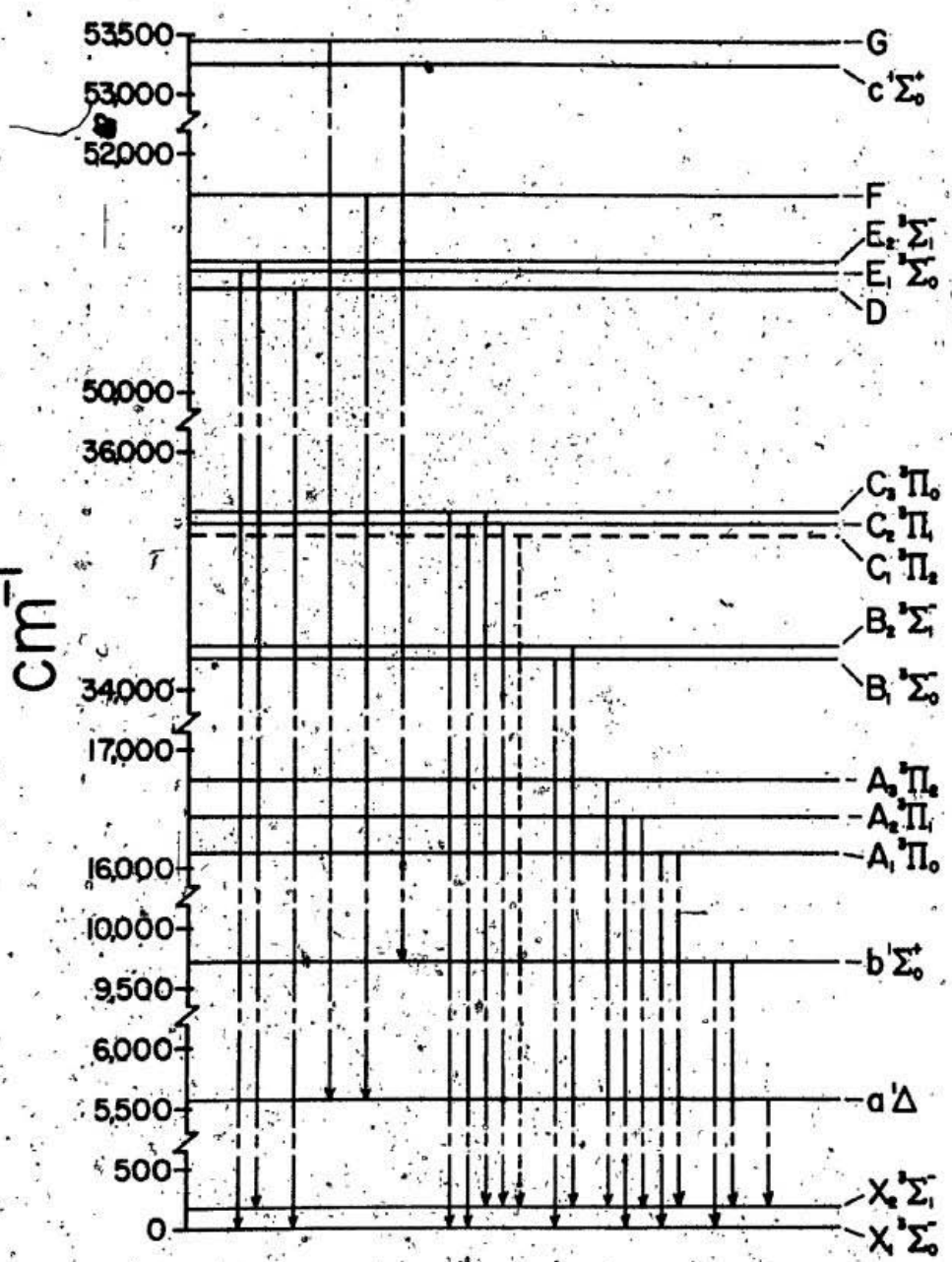

Fig. 21. A schematic energy level diagram showing all the observed electronic transitions of SeO.

The expected low-lying excited electron configurations of SeO are obtained by bringing the electrons from the v, x, or w orbitals to the higher orbitals. These are written as follows

$$KKLM\ (z\sigma)^2\ (y\sigma)^2\ (w\pi)^4\ (x\sigma)^2\ (v\pi)\ (u\sigma) : {}^1\Pi, {}^3\Pi_{reg} \quad (6\text{-}2)$$

$$KKLM\ (z\sigma)^2\ (y\sigma)^2\ (w\pi)^4\ (x\sigma)\ (v\pi)^2\ (u\sigma) : {}^1\Sigma^+, {}^1\Sigma^-, {}^1\Delta, {}^3\Sigma^+, {}^3\Sigma^-\ (2), {}^3\Delta, {}^5\Sigma^+ \quad (6\text{-}3)$$

$$KKLM\ (z\sigma)^2\ (y\sigma)^2\ (w\pi)^4\ (x\sigma)\ (v\pi)^3 : {}^1\Pi, {}^3\Pi_{inv}. \quad (6\text{-}4)$$

Further higher electron configurations involve excitation from the $(w\pi)^4$ orbital and require rather somewhat more energy than the configurations (6-2) to (6-4). Among the excited electronic states of SeO observed in the present work, A $^3\Pi_{reg}$ most probably belongs to the configuration (6-2) and C $^3\Pi_{inv}$ to the configuration (6-4). States B, c and E may belong to the configuration (6-3). States D, F and G whose nature is not yet known may belong to any of the configurations from (6-2) to (6-4).

6.3. Potential Energy Curves of States X_1O^+, bO^+, A_1O and B_1O^+

The electronic states selected for the calculation of the potential energy curves are X, b, A and B because only for these states the rotational constants (B_v) are known

(although approximately for state A). The potential energy curves for X_1O^+, bO^+, A_1O and B_1O^+ are derived by Klein-Dunham method (described in Chapter 2). A computer program written in FORTRAN IV (TRABRB 1970) was used on the IBM 370 computer to calculate the vibrational wavefunctions, Franck-Condon factors and r-centroids. It uses as its input the observed vibrational energy levels $G(v)$ [$= \omega_e(v+\frac{1}{2}) - \omega_e x_e (v+\frac{1}{2})^2$], the rotational constants B_v [$= B_e - \alpha_e(v+\frac{1}{2})$], the dissociation energies D_e and the reduced-mass μ[$\mu(^{80}SeO) = 13.32747$ amu]. The B_e and α_e values for the bO^+ state were estimated with the help of the derived B_o value, observed separations of R and Q heads in the $bO^+ - X_2 1$ subsystem and also from the Pekeris relation (cf. Herzberg, 1950)

$$\alpha_e = \sqrt{\frac{6\ \omega_e x_e\ B_e^3}{\omega_e}} - \frac{6B_e^2}{\omega_e} .$$

Their values are $B_e = 0.4578$ cm^{-1} and $\alpha_e = 0.0035$ cm^{-1}. The estimation of B_e and α_e for the A_1O state was based upon the results given in Chapter 5 and the resulting values are $B_e = 0.473_5$ and $\alpha_e = 0.003_5$. The dissociation energies D_e were calculated from the expression $D_e = (4/5)\omega_e^2/4\omega_e x_e$. As pointed out in Chapter 5, the factor 4/5 in this expression was used because of the fact that for the analogous molecules O_2, S_2, and SO the linear extrapolation of vibrational levels gives dissociation energies which are about

25% higher than the actual values. The corrected values* of D_e for states X, b, A and B are 37 020, 27 540, 30 400, and 13 990 cm^{-1} respectively.

The computer program calculates the Klein-Dunham potential curves and then extrapolates them by means of fitted Morse function. The values of the step size, r_{min} and r_{max} used in the present calculations are 0.005 Å, 0.750 Å, and 4.500 Å, respectively. The derived Klein-Dunham turning points are given in Table 19 and the potential energy curves are shown in Fig. 22. In this figure the dots represent the calculated turning points and the solid curves beyond the dots represent the fitted Morse function. The maximum value of the noise-factor in these calculations was $\leq 10^{-11}$.

The values of the low-lying spectral terms (in cm^{-1}) of Se and O atoms are given below (cf. Moore, 1949, 1952):

State	Se	O
$^3P_2$	0	0
$^3P_1$	1989.5	158.5
^3P_o	2534.4	226.5
^1D	9576.08	15867.7
^1S	22446.03	33792.4

Based on these values and the calculated values of D_e for SeO, it is inferred that states X and b dissociate into the

---

* These values are probably accurate within 100 cm^{-1} or so.

TABLE 19

Klein-Dunham turning points for $X_1 0^+$, $b0^+$, $A_1 0$ and $B_1 0^+$ states of ^{80}SeO

v	U(r) (cm^{-1})	r_{min} (Å)	r_{max} (Å)	U(r) (cm^{-1})	r_{min} (Å)	r_{max} (Å)
	$X_1 0^+$ state			$b0^+$ state		
0	0	1.6484	1.6484	9 725.55	1.6622	1.6622
1	456.22	1.5986	1.7039	10 143.69	1.6101	1.7202
2	1 357.35	1.5650	1.7488	10 972.30	1.5754	1.7671
3	2 258.48	1.5438	1.7811	11 790.69	1.5531	1.8018
4	3 146.05	1.5270	1.8093	12 598.86	1.5358	1.8316
5	4 024.58	1.5130	1.8346	13 396.81	1.5214	1.8586
6	4 894.07	1.5010	1.8580	14 184.54	1.5089	1.8838
7	5 754.52	1.4904	1.8802	14 962.05	1.4979	1.9077
8	6 605.93	1.4808	1.9014	15 729.34	1.4880	1.9306
9	7 448.30	1.4722	1.9219	16 486.41	1.4790	1.9528
10	8 281.63	1.4642	1.9418			
	$A_1 0$ state			$B_1 0^+$ state		
0	16 130.6	1.6344	1.6344	34 277.7	1.9162	1.9162
1	16 626.0	1.5868	1.6878	34 535.9	1.8553	2.0081
2	17 607.0	1.5549	1.7311	35 052.4	1.8157	2.1174
3	18 575.0	1.5343	1.7630	35 559.1	1.7904	2.2008

Figure 22

Fig. 22. Potential energy curves for the $X_1 0^+$, $b0^+$, $A_1 0$ and $B_1 0^+$ states of SeO. The dots are Klein-Dunham turning points. Solid curves beyond the dots are Morse curves. A schematic potential energy curve for the a2 state is also shown. The Morse curve for the B state beyond v = 3 is found to be almost linear and hence is represented by a dashed curve.

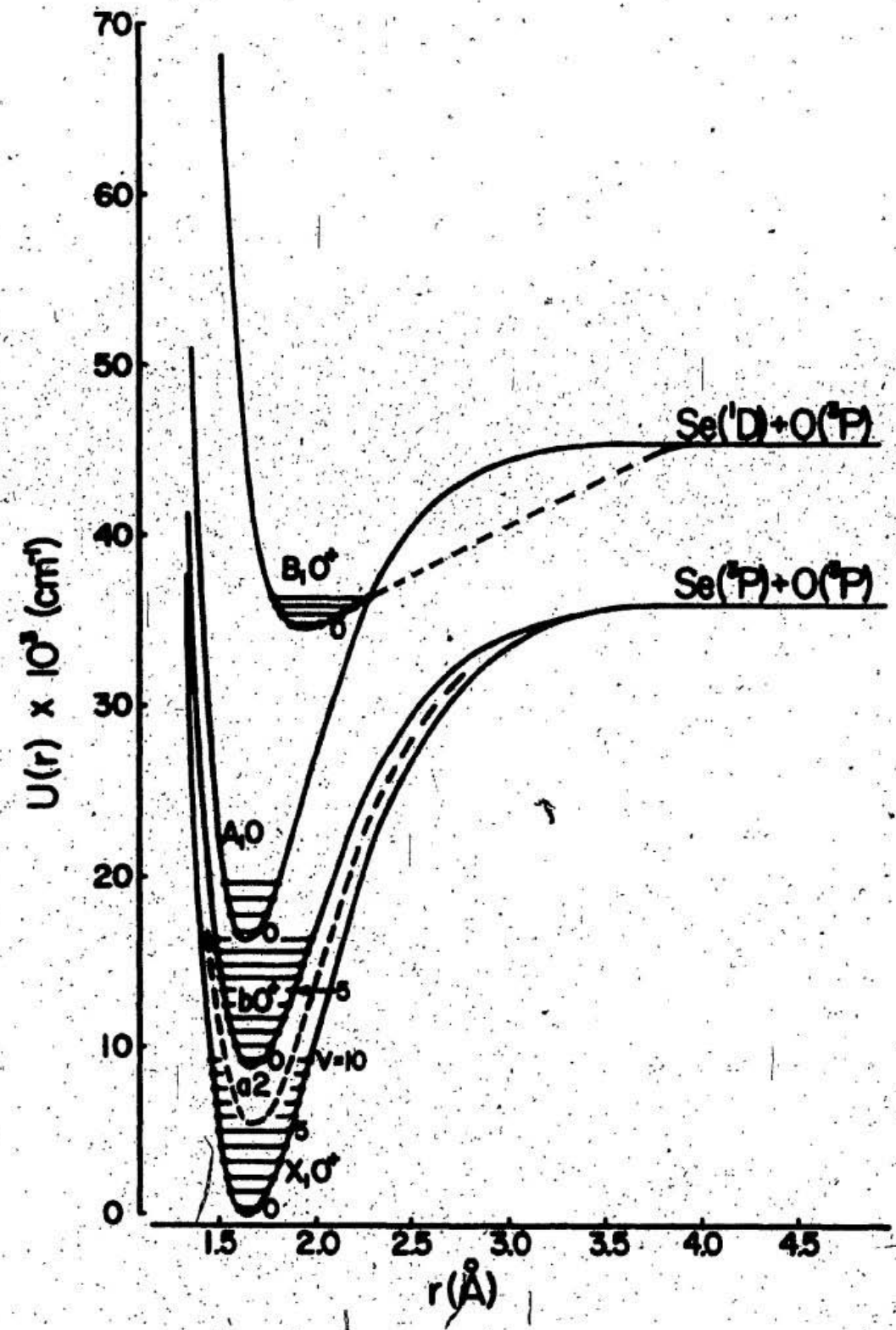
70
60
50
40
30
20
10
0
U(r) x 10³ (cm⁻¹)
Se(¹D)+O(³P)
Se(³P)+O(³P)
B,0⁺
A,0
bΠ
a2
X,Σ⁺
V=10
0
5
1.5
2.0
2.5
3.0
3.5
4.0
4.5
r(Å)

ground state products $Se(^3P) + O(^3P)$. The third state which also dissociates into these atomic products is $a^1\Delta$ (or a2) whose T_{oo} value is known (Table 18). States B and A of SeO dissociate into the atomic products $Se(^1D) + O(^3P)$ whereas for the analogous molecule SO, state B dissociates into $S(^1D) + O(^3P)$ but state A dissociates into $S(^3P) + O(^3P)$ (see section 5.2). Among the other states of SeO, $C^3\Pi_{inv}$ seems to dissociate into $Se(^3P) + O(^1D)$. It is noticed from Fig. 22 that state A_1 crosses state B_1 around $v = 3$ and this may be the reason why state B is highly perturbed (Barrow & Deutsch, 1963). In conclusion it must be pointed out that the extended parts of the potential energy curves well beyond the actual experimental points in Fig. 22 by Morse functions are considered to be approximate.

CHAPTER 7

ROTATIONAL ANALYSIS OF THE $B^2\Sigma^+ - X^2\Pi_{reg}$ SYSTEM OF SbO

7.1. Introduction

A brief review of the previous work on the electronic band spectrum of SbO was given in Chapter 1 of this thesis. It was Sengupta (1939) who first proposed the vibrational analysis of the $B^2\Sigma - X^2\Pi_{reg}$ system of SbO in the region 3240 - 4720 Å. The first high resolution work on SbO was that of Lakshman (1960b) who analyzed the rotational structure of the two 0 - 0 subbands of the B - X system from the spectrum photographed at a dispersion of 1.25 Å/mm. Singh and Upadhyay (1967) photographed the same two bands at a dispersion of 0.33 Å/mm and have identified the rotational lines due to both isotope molecules ^{121}SbO and ^{123}SbO. However, no further results of this work are given in their short note. Subsequently, Rao and Rao (1968) reanalyzed the rotational structure of the same two subbands which were photographed at a dispersion of 0.63 Å/mm. The present work is concerned with a detailed rotational analysis of the 0 - 0 and 1 - 0 bands of the $B^2\Sigma^+ - X^2\Pi_{3/2}$ subsystem.

The emission spectrum of SbO was excited in an electrodeless quartz discharge tube by the Raytheon model

PGM-100 microwave generator. Spectra were initially photographed with the 2 m Bausch and Lomb spectrograph at medium dispersion (~3.9 Å/mm). The rotational structure of several bands of the B - X system was photographed with the 3.4 m Jarrell-Ash Ebert spectrograph in the third order of the Bausch and Lomb special grating with 1200 grooves/mm (cf. Chapter 3) at a dispersion of ~0.56 Å/mm. The slit width of the spectrograph was maintained at 30 μm. Kodak 103a-O plates were used to photograph the spectra. Higher orders in the high resolution spectra were removed by a Corning filter CS 0-52. The exposure times varied between 30 sec and 3 min. The error in the measurement of sharp lines is estimated to be 0.008 Å; however, it is considerably more for diffuse and blended lines.

A spectrogram showing a part of both the subsystems $B - X^2\Pi_{\frac{1}{2}}$ and $B - X^2\Pi_{3/2}$ of SbO photographed with Bausch and Lomb spectrograph is given in Fig. 23. The measured wavelengths of the intense bands 1 - 0, 0 - 0 and 0 - 1 of these subsystems are given below (Sengupta, 1939):

Band	Subsystem	λ_{air} (Å)
1-0 R_{21}	$B^2\Sigma^+ - X^2\Pi_{\frac{1}{2}}$	3696.45
0-0 R_{21}	"	3776.00
0-1 R_{21}	"	3894.84
1-0 Q_2	$B^2\Sigma^+ - X^2\Pi_{3/2}$	4035.00
0-0 Q_2	"	4130.22
0-1 Q_2	"	4272.74

Figure 23

Fig. 23. Intense bands of the $B^2\Sigma^+ - X^2\Pi$ system of SbO in the region 3620 - 4280 Å.

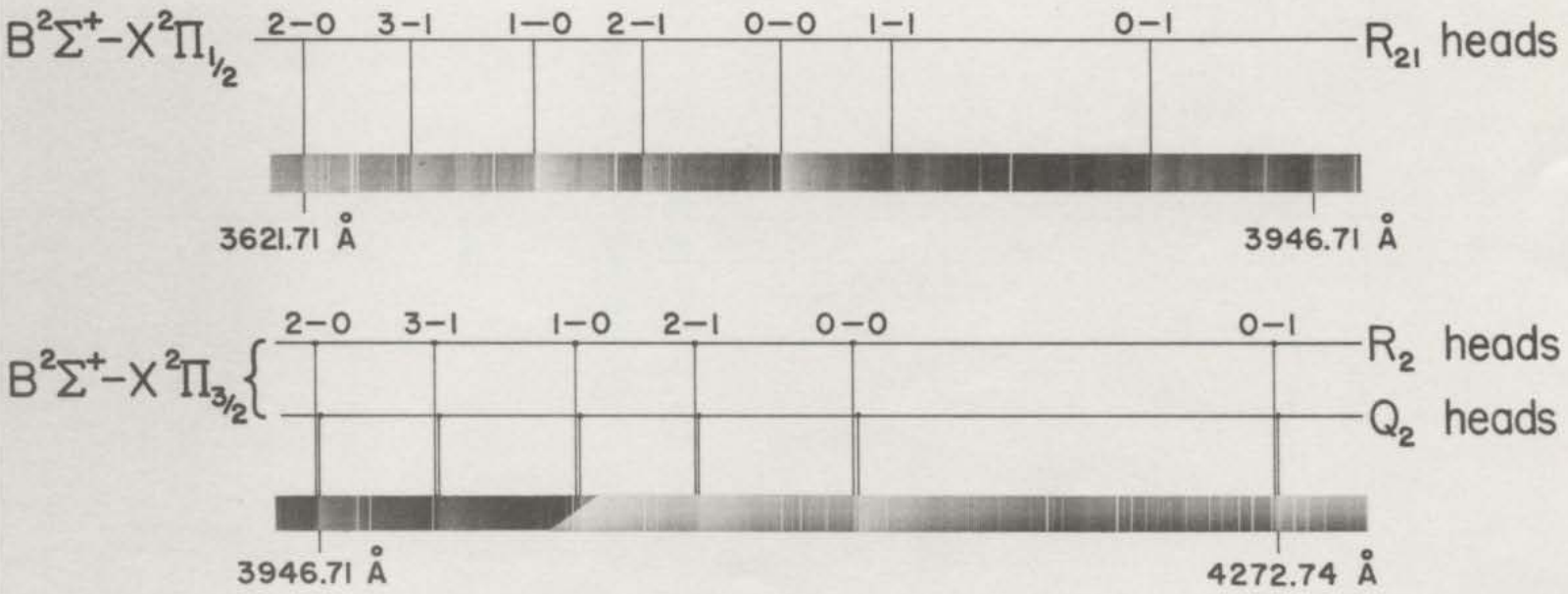
$B^2\Sigma^+ - X^2\Pi_{1/2}$
2–0
3–1
1–0
2–1
0–0
1–1
0–1
R_{21} heads
3621.71 Å
3946.71 Å
$B^2\Sigma^+ - X^2\Pi_{3/2}$
2–0
3–1
1–0
2–1
0–0
0–1
R_2 heads
Q_2 heads
3946.71 Å
4272.74 Å

7.2. Rotational Structure of a $^2\Sigma^+ - {}^2\Pi_{reg}$ Transition

It is known from the earlier work that the spin-orbit splitting in the ground state $X^2\Pi_{reg}$ of SbO is very large (~2270 cm^{-1}) and there is no sign of any large splitting in its $B^2\Sigma^+$ state. This implies that $X^2\Pi_{reg}$ belongs to Hund's case (a) and $B^2\Sigma^+$ retains its case (b) character. Thus the B - X system of SbO is an example of a "mixed case" transition.

The rotational term values for case (b) $^2\Sigma$ state are given by (cf. Eq. (2-12))

$$F_1(N) = B_v N(N+1) - D_v N^2(N+1)^2 + \tfrac{1}{2}\gamma N, \qquad (7\text{-}1a)$$

$$F_2(N) = B_v N(N+1) - D_v N^2(N+1)^2 - \tfrac{1}{2}\gamma (N+1), \qquad (7\text{-}1b)$$

where γ is the splitting constant, and $F_1(N)$ and $F_2(N)$ refer to the components with $J = N+\frac{1}{2}$ and $N-\frac{1}{2}$ respectively. In terms of J we have

$$F_1(J) = B_v(J-\tfrac{1}{2})(J+\tfrac{1}{2}) - D_v(J-\tfrac{1}{2})^2(J+\tfrac{1}{2})^2 + \tfrac{1}{2}\gamma(J-\tfrac{1}{2}), \qquad (7\text{-}2a)$$

$$F_2(J) = B_v(J+\tfrac{1}{2})(J+3/2) - D_v(J+\tfrac{1}{2})^2(J+3/2)^2 - \tfrac{1}{2}\gamma(J+3/2). \qquad (7\text{-}2b)$$

Normally the value of γ is very small compared to B_v and from the above two equations we find that

$$F_1(N) - F_2(N) = \gamma(N+\tfrac{1}{2}), \qquad (7\text{-}3)$$

which shows that the splitting increases linearly with N.

Assuming that the Λ-doubling in the $^2\Pi_{1/2}$ component is significant and that in the $^2\Pi_{3/2}$ component is small and can be neglected, the rotational term values for a $^2\Pi_{reg}$ state belonging to case (a) (large separation between $^2\Pi_{1/2}$ and $^2\Pi_{3/2}$ components) can be represented by the following expressions (Mulliken, 1931; Mulliken & Christy, 1931; Herzberg, 1950; and cf. Eq. (2-10)):

$$^2\Pi_{1/2}: \quad F_{1c}(J) = B^{(1)}J(J+1) - D^{(1)}J^2(J+1)^2 + \tfrac{1}{2}p(J+\tfrac{1}{2}), \quad (7\text{-}4a)$$

$$F_{1d}(J) = B^{(1)}J(J+1) - D^{(1)}J^2(J+1)^2 - \tfrac{1}{2}p(J+\tfrac{1}{2}), \quad (7\text{-}4b)$$

$$^2\Pi_{3/2}: \quad F_{2c}(J) \simeq F_{2d}(J) = B^{(2)}J(J+1) - D^{(2)}J^2(J+1)^2, \quad (7\text{-}5)$$

where p is the Λ-doubling constant, $B^{(i)}$ and $D^{(i)}$ (i=1,2) are the effective rotational and stretching constants, respectively. The relation between the effective and true values of the rotational constant B is given by (Mulliken, 1931)

$$B^{(i)} = B_v^{(i)} \left(1 \pm \frac{2B_v^{(i)}}{A\Lambda} + \ldots\right), \quad (7\text{-}6)$$

where + sign out of (±) stands for $^2\Pi_{3/2}$ and − sign for $^2\Pi_{1/2}$. A is the spin-orbit coupling constant and Λ = 1 for a Π state. The Λ-doublings in the $^2\Pi_{1/2}$ and $^2\Pi_{3/2}$ components can be expressed as (Mulliken & Christy, 1931)

$$^2\Pi_{1/2}: \quad \Delta\nu_{dc}(J) = -p(J+\tfrac{1}{2}), \quad (7\text{-}7)$$

$$^2\Pi_{3/2}: \quad \Delta\nu_{dc}(J) = (p/Y^2 + 2q/Y)(J-\tfrac{1}{2})(J+\tfrac{1}{2})(J+3/2) + \ldots, \quad (7\text{-}8)$$

where q is a constant and $Y = A/B_v$. Since A is too large for SbO (~2270 cm^{-1}), the Λ-doubling in $^2\Pi_{3/2}$ component is expected to be very small, at least theoretically.

In Fig. 24 an energy level diagram is shown which illustrates a $^2\Sigma^+ - {}^2\Pi_{reg}$(a) transition. In this diagram, notations c, d, + and - are taken from Mulliken (1931) and those of the branches are taken from Herzberg (1950); the Λ-type doubling in $^2\Pi$ state and the spin-splitting in $^2\Sigma$ state are exaggerated and the spin-orbit splitting of the $^2\Pi$ state is drawn on a much smaller scale than the separation of the rotational levels. Since the separation between the $^2\Pi_{1/2}$ and $^2\Pi_{3/2}$ components is large, each band of the $^2\Sigma^+ - {}^2\Pi_{reg}$ transition is divided into two subbands, $^2\Sigma^+ - {}^2\Pi_{1/2}$ and $^2\Sigma^+ - {}^2\Pi_{3/2}$, which are separated from each other by the amount of the doublet splitting of the $^2\Pi$ state. Correspondingly, there are two zero lines for each band.

It can be seen from Fig. 24 that according to the selection rules $\Delta J = 0, \pm 1$ and $+ \leftrightarrow -$, six branches are possible for each subband. The branches of the subband $^2\Sigma^+ - {}^2\Pi_{1/2}$ are designated as

$$R_{21}\ ,\ R_1\ ,\ Q_{21}\ ,\ Q_1\ ,\ P_{21} \text{ and } P_1$$

and those of the subband $^2\Sigma^+ - {}^2\Pi_{3/2}$ are designated as

$$R_2\ ,\ Q_2\ ,\ R_{12}\ ,\ P_2\ ,\ Q_{12} \text{ and } P_{12}.$$

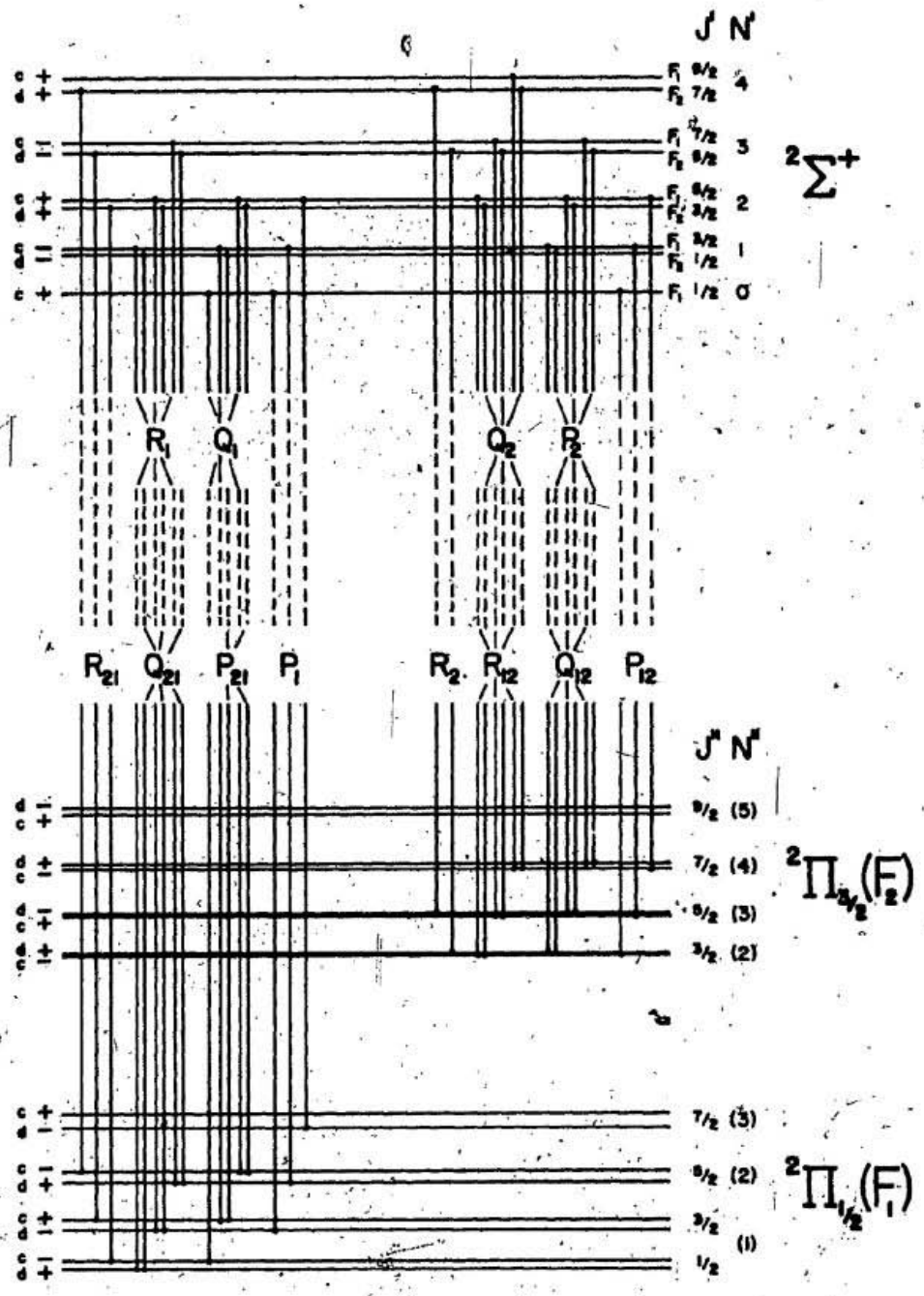

Fig. 24. A schematic energy level diagram for a band of a $^2\Sigma^+ - {}^2\Pi$ transition. Refer to text for other details.

However, we have a choice of using alternative notations as follows

$R_{21} \equiv R_{dc}$, $R_1 \equiv R_{cd}$, $Q_{21} \equiv Q_d$, $Q_1 \equiv Q_c$, $P_{21} \equiv P_{dc}$, $P_1 \equiv P_{cd}$

$R_2 \equiv R_d$, $R_{12} \equiv R_c$, $Q_2 \equiv Q_{dc}$, $Q_{12} \equiv Q_{cd}$, $P_2 \equiv P_d$, $P_{12} \equiv P_c$.

With the help of Eqs. (7-2), (7-4) and (7-5), it should be possible to write the equations for each of the above branches in terms of the molecular constants. It should be noted, however, that if the spin doubling in the $^2\Sigma^+$ state is too small to be resolved then the two branches of the pairs R_1 and Q_{21}, Q_1 and P_{21}, R_{12} and Q_2, and P_2 and Q_{12} will coincide. As a result only four branches will be observed for each subband.

7.3. Rotational Analysis

Attempts were made to photograph most of the intense bands of the B - X system at high resolution but not with all success. Because of the extensive overlapping of the rotational lines from one band to the other and of the presence of two almost equally abundant isotopes of Sb, the structure of most of the bands is complex. In addition, the bands belonging to the $B^2\Sigma^+ - X^2\Pi_{\frac{1}{2}}$ component do not show extensive and sharp rotational structure. Consequently, the present rotational analysis is confined to the 0 - 0 and 1 - 0 bands of the $B^2\Sigma^+ - X^2\Pi_{3/2}$ subsystem.

A spectrogram showing the rotational structure of the 0 - 0 band of $^2\Sigma^+ - {}^2\Pi_{3/2}$ component is given in Fig. 25. The rotational lines are reasonably well resolved, and at longer wavelengths a doubling of the rotational lines owing to the two abundant isotopes ^{121}SbO and ^{123}SbO is observed. The structure of this 0 - 0 band is fairly extensive and hence rotational analysis is possible for a large range of J values. The spin splitting in the upper state appears to be small and is not resolved. Therefore, as indicated earlier, only four branches, namely, R_2, Q_2+R_{12}, P_2+Q_{12} and P_{12}, are observed. At first the relative J assignments to these branches were made with the help of combination relations and the final J numbering was fixed with the help of a plot of $\Delta_2F''(J)$ or $\Delta_2F'(N)$ against $(J''+\frac{1}{2})$ or $(N'+\frac{1}{2})$ (Fig. 26) which passes through J or N = $-\frac{1}{2}$, when extrapolated. Table 20 lists the J assignments and wavenumbers of all the four branches of the 0 - 0 band. The constants B_o and D_o were derived from the least squares fit of the following equation from the four branches mentioned above:

$$\Delta_1F'(J) = R_{12}(J) - Q_{12}(J) = 2B'_o(J+\tfrac{1}{2}) - 4D'_o(J+\tfrac{1}{2})^3, \qquad (7\text{-}9)$$

$$\Delta_1F''(J) = R_{12}(J) - Q_{12}(J+1) = 2B''_o(J+1) - 4D''_o(J+1)^3, \qquad (7\text{-}10)$$

$$\Delta_2F'(J) = R_{12}(J) - P_{12}(J) = 4B'_oJ - 8D'_oJ^3, \qquad (7\text{-}11)$$

$$\Delta_2F''(J) = R_{12}(J-1) - P_{12}(J+1) = 4B''_o(J+\tfrac{1}{2}) - 8D''_o(J+\tfrac{1}{2})^3. \qquad (7\text{-}12)$$

Figure 25

Fig. 25. Rotational structure of the 0-0 band of the $B^2\Sigma^+ - X\ ^2\Pi_{3/2}$ subsystem of SbO.

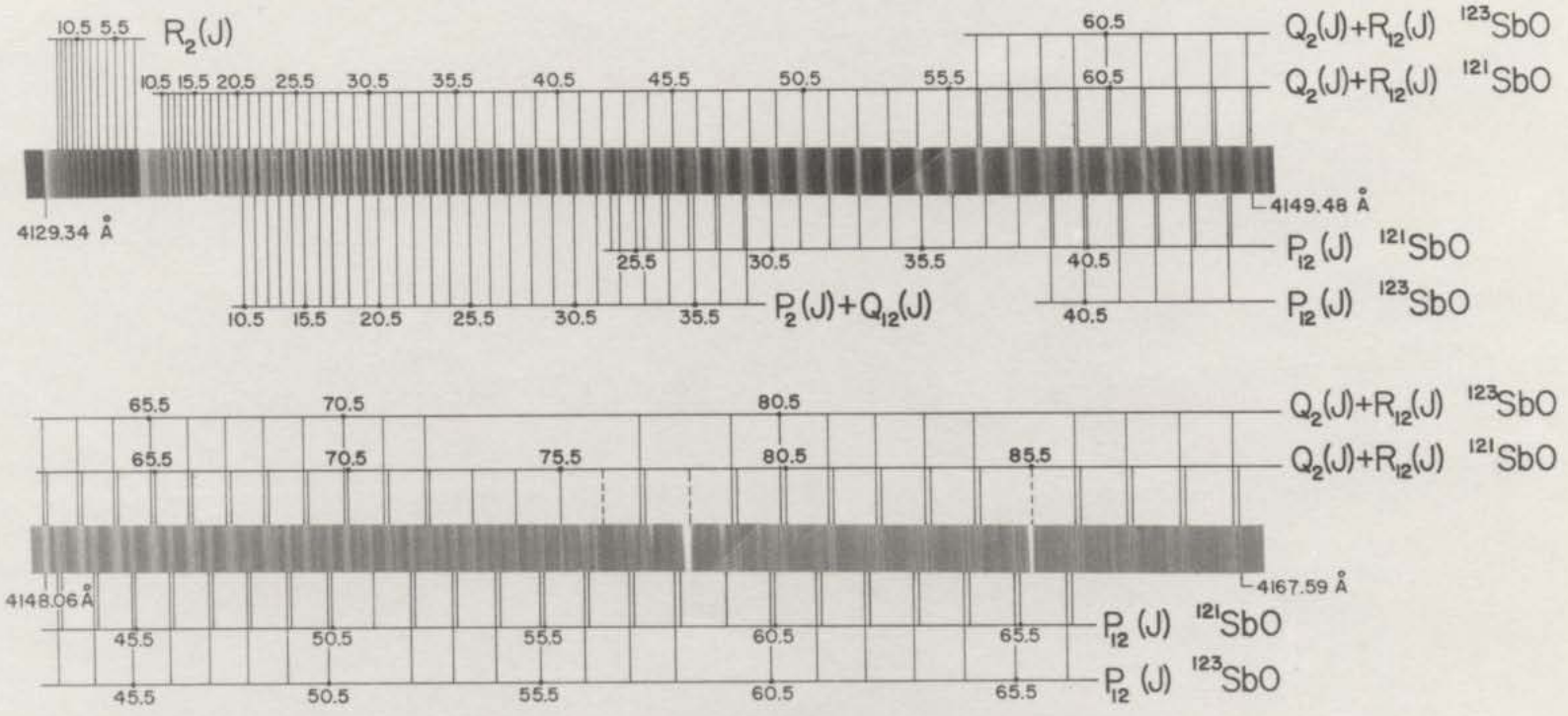
10.5 5.5
R2(J)
10.5 15.5 20.5 25.5 30.5 35.5 40.5 45.5 50.5 55.5 60.5
60.5
Q2(J)+R12(J) 123SbO
Q2(J)+R12(J) 121SbO
4129.34 Å
4149.48 Å
P12(J) 121SbO
P12(J) 123SbO
25.5 30.5 35.5 40.5
10.5 15.5 20.5 25.5 30.5 35.5
P2(J)+Q12(J)
40.5
65.5 70.5 80.5
65.5 70.5 75.5 80.5 85.5
Q2(J)+R12(J) 123SbO
Q2(J)+R12(J) 121SbO
4148.06Å
4167.59 Å
45.5 50.5 55.5 60.5 65.5
P12(J) 121SbO
P12(J) 123SbO

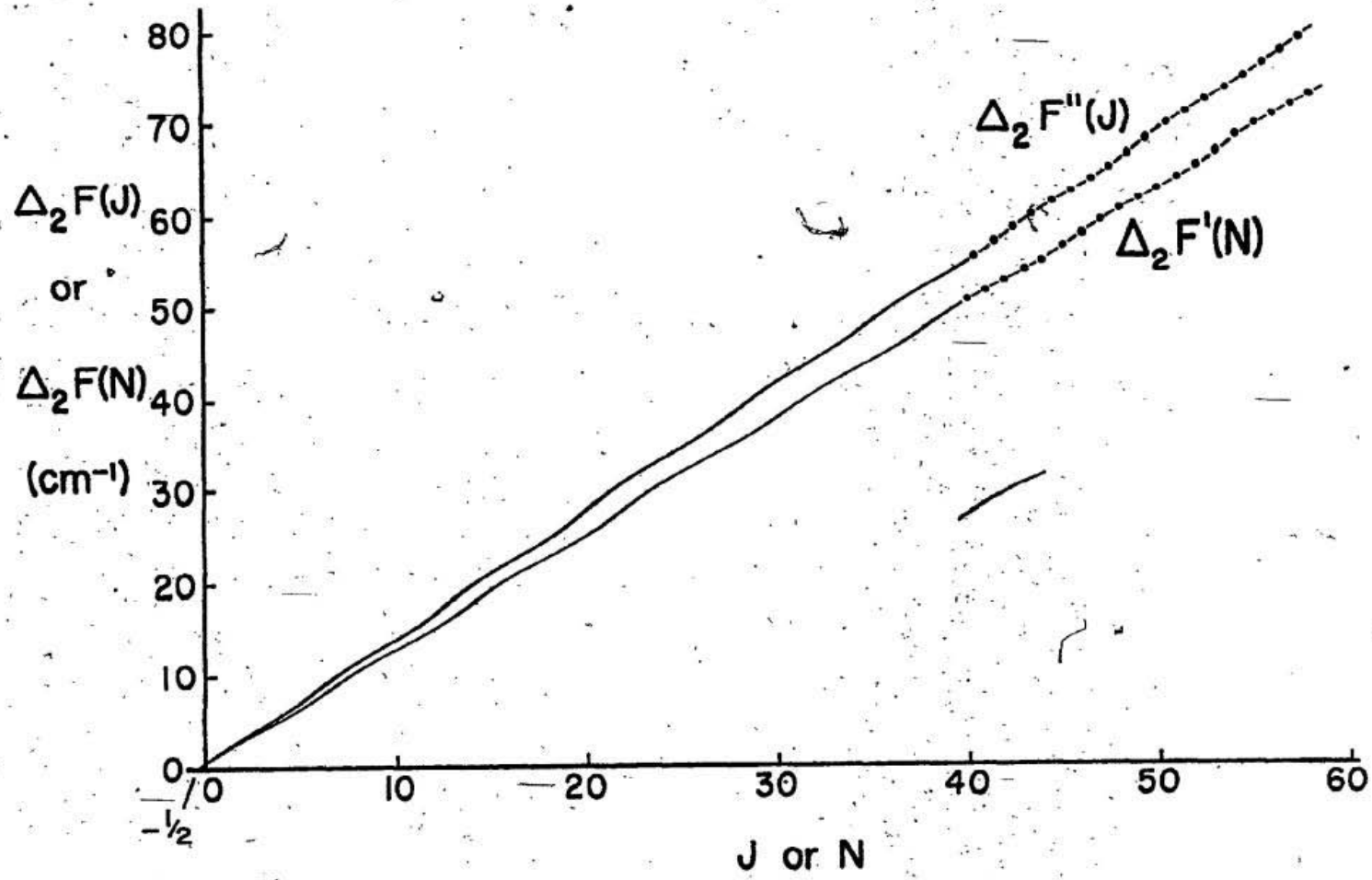

Fig. 26. Plots of $\Delta_2F(J)$ against J and of $\Delta_2F(N)$ against N for the 0-0 band of the $B^2\Sigma^+ - X^2\Pi_{3/2}$ subsystem of SbO.

TABLE 20

Vacuum wavenumbers (cm^{-1}) of the rotational lines in the 0-0 band of $B^2\Sigma-X^2\Pi_{3/2}$ subsystems

J	$R_2(J)$	$Q_2(J)+R_{12}(J)$	$P_2(J)+Q_{12}(J)$	$R_{12}(J)$
3.5	24 201.22			
4.5	24 202.19			
5.5	24 203.10			
6.5	24 203.96			
7.5	24 204.79			
8.5	24 205.49			
9.5	24 206.18			
10.5	24 206.82	24 198.52	24 190.96*	
11.5	24 207.35	24 198.01	24 189.93*	
12.5		24 197.43	24 188.77*	
13.5		24 196.84	24 187.52	
14.5		24 196.18	24 186.29	
15.5		24 195.50	24 185.07	
16.5		24 194.68	24 183.63	
17.5		24 193.86*	24 182.33	
18.5		24 193.10*	24 180.81	
19.5		24 192.20*	24 179.35	
20.5		24 191.32*	24 177.81	
21.5		24 190.21*	24 176.12	
22.5		24 189.11*	24 174.47	
23.5		24 188.00	24 172.75	
24.5		24 186.82	24 171.00	24 155.41
25.5		24 185.60	24 169.06	24 153.01
26.5		24 184.25	24 167.16	24 150.51
27.5		24 182.92	24 165.23	24 147.72
28.5		24 181.52	24 163.20	24 145.22*
29.5		24 180.03	24 161.07	24 142.45*
30.5		24 178.54	24 159.01	24 139.84*
31.5		24 176.97	24 156.80	24 137.15*
32.5		24 175.31	24 154.57	24 134.19*
33.5		24 173.66	24 152.23	24 131.43*
34.5		24 171.91	24 149.90	24 128.39*
35.5		24 170.21	24 147.47	24 125.42*
36.5		24 168.30	24 144.99*	24 122.48*
37.5		24 166.40	24 142.45*	24 119.22*
38.5		24 164.50		24 116.07*
39.5		24 162.29		24 112.87*
40.5		24 160.21		24 109.56
41.5		24 158.04		24 106.26
42.5		24 155.89		24 102.80
43.5		24 153.82		24 099.36
44.5		24 151.54		24 096.19
45.5		24 149.20		24 092.38

TABLE 20 (Continued)

J	$R_2(J)$	$Q_2(J)+R_{12}(J)$	$P_2(J)+Q_{12}(J)$	$P_{12}(J)$
46.5		24 146.82		24 088.76
47.5		24 144.34		24 085.00
48.5		24 141.84		24 081.28
49.5		24 139.28		24 077.51
50.5		24 136.64*		24 073.67
51.5		24 134.19*		24 069.88
52.5		24 131.43*		24 065.82
53.5		24 128.66*		24 061.76
54.5		24 125.82*		24 057.65
55.5		24 122.71*		24 053.47
56.5		24 119.58*		24 049.30
57.5		24 116.59		24 045.05
58.5		24 113.45		24 040.66
59.5		24 110.37		24 036.35
60.5		24 107.18		24 031.56
61.5		24 103.88		24 027.40
62.5		24 100.53		24 022.81
63.5		24 097.16		24 018.16
64.5		24 093.77		24 013.44
65.5		24 090.25		24 008.63
66.5		24 086.65		24 003.72
67.5		24 083.08		
68.5		24 079.38		
69.5		24 075.65		
70.5		24 071.86		
71.5		24 067.96		
72.5		24 064.08		
73.5		24 060.09		
74.5		24 055.97		
75.5		24 051.76		
76.5		x		
77.5		24 043.72		
78.5		†		
79.5		24 035.04		
80.5		24 030.60		
81.5		24 026.14		
82.5		24 021.58		
83.5		24 016.92		
84.5		24 012.28		
85.5		†		
86.5		24 002.71		
87.5		23 997.85		
88.5		23 992.93		
89.0		23 987.92		

*Blended line; †Superposed by atomic line; xToo weak to be measured.

In the (Q_2+R_{12}) branch, there seems to be an irregularity at J = 76.5. However, the structure of the 1 - 0 band does not show any irregularity in the (Q_2+R_{12}) branch at J = 76.5. It is therefore possible that the v' = 0 level of the $B^2\Sigma^+$ state has some perturbation at N = 77. However, some more bands involving v' = 0 should be analyzed before drawing any definite conclusion regarding this irregularity.

A reproduction of the 1 - 0 band of the $^2\Sigma^+ - {}^2\Pi_{3/2}$ component is shown in Fig. 27. In comparison with the 0 - 0 band, the structure of this band near its head is somewhat complex and the analysis was possible only for higher values of J. The analysis of the 0 - 0 band was helpful in assigning correct J values to the rotational lines of the 1 - 0 band. Different combination relations involving the common v'' = 0 state were used. For the 1 - 0 band also, only four branches are resolved. However, the R_2 branch is diffuse and weak (not shown in Fig. 27). The J assignments and wavenumbers of the rotational lines of this band are given in Table 21. As most of the rotational lines of the (P_2+Q_{12}) branch are diffuse or blended, the rotational constants for this band were calculated by the linear least squares fit of the following equations:

$$\Delta_2 F'(J) = R_{12}(J) - P_{12}(J) = 4B_1'J - 8D_1'J^3, \qquad (7\text{-}13)$$

$$\Delta_2 F''(J) = R_{12}(J-1) - P_{12}(J+1) = 4B_0''(J+\tfrac{1}{2}) - 8D_0''(J+\tfrac{1}{2})^3. \qquad (7\text{-}14)$$

Figure 27

Fig. 27. Rotational structure of the 1-0 band of the $B^2\Sigma^+ - X\ ^2\Pi_{3/2}$ subsystem of SbO.

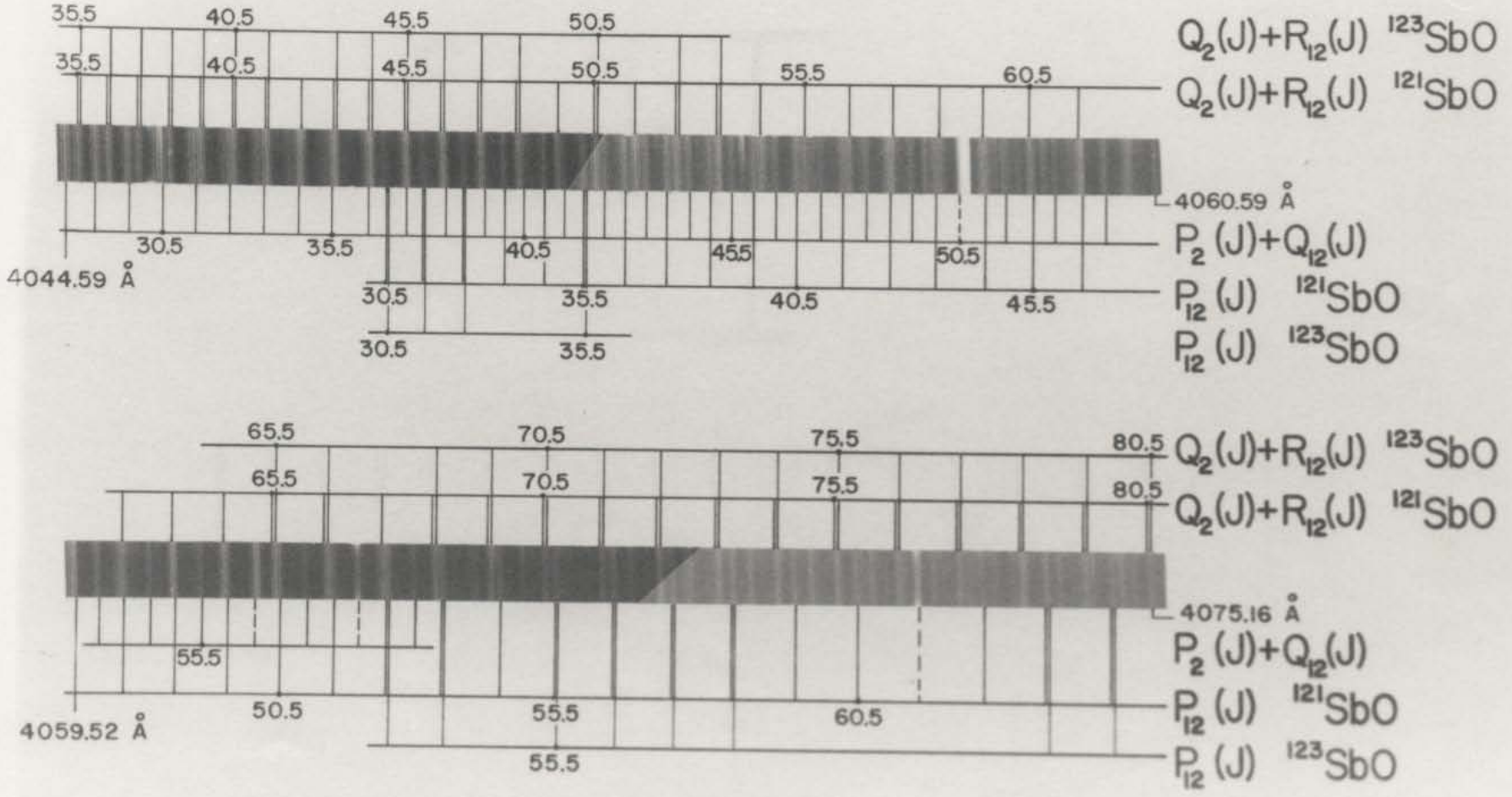
35.5
40.5
45.5
50.5
35.5
40.5
45.5
50.5
55.5
60.5
Q2(J)+R12(J) 123SbO
Q2(J)+R12(J) 121SbO
4060.59 Å
30.5
35.5
40.5
45.5
50.5
4044.59 Å
P2(J)+Q12(J)
30.5
35.5
40.5
45.5
P12(J) 121SbO
30.5
35.5
P12(J) 123SbO
65.5
70.5
75.5
80.5
65.5
70.5
75.5
80.5
Q2(J)+R12(J) 123SbO
Q2(J)+R12(J) 121SbO
4075.16 Å
55.5
50.5
55.5
60.5
4059.52 Å
P2(J)+Q12(J)
P12(J) 121SbO
55.5
P12(J) 123SbO

TABLE 21

Vacuum wavenumbers (cm^{-1}) of the rotational lines in the 1-0 band of $B^2\Sigma-X^2\Pi_{3/2}$ subsystem

J	$Q_2(J)+R_{12}(J)$	$P_2(J)+Q_{12}(J)$	$P_{12}(J)$
27.5		24 717.42	
28.5		24 714.79	
29.5		24 711.78	
30.5		24 708.88	24 688.62*
31.5		24 705.57	24 685.34
32.5		24 702.86	24 681.77
33.5		24 699.81	24 678.25
34.5		24 696.71*	24 674.67
35.5	24 715.97	24 693.73	24 671.07
36.5	24 713.34	24 690.60*	24 667.40
37.5	24 710.64	24 687.06	24 663.64
38.5	24 707.90	24 683.49	24 659.83
39.5	24 705.07	24 679.97*	24 655.88
40.5	24 702.19	24 676.47*	24 652.05*
41.5	24 699.27	24 672.84*	24 648.02*
42.5	24 696.28*	24 669.18	24 643.64*
43.5	24 693.16	24 665.46	24 639.39*
44.5	24 689.98	24 661.68	24 635.02*
45.5	24 686.80	24 658.07	24 630.84*
46.5	24 683.49	24 653.88	24 626.48*
47.5	24 680.17	24 649.88	24 622.39*
48.5	24 676.74	24 645.82	24 617.83
49.5	24 673.31*	24 641.73	24 613.26
50.5	24 669.74	†	24 608.62
51.5	24 666.05	24 633.30*	24 603.93
52.5	24 662.45	24 628.99*	24 599.05
53.5	24 658.72	24 624.54*	24 594.16
54.5	24 655.11*	24 620.03*	24 589.20
55.5	24 651.20*	24 615.57*	24 584.20
56.5	24 647.18*	24 610.78*	24 579.10
57.5	24 643.33*	24 606.24*	24 573.91
58.5	24 639.10	†	24 568.64
59.5	24 635.42*	24 596.75*	24 563.29
60.5	24 631.17*		24 557.90
61.5	24 626.81*		†
62.5	24 622.39*		24 546.75
63.5	24 618.13*		24 541.04

TABLE 21 (Continued)

J	$Q_2(J)+R_{12}(J)$	$P_2(J)+Q_{12}(J)$	$P_{12}(J)$
64.5	24 613.54		24 535.32
65.5	24 608.94		
66.5	24 604.31		
67.5	24 599.59		
68.5	24 594.81		
69.5	24 589.96		
70.5	24 585.09		
71.5	24 580.09		
72.5	24 575.04		
73.5	24 569.88		
74.5	24 564.68		
75.5	24 559.43		
76.5	24 554.05		
77.5	24 548.67		
78.5	24 543.16		
79.5	24 537.57		
80.5	24 531.95		

*Blended or diffuse line.

†Superposed by atomic line.

Graphical plots of these fits are shown in Fig. 28. The additional weak lines in the 0 - 0 and 1 - 0 bands at longer wavelengths (see Figs. 25 and 27) for which no J assignments were possible may possibly belong to some overlapping bands.

The molecular constants of the $B^2\Sigma^+$ and $X^2\Pi_{3/2}$ states are listed in Table 22. The vibrational constants are from Sengupta (1939). The rotational constant B_o'' of the $X^2\Pi_{3/2}$ state and B_o' of the $B^2\Sigma^+$ state given in Table 22 are the average values obtained from different branches of the 0 - 0 and 1 - 0 bands. It should be noted that the values of the ground-state constants B_o and D_o given in this table are the effective values. The values of ν_o for the 0 - 0 and 1 - 0 bands were determined by fitting the equations for the (Q_2+R_{12}) and P_{12} branches to a third order polynomial.

7.4. Isotope Effect

Many rotational lines in the 0 - 0 band and most of the lines in the 1 - 0 band show doublet structure which is assigned to the isotopes ^{121}SbO and ^{123}SbO. The observed intensities of the two components of the doublets in these bands is in accordance with the relative abundance of the two isotope species (^{121}Sb : 57.25%; ^{123}Sb : 42.75%). The vibrational isotope shifts $\Delta\nu_v$ were calculated by using Eqn. (4-7a). [Note: $\mu_A(^{121}\text{SbO}) = 14.1261$ amu; $\mu_A(^{123}\text{SbO} = 14.1530$

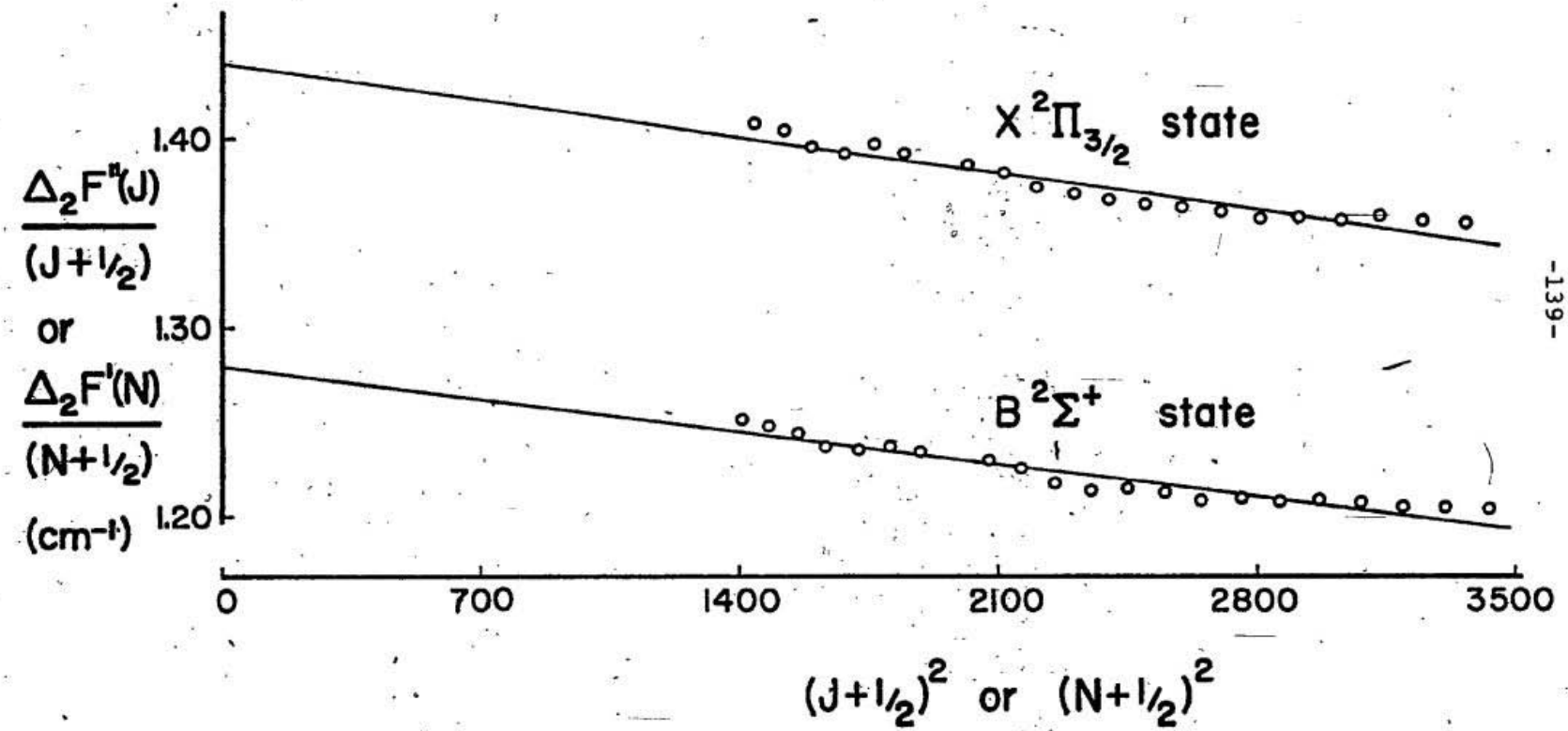

Fig. 28. Plots of $\Delta_2F''(J)/(J+\frac{1}{2})$ versus $(J+\frac{1}{2})^2$ for the $X^2\Pi_{3/2}$ substate and that of $\Delta_2F'(N)/(N+\frac{1}{2})$ versus $(N+\frac{1}{2})^2$ for the $B^2\Sigma^+$ state, of SbO.

TABLE 22

Molecular constants of the $B^2\Sigma^+$ and $X^2\Pi_{3/2}$ states

	$B^2\Sigma^+$	$X^2\Pi_{3/2}$
ω_e (cm^{-1})	582.0[a]	817.0[a]
$\omega_e x_e$ (cm^{-1})	6.50[a]	5.40[a]
$\Delta G(\frac{1}{2})$ (cm^{-1})	570.3	
B_1 (cm^{-1})	0.3197±0.0009	
I_1 (gm cm^2)	87.65×10^{-40}	
r_1 (Å)	1.9331	
B_o (cm^{-1})	0.3238±0.0006[†]	0.3563±0.0007*
D_o (cm^{-1})	5×10^{-6}	4×10^{-6}*
I_o (gm cm^2)	86.54×10^{-40}	78.65×10^{-40}
r_o (Å)	1.9208	1.8311
B_e (cm^{-1})	0.3259	
α_e (cm^{-1})	0.0041	
I_e (gm cm^2)	85.98×10^{-40}	
r_e (Å)	1.9146	

ν_o for the 0 - 0 band of $B^2\Sigma - X^2\Pi_{3/2}$ = 24199.6 cm^{-1}

ν_o for the 1 - 0 band of $B^2\Sigma - X^2\Pi_{3/2}$ = 24769.9 cm^{-1}

[a] Sengupta (1939).

* Effective values.

[†] Value obtained by Rao and Rao (1968) is 0.321_2 cm^{-1}.

amu; $\rho^2 = [\mu(^{121}SbO)/\ \mu(^{123}SbO)] = 0.9981]$. The values obtained are as follows:

$$0 - 0 \text{ band: } \Delta\nu_v(^{121}SbO - {}^{123}SbO) = -0.11 \text{ cm}^{-1}$$

$$1 - 0 \text{ band: } \Delta\nu_v(^{121}SbO - {}^{123}SbO) = +0.42 \text{ cm}^{-1}$$

The observed isotope shifts in the rotational lines of different branches in 0 - 0 and 1 - 0 bands are listed in Tables 23, 24 and 25. However, in the absence of sufficient rotational constants, it was not possible to calculate the total (i.e., vibrational + rotational) isotope shifts in these branches. Equation (4-7b) can be approximated as

$$\Delta\nu_r \simeq (1 - \rho^2)\nu_r \qquad (7\text{-}15)$$

According to this relation one expects a linear fit when the $\Delta\nu_r$ values are plotted against ν_r. A representative plot for the observed $\Delta\nu_{total}$ against wavenumber of the rotational lines for the (Q_2+R_{12}) branch is shown in Fig. 29. As the vibrational isotope shift $\Delta\nu_v$ is constant for the rotational lines of a given band, the slope of this plot gives the value of $(1-\rho^2)$.

The values obtained for ρ^2 from different branches by this procedure are as follows:

(Q_2+R_{12}) branch (0-0 band) : $\rho^2 = 0.9984$

P_{12} branch (0-0 band) : $\rho^2 = 0.9979$

TABLE 23

Observed isotope shifts $\Delta\nu(^{123}SbO - ^{121}SbO)$ in $Q_2(J) + R_{12}(J)$ branch of 0 - 0 band

J	$\Delta\nu(^{123}SbO-^{121}SbO)$ (cm^{-1})	J	$\Delta\nu(^{123}SbO-^{121}SbO)$ (cm^{-1})
56.5	0.30	70.5	0.37
57.5	0.30	71.5	0.38
58.5	0.31	72.5	0.38
59.5	0.31	77.5	0.40
60.5	0.32	79.5	0.42
61.5	0.31	80.5	0.43
62.5	0.32	81.5	0.44
63.5	0.33	82.5	0.46
64.5	0.34	83.5	0.47
65.5	0.36	84.5	0.48
66.5	0.35	86.5	0.48
67.5	0.35	87.5	0.49
68.5	0.37	88.5	0.50
69.5	0.36	89.5	0.50

TABLE 24

Observed isotope shifts $\Delta\nu(^{123}SbO - ^{121}SbO)$ in $P_{12}(J)$ branch of the 0 - 0 band

J	$\Delta\nu(^{123}SbO-^{121}SbO)$ (cm^{-1})	J	$\Delta\nu(^{123}SbO-^{121}SbO)$ (cm^{-1})
39.5	0.27	52.5	0.37
40.5	0.30	53.5	0.39
41.5	0.29	54.5	0.40
42.5	0.30	55.5	0.40
43.5	0.31	56.5	0.42
44.5	0.30	57.5	0.41
45.5	0.32	58.5	0.44
46.5	0.34	61.5	0.47
47.5	0.33	63.5	0.46
48.5	0.35	64.5	0.48
49.5	0.35	65.5	0.51
50.5	0.36	66.5	0.51

TABLE 25

Observed isotope shifts $\Delta\nu(^{121}SbO - ^{123}SbO)$ in the 1 - 0 band

J	$\Delta\nu$ (^{121}SbO-^{123}SbO) in (Q_2+R_{12} branch)	$\Delta\nu$ (^{121}SbO-^{123}SbO) in P_{12} branch	J	$\Delta\nu$ (^{121}SbO-^{123}SbO) in (Q_2+R_{12} branch
30.5		0.31	65.5	0.26
31.5		0.31	66.5	0.26
32.5		0.30	68.5	0.25
35.5	0.34	0.30	69.5	0.25
36.5	0.34		70.5	0.24
37.5	0.33		71.5	0.25
38.5	0.32		72.5	0.24
39.5	0.33		73.5	0.23
40.5	0.31		74.5	0.23
41.5	0.32		75.5	0.22
43.5	0.30		76.5	0.21
44.5	0.31		77.5	0.22
45.5	0.31		78.5	0.20
46.5	0.29		79.5	0.19
47.5	0.30		80.5	0.19
48.5	0.30			
50.5	0.29			
52.5	0.28	0.26		
53.5	0.28	0,25		
55.5		0.23		
56.5		0.24		
57.5		0.23		
58.5		0.23		
63.5		0.21		
64.5		0.20		

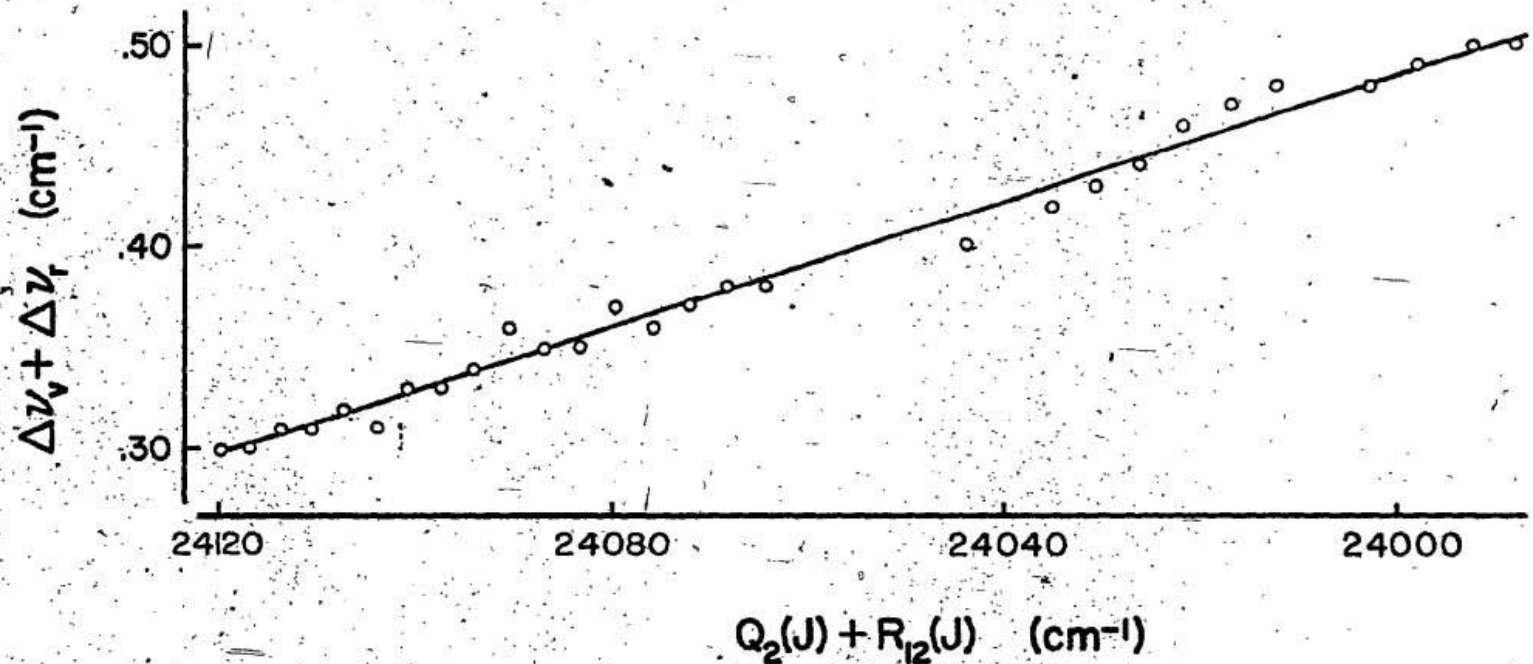

Fig. 29. Total isotope shift ($\Delta\nu_v + \Delta\nu_r$) versus the wavenumber (cm^{-1}) of the rotational lines of the $^{v}Q_2(J)^{r} + R_{12}(J)$ branch of ^{121}SbO in 0-0 band.

(Q_2+R_{12}) branch (1-0 band) : $\rho^2 = 0.9990$

These estimated values are in close agreement with the calculated value of ρ^2 (=0.9981) from the reduced masses of ^{121}SbO and ^{123}SbO. This fact supports the J assignments in the 0 - 0 and 1 - 0 bands in the present analysis.

7.5. Electron Configurations

The lowest electron configuration of SbO just as for the analogous molecules NO, PO and AsO may be written as

$$\ldots (w\pi)^4 (x\sigma)^2 (v\pi) : {}^2\Pi_{reg} \qquad (7\text{-}16)$$

The low-lying excited electronic states of SbO arise from the configuration

$$\ldots (w\pi)^3 (x\sigma)^2 (v\pi)^2 : {}^2\Pi_{reg},\ {}^2\Pi(2),\ {}^4\Pi_{inv},\ {}^2\Phi_{inv}. \qquad (7\text{-}17)$$

$$\ldots (w\pi)^4 (x\sigma) (v\pi)^2 : {}^2\Sigma^+,\ {}^2\Sigma^-,\ {}^2\Delta,\ {}^4\Sigma^-. \qquad (7\text{-}18)$$

For SbO, state X belongs to the configuration (7-16) and state B to the configuration (7-18).

REFERENCES

Adam Hilger Ltd. "Arc Spectra of Copper", 2nd edition.

Ahmed, F. and Barrow, R.F. 1974. J. Phys. B 7, 2256.

Ahmed, F., Barrow, R.F., and Yee, K.K. 1975. J. Phys. B 8, 649.

Asundi, R.K., Jan-Khan, M., and Samuel, R. 1936. Proc. Roy. Soc. A 157, 28.

Azam, M. and Reddy, S.P. 1973. Canad. J. Phys. 51, 2166.

Babcock, H.D. and Herzberg, L. 1948. Astrophys. J. 108, 167.

Barrow, R.F. and Deutsch, E.W. 1963. Proc. Roy. Soc. 82, 548.

Barrow, R.F. and du Parcq, R.P. 1965. Elemental Sulphur (Interscience Publishers, New York), Chap. 13.

Barrow, R.F. and du Parcq, R.P. 1968. Proc. Phys. Soc. B 1, 283.

Barrow, R.F., du Parcq, R.P., and Ricks, J.M. 1969. J. Phys. B 2, 413.

Barrow, R.F. and Hitchings, M.R. 1972. J. Phys. B 5, L132.

Barrow, R.F. and Ketteringham, J.M. 1963. Canad. J. Phys. 41, 419.

Barrow, R.F. and Lemanczyk, R.Z. 1975. Canad. J. Phys. 53, 553.

Barrow, R.F. and Ricks, J.M. (unpublished), (cf. B. Rosen, 1970).

Barrow, R.F. and Yee, K.K. 1974. Acta Physica Acad. Hung. 35, 239.

Bowers, K.D., Kamper, R.A., and Lustig, C.D. 1959. Proc. Roy. Soc., A 251, 565.

Carrington, A., Levy, D.H., and Miller, T.A. 1966. Proc. Roy. Soc. A 293, 108.

Carrington, A., Levy, D.H., and Miller, T.A. 1967. Proc. Roy. Soc. A 298, 340.

Carrington, A., Currie, G.N., Levy, D.H., and Miller, T.A. 1969. Mol. Phys. 17, 535.

Chatalic, A., Danon, N., Iacocca, D. and Pannetier, G. 1973. J. Chim. Phys. 70, 1600.

Choong, S.P. 1938. Ann. Phys. Paris 10, 173.

Colin, R. 1968. Canad. J. Phys. 46, 1539.

Colin, R. 1969. Canad. J. Phys. 47, 979.

Daniel, J.M. and Dorain, P.B. 1966. J. Chem. Phys. 45, 26.

Douglas, A.E. and Jones, W.E. 1966. Canad. J. Phys. 44, 2251.

Dunham, J.L. 1932. Phys. Rev. 41, 713.

Edlen, B. 1953. J. Opt. Soc. Amer. 43, 339.

Findlay, F.D. 1970. Canad. J. Phys. 48, 2107.

Gatterer, A. and Junkes, J. 1956. Arc Spectrum of Iron, 2nd ed. (Specola Vaticana, Citta del Vaticano).

Gouedard, G. and Lehmann, J.C. 1976. J. Phys. B 9, 2113.

Greenwood, D.J. and Barrow, R.F. 1976. J. Phys. B 9, 2123.

Haranath, P.B.V. 1964. J. Mol. Spectrosc. 13, 168.

Haranath, P.B.V. 1965. Indian J. Pure & Appl. Phys. 3, 75.

Hebb, M.H. 1936. Phys. Rev. 49, 610.

Herzberg, L. and Herzberg, G. 1947. Astrophys. J. 105, 353.

Herzberg, G. 1950. Spectra of diatomic molecules, 2nd ed. (D. Van Nostrand Co., Inc., Princeton, N.J.).

Herzberg, G. 1971. The spectra and structures of simple free radicals, Cornell University Press, Ithaca and London.

Humphreys, C.J. 1953. J. Opt. Soc. Amer. 43, 1027.

Hynes, D.L. 1968. B.Sc. (Honours) dissertation, Memorial University of Newfoundland, Canada.

International Union of Pure and Applied Chemistry. 1961. Tables of Wavenumbers for the Calibration of Infrared Spectrometers (Butterworths, London).

Jarmain, W.R. 1960. Canad. J. Phys. 38, 217.

Jarmain, W.R. 1971. J. Quant. Spectrosc. Radiat. Transfer 11, 421.

Jarmain, W.R. and McCallum, J.C. 1970. TRAPRB (A computer program for molecular transitions), University of Western Ontario, Canada.

Jones, W.E. 1967. Canad. J. Phys. 45, 21.

Jordan, P.C. 1964. J. Chem. Phys. 41, 1442.

Klein, O. 1932. Z. Phys. 76, 226.

Kopp, I., Lindgren, R., and Rydh, B. 1974. Table of Band Features of diatomic molecules in wavelength order A, (Inst. of Phys., University of Stockholm).

Kovacs, I. 1962. Phys. Rev. 128, 663.

Kovacs, I. 1969. Rotational Structure in the spectra of diatomic molecules, American Elsevier Publishing Co., Inc., N.Y.

Kramers, H.A. 1929. Z. Physik 53, 422.

Kushawaha, V.S. and Pathak, C.M. 1972. Spectrosc. Lett. 5, 393.

Lakshman, S.V.J. 1960a. Z Physik 158, 367.

Lakshman, S.V.J. 1960b. Z. Physik 158, 386.

Maeder, R. and Miescher, E. 1948. 161, 393.

Mohan, H. and Majumdar, K. 1961. Proc. Phys. Soc. 77, 147.

Moore, C.E. 1949 (Vol. I) and 1952 (Vol. II). Atomic energy levels (circular 467 of National Bureau of Standards, U.S.A.).

Morse, P.M. 1929. Phys. Rev. 34, 57.

Mukherji, B.C. 1931. Z. Physik 70, 552.

Mulliken, R.S. 1930. Rev. Mod. Phys. 2, 60.

Mulliken, R.S. 1931. Rev. Mod. Phys. 3, 89.

Mulliken, R.S. and Christy, A. 1931. Phys. Rev. 38, 87.

Mulliken, R.S. 1932. Rev. Mod. Phys. 4, 1.

National Bureau of Standards monograph 108, "Oscillator Strengths and Transition Probabilities for 3288 Lines of Fe I" 1968. Washington, D.C., U.S.A.

Nicholls, R.W. and Jarmain, W.R. 1956. Proc. Phys. Soc. A 69, 253.

O'Neil, S.V. and Shaeffer III, H.F. 1971. J. Chem. Phys. 55, 394.

Plyler, E.K., Blaine, L.R., and Tidwell, E.D. 1955. J. Res. Natl. Bur. Standards 55, 279.

Powell, F.X. and Lide, D.R. 1964. J. Chem. Phys. 41, 1413.

Raftery, J., Scott, P.R., and Richards, W.G. 1972. J. Phys. B 5, 1293.

Rai, S.B., Rai, B., and Rai, D.K. 1974. Can. J. Phys. 52, 592.

Rai, B.D., Upadhyay, K.N., and Rai, D.K. 1970. J. Phys. B 3, 1374.

Rao, D.V.K. and Rao, P.T. 1968. Current Sci. 37, 310.

Reddy, S.P. and Azam, M. 1974. J. Mol. Spectrosc. 49, 461.

Rees, A.L.G. 1947. Proc. Phys. Soc. A 59, 998.

Rosen, B. 1970. International Tables of Selected Constants: Spectroscopic Data relative to Diatomic Molecules (Pergamon Press, N.Y.).

Rydberg, R. 1931. Z. Physik. 73, 376.

Schlapp, R. 1932. Phys. Rev. 39, 806.

Schlapp, R. 1937. Phys. Rev. 51, 342.

Sen Gupta, A.K. 1939. Ind. J. Phys. 13, 145.

Sen Gupta, A.K. 1943. Ind. J. Phys. 17, 216.

Shimauchi, M. 1960. Science of Light 9, 109.

Singh, R.B. and Upadhyay, K.N. 1967. Proc. of Indian Science Congress, Calcutta, India.

Suchard, S.N. 1975. Spectroscopic Data, Volume 1: Heteronuclear diatomic molecules (Plenum Publishing Co. Ltd., London, England).

Tilford, S.G., Vanderslice, J.T., and Wilkinson, P.G. 1965. Astrophys. J. 141, 1226.

Townes, C.H. and Schawlow, A.L. 1955. Microwave Spectroscopy, McGraw-Hill, New York.

TRAPRB, A computer program for molecular transitions, Jarmain, W.R. and McCallum, J.C. 1970. University of Western Ontario.

Van Vleck, J.H. 1929. Phys. Rev. 33, 467.

Verma, K.K., Azam, M., and Reddy, S.P. 1975. J. Mol. Spectrosc. 58, 367.

Verma, K.K., Azam, M., and Reddy, S.P. 1977. J. Mol. Spectrosc. 65, 289.

Verma, K.K. and Reddy, S.P. 1977. J. Mol. Spectrosc. 67, 360.

Watson, J.K.G. 1968. Canad. J. Phys. 46, 1637.

Welch, W.M. and Mizushima, M. 1972. Phys. Rev. A 5, 2692.

Yee, K.K. and Barrow, R.F. 1972. J. Chem. Soc. Faraday II 68, 1397.

Zaidel, A.N., Prokofev, V.K., Raiskii, S.M., Slavnyi, V.A., and Shreider, E. Ya. 1970. Tables of Spectral Lines (IFI/Plenum, New York-London).

PUBLICATIONS

K.K. Verma and S.P. Reddy. Rotational Analysis of the $b0^+ - X0^+,1$ System of SeO. J. Mol. Spectrosc. 67, 360 (1977).*

K.K. Verma, M. Azam, and S.P. Reddy. The $A^3\Pi_{reg} - X0^+,1$ System of the SeO Molecule. J. Mol. Spectrosc. 65, 289 (1977)*

K.K. Verma, M. Azam, and S.P. Reddy. A New Spectrum of SeO in the Region 3190 - 2690 Å. J. Mol. Spectrosc. 58, 367 (1975).*

V.D. Vankar, P.K. Gargya, K.K. Verma, and D.L. Bhattacharya. A Simple Replica Technique for Electron Microscopy of Porous Surfaces. Ind. Journal of Pure & Applied Phys. 11, 231 (1973).

---

*A copy of the publication is attached.

ROTATIONAL ANALYSIS OF THE b–X SYSTEM OF SELENIUM MONOXIDE

K.K. VERMA AND S. PADDI REDDY.

DEPARTMENT OF PHYSICS, MEMORIAL UNIVERSITY OF NEWFOUNDLAND,
ST. JOHN'S, NEWFOUNDLAND, CANADA A1C 5S7

LEAVES 360-373

PREVIOUSLY COPYRIGHTED MATERIAL,

PHAMPLET AT END OF THESIS

NOT MICROFILMED.

A NEW EMISSION BAND SPECTRUM OF SeO IN THE REGION 3190-2690 Å[1].

K.K. VERMA, M. AZAM, AND S. PADDI REDDY

DEPARTMENT OF PHYSICS, MEMORIAL UNIVERSITY OF NEWFOUNDLAND, ST. JOHN'S, NEWFOUNDLAND, CANADA

LEAVES 367-373

THE $A^3\Pi$-$X0^+$ (1) BAND SYSTEM OF THE SeO MOLECULE

K.K. VERMA, M. AZAM, AND S. PADDI REDDY

DEPARTMENT OF PHYSICS, MEMORIAL UNIVERSITY OF NEWFOUNDLAND, ST. JOHN'S, NEWFOUNDLAND, CANADA, A1C 5S7